3. Results

The results section of this thesis is arranged in three main subsections. Section 3.1 presents the statistical results of composite surface wind and SLP pressure data from the original six case studies (see Table II). Section 3.2 individually highlights and introduces the synoptic and mesoscale configuration of the six original case studies, as well as the seventh, late-addition case study of 2 January 2008. A summary of all seven case studies is presented in section 3.3.

3.1 Statistical Results

3.1.1 Wind Climatology During MHC Events

Hourly observations of surface wind direction were culled from the ASOS sites located in Glens Falls, NY (KGFL), Utica, NY (KUCA), and Albany, NY (KALB), in order to determine the prevailing wind direction at these sites during MHC events (see Fig. 1.2). These sites were used for five of the original six case studies (see Table II for case study dates). By January 2007, however, the ASOS at KUCA had been decommissioned by NOAA and its designated replacement site in Rome, NY (KRME), was not yet fully operational. So, while data from KRME would be an ideal replacement for data from KUCA, winds collected for analysis from the 29 January 2007 case made use instead of KSYR as the westernmost observation point. The wind directions from KUCA and KSYR were aggregated and treated as having come from the same station, as the two stations are both located within the Mohawk River valley and surrounded by similar topography (Fig. 1.2). Thus, wind directions upstream at KSYR are expected to be representative of those at KUCA.

Only observations that were taken during an "ongoing" MHC event were included in the wind climatology, and therefore this climatology is not representative of antecedent conditions. An hourly observation was classified to have occurred during an ongoing MHC event if:

(a) Radar echoes of at least 5 dBZ (KENX, base reflectivity, 0.5° beam elevation) were present near the intersection of the Mohawk and Hudson River valleys at the time of the observation
(b) The echoes did not originate over Lake Ontario, and therefore were not attributable to lake effects
(c) The echoes were discrete and unconnected to any larger area of synoptically forced precipitation

Or, alternatively (and, as will be shown later, less frequently)

(d) A marked enhancement of preexisting radar echoes was observed as the echoes passed through the area where the Mohawk and Hudson River valleys intersect

Hourly reports from the original six case studies which met these criteria were grouped by wind direction, into 10° bins, and counted (see Table III). The total number of reports in each 10° bin was then plotted, according to observation site, onto wind roses, where the azimuthal axis represents wind direction in degrees and the radial axis represents the number of hourly occurrences. A description of the resulting three wind roses follows,

with a comprehensive analysis of wind direction at KALB thereafter, categorized by the time the observation was made relative to the onset of MHC.

3.1.1.1 Wind Climatology at KGFL During MHC Events

Figure 3.1a shows the number of hourly wind reports at KGFL from each direction during ongoing MHC events, while Fig. 3.1b relates each report value to the total number of wind reports at KGFL during ongoing MHC events (a number which varies slightly from station to station, owing to several missing hourly observations which could not be recovered). Figure 3.1a shows a prevailing northeasterly wind direction during MHC events at KGFL. The maximum number of reports from any one bin is seven (from 050°), with 52% of wind reports coming from 040°–070°. A much weaker secondary signal, from the northwest, is also seen, with 16% of wind reports falling between 310° and 340°. It is interesting to note that, while not included in the totals or percentages shown in Figs. 3.1a,b, calm wind reports KGFL numbered six during MHC events, equaling the second-greatest number of reports for any one bin. Calm surface winds were also reported by Chien and Mass (1997) during the 26 May 1992 PSCZ event, and also by Wesley et al. (1995) during the LA event which occurred on 16 January 1991.

3.1.1.2 Wind Climatology at KUCA/KSYR During MHC Events

A strong single-mode surface wind direction signature also exists at KUCA/KSYR. Figure 3.2a shows a sharp maximum at 290° in number of occurrences (11 out of 45 total; see Table III). This one-bin maximum accounts for 24% of all

reports, with 59% of all reports coming from 270°–300° (Fig. 3.2b). This range of wind directions corresponds well with the axis of the Mohawk River valley (see Fig. 1.2). The next-largest grouping of reports is from 320°–350°, with 30% of all reports falling in this range.

3.1.1.3 Wind Climatology at KALB During MHC Events

Differing from the surface wind signatures at KGFL and KUCA/KSYR, the wind direction at KALB during MHC events is shown in Fig. 3.3a to be strongly bimodal. Seven reports, the maximum number in any one bin for KALB, are seen from 020° and 030°, and also from 310°. Figure 3.3b shows that winds from 000°–030° and from 300°–330° account for an overwhelming majority of reports (85%), with winds from the north to north-northeast occurring preferentially over winds from the west-northwest (47% to 38%, respectively). This finding is consistent with the geography that surrounds the observation site, situated at the intersection of the Mohawk valley, which opens to the west-northwest of KALB, and the Hudson valley, which opens to the north (see Fig. 1.2). This finding is also consistent the results of Wasula et al. (2002), who found prevailing wind directions of north, south, and west-northwest at KALB during severe weather events.

3.1.1.4 Wind Climatology at KALB Classified By Relative Observation Time

To determine if either wind mode tends to occur at a particular time relative to the onset of MHC (e.g., whether west-northwest winds occur as the event winds down and as high pressure builds in), each of the 46 hourly surface wind observations taken at KALB

was grouped into three time periods—"beginning," "middle," and "end." Table II contains the starting and ending times for each classification for each case study. These observation-time classifications were made based on radar presentation at the time of the report, and are inherently subjective in nature. While there are likely slight inconsistencies in how individual observations were classified, the aim is simply to generalize how winds evolve during MHC events in a qualitative sense.

3.1.1.4.1 Wind Direction at the "Beginning" of MHC Events

Observations made concurrently with the first appearance of MHC-related precipitation on radar were assigned to the "beginning" classification. Generally, this time period is characterized by a small, discrete area of echoes visible on radar (often in clear-air mode) or, alternately, the first discernable signs of enhanced radar reflectivity as preexisting echoes approach KALB.

Ten such time periods were identified, with wind directions ranging across 90° and reports from the northwest, north, and northeast (see Fig. 3.4a). The highest number of reports from any one bin is 3, from 000°, with 2 reports from 030° (see Table IV). Given the small sample size, a definitive signal is difficult to find, however the reports do skew towards the north and northeasterly directions.

3.1.1.4.2 Wind Direction at the "Middle" of MHC Events

The "middle" classification is characterized by the presence on radar of widespread, discrete echoes, which may fluctuate in intensity. Twenty-five wind

observations were made during the middle of an ongoing MHC event. A stronger bimodal wind direction signature appears during this time period, as shown in Fig. 3.4b. A peak of five wind reports occurs from both 030° and 310°, showing equal preference for north-northeast winds and west-northwest winds at this time. This bimodal nature to the winds may reflect the position of the boundary representing the two low-level flows, e.g., north or south of KALB.

3.1.1.4.3 Wind Direction at the "End" of MHC Events

Observations designated as having been taken at the "end" of an MHC event occur concurrent with a marked decrease in precipitation coverage and intensity (as visible on radar), followed within several hours by the end of MHC-induced precipitation altogether. Precipitation may still be continuing in the area, but it has become clear that its origins are not related to MHC.

Eleven such observations were identified, with wind directions ranging across 120° and reports from the west-northwest, northwest, north and north-northeast (see Fig. 3.4c). As with the "beginning" classification, no dominant wind direction signal is present, but reports are slightly skewed towards the northwest.

It should be noted that at no time during these case studies were winds observed from 90°–270°, going through 180°.

3.1.2 Pressure Differences During MHC Events

Calculations of SLP difference were made between several pairs of observation sites in order to examine the effects that pressure gradient has on MHC. Using the same

hourly ASOS observations employed to develop the wind climatology for ongoing MHC events (see section 3.1.1 for results, and Fig. 1.2 for locations of ASOS sites superimposed on terrain), SLP from KGFL and KPOU (KUCA and KPSF; later KSYR and KPSF) were differenced to determine the pressure gradient from north to south (west to east) across the domain. These pairs of stations were chosen because of the reliability of their reports, their location on the perimeter of the MHC domain, and their nearly-equal spacing (straight-line distance from KUCA to KPSF is 189 km; from KGFL to KPOU is 192 km; KSYR to KPSF is 242 km).

West-to-east SLP differences were plotted against north-to-south differences on X-Y (scatterplot) graphs, one for the case studies which utilize KUCA as the westernmost observation point and one for the case study which utilizes KSYR as the westernmost observation point. A description of these graphs follows, including an examination of SLP difference as a function of observation time relative to the onset of MHC.

3.1.2.1 Pressure Differences During MHC Events, Using KUCA

Figures 3.5a–d compare SLP differences for case studies spanning November 2002–March 2006, inclusive, with KUCA as the westernmost observation point. Irrespective of when the observation was taken, relative to the onset of MHC, Fig. 3.5a shows all north-to-south pressure differences were between 1 hPa and 5 hPa. Similarly, all west-to-east pressure differences were between 4 hPa and 7 hPa, irrespective of observational time. Furthermore, in nearly all cases the west-to-east pressure difference (and, it follows, the pressure gradient) is greater than that in the north-to-south direction;

however no calculable ratio of these two pressure differences (or gradients) exists as a threshold value for MHC formation.

In Fig. 3.5b only pressure-difference pairs observed at the "beginning" of MHC events are considered (for a definition of "beginning" as it relates to this research, see section 3.1.1.4.1). A linear regression (solid line) of west-to-east versus north-to-south pressure differences reveals no strong correlation. It is noted, however, that all north-to-south pressure differences were greater than 2 hPa.

Figure 3.5d shows only those pressure-difference pairs attributed to the "end" of MHC events. Again, a linear regression shows no strong correlation between west-to-east pressure differences and those from north-to-south. All but one pressure difference in the north-to-south direction, however, was below 2.5 hPa, suggesting that the pressure gradient along the Hudson valley tends to be higher at the "beginning" of MHC events, as compared to the "end." A comparable signal is not present in the west-to-east direction.

The worst-fitting linear regression between pressure-difference pairs appears during the "middle" of MHC events, as shown in Fig. 3.5c, where the actual values are distributed randomly.

3.1.2.2 Pressure Differences During MHC Events, Using KSYR

The cessation of hourly observations at KUCA required that KSYR be substituted as the westernmost observation point in the MHC domain for the January 2007 case study. The small sample size of the resulting SLP difference calculations prevents a meaningful pressure gradient analysis along the Mohawk valley; however, it is useful to

note that the north-to-south pressure differences fell within the 1 hPa to 4 hPa parameters developed from previous case studies (see Fig. 3.6).

3.2 Case Studies of MHC Events

In choosing which MHC events to include in this thesis, the overall goal was to select those containing precipitation that was generated entirely by flow channeling within the Mohawk and Hudson River valleys. Situations involving lake effects, upslope flows, and forcing due to the presence of strong synoptic systems were generally ignored, in the interest of researching only those events that were plainly attributable to MHC.

Precipitation produced by MHC generally follows a synoptic-scale storm and, in general, is insignificant in comparison, rarely warranting mention in storm reports or climate summaries. Additionally, a robust archive of historical radar data for the region does not exist prior to the Doppler era. Consequently, it is very difficult to identify historical occurrences of MHC through the perusal of existing data. Thus, a real-time evaluation of potential cases for study was employed for this thesis, but was limited to the period after 1 November 2002. Candidate case studies were initially identified through analysis of KENX radar images. The formation or persistence of "unexplained" radar echoes in the vicinity of KALB was an indicator to examine surface parameters; namely, to look for the presence of surface wind convergence. Events which met these basic criteria were subjected to an in-depth synoptic and mesoscale analysis.

There are, undoubtedly, drawbacks and limitations stemming from the way in which case studies were identified and selected. These include: 1) human error and lack of consistent, around-the-clock vigilance leading to missed MHC events; 2) the exclusion

of events in which the confluent surface wind signature produces no precipitation (so-called "null" cases); 3) the failure to examine all cases in which MHC leads to enhancement of preexisting precipitation, a process which is inherently difficult to identify on radar.

Ultimately six occurrences of MHC were chosen (see Table II), with a seventh added during the writing of this thesis. One of the cases (March 2006) is not a pure MHC event, complicated by a synoptic scale system which was affecting the region, but it was included nevertheless to highlight how MHC can act to enhance preexisting precipitation. Two of the final seven cases (November 2002 and January 2007) are designated as "benchmark" cases because of the strong and persistent MHC signal they reveal, and also because of the large impact they had on the general public. These cases are used as a point of reference by which to compare the remaining five cases.

3.2.1 The Benchmark Case of November 2002

This MHC event occurred on the day prior to Thanksgiving, often the busiest travel day of the year in the United States (U.S.), and provided the original impetus to study this phenomenon. A poor forecast, compounded by inopportune timing, combined to create a high-impact weather event out of very little snowfall.

A fast-moving, moisture-starved surface low pressure system ("Alberta Clipper") brought widespread light-to-moderate snowfall to eastern New York state and western New England during the overnight and pre-dawn hours (local time) of 27 November 2002. The snowfall associated with this low was universally expected by local forecasters to end during the early morning, as detailed in the public "zone" forecast for

the immediate Albany area, released at 0822 UTC on 27 November 2002 by the Albany forecast office of the NWS (KALY):

> "TODAY...SNOW LIKELY EARLY THIS MORNING...THEN CLOUDY WITH A CHANCE OF FLURRIES FROM LATE MORNING ON. NO ACCUMULATION."

A storm summary, written by meteorologists of local television station WRGB-TV (2008) and compiled using a mesoscale network of volunteer observers ("weather watchers"), indicates that approximately 2.5–10.0 cm of snow fell in most areas, due to the Clipper low, "only causing minor inconveniences to morning commuters."

Accumulating snow, however, continued to fall through the afternoon (local time) over a majority of the population centers of eastern New York, and forecast updates came too late for many travelers to adjust their plans accordingly. The NWS forecast was not updated to reflect the presence of a persistent, mesoscale area of MHC-induced precipitation until approximately 1800 UTC, as indicated in the area forecast discussion issued by KALY at 1805 UTC:

> "AN AREA OF LIGHT SNOW HOWERS/FLURRIES HAS FORMED ALONG THE MOHAWK/HUDSON CONVERGENCE ZONE WITH A MOSIT [sic] N/NNW FLOW. WL UPDATE ZONES AND FCST SNOW SHOWERS LIKELY IN THIS REGION WITH UP TO AN INCH OF SNOW POSSIBLE."

Additional snowfall totals from this MHC-induced precipitation ranged from 2.5 to 5.0 cm across the region, as recorded from the weather watchers of WRGB-TV (2008). It was this snowfall that generated scores of minor accidents on the roads of eastern New York, creating a harrowing pre-holiday period for both travelers and forecasters alike.

3.2.1.1 SYNOPTIC SUMMARY

The MHC event of November 2002 formed in the wake of a passing Alberta Clipper low, and Figs. 3.7a–d reveal the evolution of the resultant surface features, with high- (low-) pressure centers labeled by a blue "H" (red "L"). At 0600 UTC 27 November (time and date hereafter denoted as 0600/27) a broad area of high pressure extended from the southern shores of Hudson Bay into the midwestern U.S., and a broad area of low pressure was located from the Canadian Maritime provinces southward along and just off the U.S. East Coast (Fig. 3.7a). Also at that time a west-to-east zone of lower pressure ("inverted trough") extended from the Delmarva Peninsula to southeastern lower Michigan, while a zonally oriented ridge of high pressure ran from central Maine to north of Lake Huron. By 1200/27 (Fig. 3.7b), low pressure off the U.S. eastern seaboard had consolidated, deepening to a 1007-hPa low centered well south of Cape Cod, near 38°N, 71°W. The inverted trough extended northwestward from the low center towards southeastern lower Michigan, crossing northeastern Pennsylvania and into western New York. The high pressure ridge remained located near where it was at 0600/27, and a "reverse-S" shaped SLP pattern over New York and western New England is noted (Fig. 3.7b). As low pressure deepened to 999 hPa and moved northeastward to near 40°N, 65°W by 1800/27, the inverted trough and zonal ridge located over the northeastern U.S. were reflected more weakly compared to 1200/27 (Fig. 3.7c). The orientation of isobars was more meridional, but a slight "reverse-S" shaped curve is still noticeable (Fig. 3.7c). The low pressure system continued to deepen through 0000/28, with a 6-hPa decrease in central pressure in the preceding 6 h, as it accelerated to southeast of Nova Scotia, near 41.5°N, 60.5°W (Fig. 3.7d).

The 850-hPa analysis at 0600/27 (Fig. 3.8a) shows a trough of lower geopotential heights, oriented from northeast-to-southwest, from Maine to the Piedmont of North Carolina, with a cyclonic circulation evident and centered in the vicinity of central Pennsylvania. An attendant zone of enhanced baroclinicity was present, along with weak warm advection, over New York and southern New England. By 1200/27, CAA had begun over eastern New York and western New England though there was little-to-no change in temperatures over the region during the preceding six hours (Fig. 3.8b). The center of cyclonic circulation moved to eastern Long Island as the baroclinic zone and geopotential height trough sharpened, running from south of Nova Scotia to Virginia and North Carolina (Fig. 3.8b). Weak cold advection, driven by 15 m s^{-1} winds, continued over New York and New England, with temperatures falling approximately 3°C (to −12°C) over KALB during the 6 h ending 1800/27 (Fig. 3.8c). The trough and center of circulation continued to move offshore through 1800/27. At 0000/28 (Fig. 3.8d), winds had increased to 15 m s^{-1} in the vicinity of KALB as weak cold advection continued. Also at this time, a closed geopotential height contour had appeared around the center of circulation located southeast of Nova Scotia, which continued to move northeast.

As illustrated by relative humidity (RH) values, the atmosphere at 700 hPa was saturated (with respect to water) over eastern New York and western New England during 0600–1200/27 (Figs. 3.9a,b). At that time, a geopotential height trough was moving from western New York to eastern New York. Moderate ascent of approximately −4.0 to −7.0 μb s^{-1} was present over eastern New York and western New England at 0600/27, and a broad area of weak ascent (−2.0 to −4.0 μb s^{-1}), connected with the developing area of surface low pressure, was located off the mid-Atlantic coast

(Fig. 3.10a). Ascent over the ocean and over central and eastern New England increased to −10.0 to −12.0 μb s^{-1} by 1200/27, and was associated with the deepening surface low located south of Cape Cod (Fig. 3.10b). Also at that time, ascent was weakening over eastern New York and western New England. By 1800/27, as the 700-hPa trough moved east of the region, RH values fell to near 70% over extreme eastern New York and western New England, before falling below 70% at 0000/28 (Figs. 3.9c,d). From 1800/27 to 0000/28 (Figs. 3.10c,d), little or no ascent is diagnosed over eastern New York or western New England, but upward motion does increase dramatically well offshore. Some horizontal advection of cyclonic 700-hPa geostrophic relative vorticity by the 1000–500-hPa thermal wind exists over eastern New York and western New England during 0600–1200/27 (Figs. 3.11a,b), however this advection ends by 1800/27, replaced by neutral or anticyclonic advections from 1800/27 to 0000/28 (Figs. 3.11c, d). The advection of lower 1000–500-hPa thickness values by surface winds implies CAA in the lower and middle troposphere, beginning at 1200/27 and continuing through 0000/28.

At 0600/27 (Fig. 3.12a), a positively tilted 500-hPa geopotential height trough was located over the eastern Great Lakes and western New York, with eastern New York and western New England experiencing advection of cyclonic absolute vorticity (CVA). By 1200/27 (Fig. 3.12b), the trough axis has sharpened a bit and progressed to a line from Montreal, Quebec, to the southern tier (Binghamton area) of New York to southwest Pennsylvania, with advection of anticyclonic absolute vorticity (AVA) just beginning over eastern New York. This AVA continued through 1800/27 (Fig. 3.12c), and by 0000/28 little or no absolute vorticity advection was occurring over eastern New York or western New England (Fig. 3.12d). From 1800/27 to 0000/28, MHC-related precipitation

was occurring in the absence of CVA at 500 hPa. Geopotential heights at 500 hPa increased 2 dam between 1800/27 and 0000/28 over eastern New York and western New England, and a confluent wind signature was evident at that level as well at 0000/28 (Fig. 3.12d).

At 0600/27, the core of a 55 m s^{-1} wind maximum (jet streak) at 300 hPa ran from the Adirondack Park region of upstate New York across southeastern Quebec, placing eastern New York and western New England under rising air in its right-rear quadrant (Fig. 3.13a). This jet streak translated northeastward, to over the Canadian Maritime provinces, by 1200/27, placing eastern New York and western New England under sinking air in its left-rear quadrant (Fig 3.13b). The region remains under the sinking air associated with this jet streak until 0000/28, as a confluent wind signature develops over eastern New York and western New England (Figs. 3.13c,d).

The radar mosaics (NOWrad) for eastern New York and western New England at 0900/27 (Fig. 3.14a) and 1200/27 (Fig. 3.14b) show eastern New York and western New England on the northwestern fringe of a large precipitation shield which runs along the coast of New England southward to New Jersey. Scattered precipitation (snow) associated with lake moisture and lingering upper-air dynamics existed over western New York at these times. Synoptic-scale precipitation had ended across the region by 1500/27 (Fig. 3.14c). The first signs of a discrete area of scattered precipitation echoes appeared at 1800/27 and are highlighted with a red circle on Fig. 3.14d. This precipitation area expands over eastern New York and western New England by 2100/27 (Fig. 3.14e) before contracting by 2345/27 (Fig. 3.14f).

A higher-resolution view of the precipitation is provided by the East Berne, NY (KENX), Weather Surveillance Radar-1988 Doppler (WSR-88D). The departure of the synoptically forced precipitation, from northwest to southeast across eastern New York and western New England is shown on the KENX radar in Figs. 3.15a and 3.15b. By 1400/27 (Fig. 3.15c), only weak radar echoes were left over central Massachusetts and northwest Connecticut. A small area of precipitation (snow flurries) had developed about 45 km west of KALB, over north-central Schoharie county. By 1558/27 (Fig. 3.15d), this small area of precipitation had blossomed into a quasi-linear area of light snow, running approximately parallel to and just of the Hudson River valley. At 1803/27 (Fig. 3.15e), snow had increased both in coverage and intensity across eastern New York, with maximum base reflectivity (0.5° beam tilt) values of 25–28 dBZ centered just northwest of KALB, over Schenectady county. The area of moderate snow persists through 2001/27 (Fig. 3.15f), with some areas of spotty, lighter precipitation developing around it.

3.2.1.2 Mesoscale Summary

Inspection of WSR-88D radar imagery from KENX (see Fig. 3.15) shows that precipitation associated with MHC was near peak intensity and maximum areal coverage across eastern New York at 2001/27. This section will examine the mesoscale weather conditions present in the vicinity of KALB around this time.

Figure 3.16 is a manual surface analysis for eastern New York and much of New England, generated using the 2100/27 ASOS and marine weather reports, which shows a confluent surface wind signature in the vicinity of KALB. Winds KALB at that time

were light from the north-northwest; winds at KUCA were light from the northwest; and light north-northeast winds were reported at KGFL. At the same time, Fig. 3.16 shows northwest winds at a station approximately 60 km to the northeast of KALB (Rutland, Vermont; KRUT), and no other north-northeast wind reports in the region to match those at KGFL. Isobars reveal an inverted surface pressure trough across coastal New England and northeast Pennsylvania, as well as a zonally oriented ridge of high pressure across the Adirondack Mountains of upstate New York. The "reverse-S" isobar pattern seen in Figs. 3.7b,c, is also apparent in Fig. 3.16.

Surface meteograms show confluent surface winds between KUCA and KGFL from 1300 to 2100/27 (Figs. 3.17a,b) and between KUCA and KALB from 1700 to 2000/27 (Fig. 3.17a,c), coincident with reports of moderate snowfall at KALB from 1800 to 2100/27 (Fig. 3.17c).

During the period 1200/27–0000/28, Fig. 3.18 shows that SLP values were higher to the north and west of KALB. The difference in SLP was significantly greater from west-to-east across the region (as seen between KUCA and KPSF in Fig. 3.18) than from north-to-south (KGFL to KPOU) across approximately the same distance. At any given station, SLP values changed relatively little between 1200/27 and 0000/28, with the greatest change during this time period (approximately 3 hPa) occurring at KPOU.

The radiosonde sounding (in skew T–log p format) from Albany, NY (KALY), for 1200/27 (Fig. 3.19a) reveals a saturated layer between the surface and approximately 550 hPa. By 0000/28 (Fig. 3.19b), the top of the moist layer had subsided to approximately 850 hPa, and the height of the temperature inversion had decreased in a similar fashion.

A wind profiler located at Schenectady, NY (KSCH; approximately 15 km northwest of KALB), recorded wind direction and speed in a vertical profile, the data from which are presented with hourly resolution from 1200/27 to 0000/28 in Fig. 3.20. Wind speeds remained at 5 m s^{-1} or less from 950 hPa and below during the period 1300/27–0000/28. The profiler showed a backing wind signature with height, consistent with the horizontal advection of colder air over KSCH. By 2000/27, winds below 950 hPa had decoupled, shown in Fig. 3.20 as the wind direction discontinuity which occurs at approximately that pressure height. The lowest 50 hPa of the atmosphere remained isolated from the atmosphere above through 2100/27. Recoupling of the lower atmosphere to the remainder of the air column above occurred beginning at 2200/27, at which time near-surface northwesterly winds increased.

Zero-hour gridded, initialized data from the NARR were utilized to generate time series plots of horizontal temperature advection over KALB. Figure 3.21 shows CAA was occurring from the bottom to the top of the column at 1800 and 2100/27, and 0000/28. Temperature advection values from 850 hPa and below are modest, with a mean value around $-12°C \times 10^{-5}$ s^{-1}. Vertical velocity values over KALB (also derived from 0-h gridded NARR initializations), are presented in Fig. 3.22. Weak ascent is evident in the lower troposphere at 1800 and 2100/27, with maximum ascent values at 925 hPa of -1.5 μb s^{-1} and -1.0 μb s^{-1}, respectively. Downward motion in the remainder of the atmospheric profile increases both in magnitude and depth between 1800/27 and 0000/28, at which time no upward motion is diagnosed at all (Fig. 3.22).

An infrared image of the northeastern U.S. is presented in Fig. 3.23 from the Geostationary Operational Environmental Satellite-8 (GOES-8) satellite. At 1732/27, the

satellite shows CTTs of approximately −14°C located over KALB. This CTT corresponds to an approximate pressure level of 840 hPa, inferred from the KALY radiosonde soundings from 1200/27 and 0000/28 (see Fig. 3.19).

3.2.2 The Benchmark Case of January 2007

The MHC event of January 2007 began during the nighttime hours (local time) of 28 January 2007, and continued overnight and into the morning hours of 29 January 2007. Its societal impact (on morning drivers), unambiguous synoptic pattern, and its duration make it an ideal benchmark case. It is one of the longer-lived cases included in this thesis (see Table II for dates and times of all included case studies), despite associated snowfall totals that were very light, with only trace–2.5 cm amounts reported in the storm summary provided by WRGB-TV (2008). Nevertheless, this small amount of snow was able to create slippery spots on some roads in eastern New York, causing distress to morning travelers in this area.

3.2.2.1 SYNOPTIC SUMMARY

Precipitation resulting from MHC began as several areas of surface low pressure developed off the U.S. East Coast. Figure 3.24a reveals that an inverted low-pressure trough extended from the southern tier of New York westward to near Minneapolis, Minnesota, prior to the MHC event, at 1200/28. A weak zone of low pressure, as indicated by "baggy" isobars, hinted at the development of a surface low over the Piedmont region of North Carolina. A nearly uniform 1000–500 hPa thickness gradient also existed at that time from the southern shores of Hudson Bay in Canada to coastal

North Carolina. At 1800/28 (Fig. 3.24b), a single, closed isobar had formed around a 999-hPa low, centered several hundred kilometers southeast of Cape Hatteras, North Carolina. The isobars located over New York and New England were arranged in an revere-S shape at this time. Figure 3.24c shows the inverted trough of low pressure pivoting farther south by 0000/29, aligned from southeast Pennsylvania to southeastern lower Michigan, as the low-pressure center located offshore deepened to 993 hPa and moved to near 38°N, 67°W. By 0600/29, this low center had deepened to 988 hPa and was centered at 40°N, 63°W (Fig. 3.24d), the pressure trough located over Pennsylvania had drifted slightly northward at this time, and some weak pressure ridging was oriented along a west-to-east axis over northern New York. Light snow was also detected in the vicinity of KALB on the KENX radar beginning at 0601/29 (Fig. 3.32c), and this precipitation continued through 1203/29 (Fig. 3.32e). As the original ocean low deepened to 987 hPa and moved well southeast of Nova Scotia, a second ocean low, located at approximately 38°N, 67°W, deepened to 988 hPa by 1200/29 (Fig. 3.24e). Slight cyclonic curvature to isobars, which existed over southern New York, indicated that the weak inverted surface trough remained at this time. Weak high pressure had also developed over southern Ontario and Quebec provinces. The second ocean low deepened sharply to 980 hPa by 1800/29 and was centered at 40°N, 60.5°W (Fig. 3.24f). Surface isobars had become more meridional (i.e., "straightened out") over eastern New York and western New England at this time.

The 850-hPa analysis shows that very weak cooling due to CAA occurred over New York from 1200/28 to 0600/29, no more than 3°C during this period (Figs. 3.25a–d). A stronger thermal gradient was located over the Appalachian Mountains, and this

gradient moved slowly offshore during these times, along with areas of increasingly cyclonic circulation. From 0600 to 1200/29, CAA over eastern New York and western New England increased (a temperature change of 5°C over KALB during this period), presumably in response to two areas of offshore geopotential height falls (Figs. 3.25d,e). Winds over eastern New York and western New England, which had been light (around 5 m s^{-1} at previous times), increased to approximately 12.5 m s^{-1} between 0600 and 1200/29 as well (Figs. 3.25d,e).

Beginning at 1200/28 and continuing through 0600/29, weak cyclonic curvature in the 700-hPa geopotential height contours existed over eastern New York and western New England (Figs. 3.26a–d). Small geopotential height falls occurred with the passage of a trough axis from 0000 to 0600/29, with ensuing geopotential height rises from 1200 to 1800/29 (Figs. 3.26e,f). Concurrent with the passage of the height trough, RH values in excess of 70% occurred over eastern New York and western New England (Figs. 3.26c,d), but RH values were below 70% at the other times (3.26a,b,e,f). Model-diagnosed ascent values were −2.0 μb s^{-1} or less over eastern New York and western New England at every time shown in Fig. 3.26. Several areas of moderate to vigorous ascent developed over the western Atlantic Ocean, the first of which was evident south of coastal North Carolina at 1200/28 (Fig. 3.27a), and increased to −20.0 μb s^{-1} as it moved south of Newfoundland by 1200/29 (Figs. 3.28b–e). A second center of strong vertical motion developed from broad areas of weak ascent along the mid-Atlantic coast at 0000/29 (Fig. 3.27c), to an area of ascent greater than −28.0 μb s^{-1} by 1800/29 (Figs. 3.27d–f). This area of upward motion at 700 hPa was collocated with the intense surface low-pressure system centered near 40°N, 60.5°W at this time (Figs. 3.24f, 3.27f).

Horizontal advection of cyclonic 700-hPa geostrophic relative vorticity by the 1000–500-hPa thermal wind was either very weak or neutral during the period from 1200/28 to 0600/29 (Figs. 3.28a–d), with weak anticyclonic vorticity advection over far northern New York from 1200 to 1800/29 (Figs. 3.28e,f).

Neutral or slightly anticyclonic curvature in the 500-hPa geopotential height contours was present over eastern New York and western New England at 1200/28 and 1800/28 as a sharp trough dropped out of the Great Lakes and into the Ohio River valley (Figs. 3.29a–c). The trough dug to the mid-Atlantic seaboard and had acquired a slightly negative tilt by 0600/29 (Fig. 3.29d). At this time, weak CVA was occurring over eastern New York and western New England. By 1200/29 the northern end of the trough axis was situated over KALB, where weak AVA had begun; the southern extent of the trough axis had taken on a negative tilt, extending from the southern New Jersey shore to near 35°N, 70°W (Fig. 3.29e). The trough axis continued to pivot eastward through 1800/29, leaving eastern New York and western New England in northwesterly flow at 500 hPa and with little or no absolute vorticity advection (Fig. 3.29f).

Slight anticyclonic curvature in the 300-hPa geopotential height contours was evident over eastern New York and western New England from 1200 to 1800/28, and this area was also located under the left-rear quadrant of a 55 m s^{-1} jet streak (Figs. 3.30a,b). A 65–75 m s^{-1} jet streak developed over coastal North Carolina by 0000/29 but translated offshore well south of the northeast U.S. by 1200/29 (Figs. 3.29c–e). This configuration of the jet stream left the Northeast under a zone of relatively lighter winds (35–45 m s^{-1}) associated with the northern extent of the trough axis (Figs. 3.30d,e).

NOWrad radar images show that scattered light precipitation developed over eastern New York and western New England between 1800/28 and 0000/29 (Figs. 3.31a, b). This area of precipitation was detached from a larger area of synoptically forced precipitation, which affected the lower Hudson Valley and brushed coastal New England from 0600 to 1500/29 (Figs. 3.31c–e). The discrete area of precipitation over eastern New York and western New England was no longer evident at 1800/29, with lake-effect precipitation apparent in western and central New York (Fig. 3.31f).

The WSR-88D located at KENX showed the last of the synoptically forced precipitation (snow) departing eastern New York by 2300/28 (not shown). By 2359/28 an area of light snow had developed just north and northwest of KGFL (Fig. 3.32a). Through 0601/29 this area of light snow expanded in coverage, with some echoes to 10 dBZ shown in Figs. 3.32b,c. A flare-up of light-to-moderate snow was centered over KALB at 0857/29 (Fig. 3.32d), and precipitation continued, though diminishing in intensity through 1203/29 (Fig. 3.32e). Precipitation had ended in the region by 1500/29, at which time only ground clutter is present on the radar (Fig. 3.32f).

3.2.2.2 Mesoscale Summary

An inverted surface trough and accompanying baroclinic zone seen on the surface analysis for eastern New York and much of New England at 0600/29 (Fig. 3.33) reveals a cold front extending from an offshore low to along the New York–Pennsylvania border. Higher SLP was located across northern New York, oriented along a west-northwest to east-southeast ridge axis. Surface CAA was ongoing in New York and across New England, though surface winds in these areas were quite light, on the order of 2.5 m s^{-1}.

A weakly confluent wind signature was evident between KGFL, KALB (both with some easterly wind component) and KSYR (with a slightly westerly component).

Figure 3.34 contains surface meteograms for bellwether sites, with KSYR substituting for KUCA. The wind direction at KSYR is shown to vary throughout the time series (2000/28–1200/29), from west-northwesterly to more northerly, then back to west-northwesterly (Fig. 3.34a). Winds at KGFL (Fig. 3.34b) were very light during the entire event, with reported wind speeds under 2.5 m s^{-1} and six calm reports during the time series. The wind direction at KGFL was consistently northeast or easterly throughout the event. Several periods of strongly confluent winds occurred between KSYR and KGFL, including 2300/28–0100/29 and 0700–1000/29, with over 100° of difference in wind direction reported during these times (Figs. 3.34a,b). The wind direction at KALB (Fig. 3.34c) remains comparatively constant, from the north and north-northeast throughout the event.

Time series plots of SLP reveal higher values at KSYR compared to KALB and KPSF throughout the entire event (Fig. 3.35). Greater SLP was reported at KGFL than at KALB and KPOU during the event as well; however the relative SLP differences between these stations decreased with time (Fig. 3.35). From 0900 to 1400/29, SLP differences between KGFL and KALB approached zero, and the SLP difference between KGFL and KPOU dropped appreciably after 0700/29 (Fig. 3.35). The overall SLP change at any one station during the time period 0000–1200/29 is approximately 6 to 7 hPa (Fig. 3.35), which is approximately double that seen over the same period of time during the November 2002 case (Fig. 3.18). These greater SLP changes are consistent with the presence of a stronger upper-level storm during the January 2007 MHC event

(see 500-hPa analyses in Figs. 3.12a–d for November 2002; Figs. 3.29a–f for January 2007).

The radiosonde sounding from KALY at 1200/29 (Fig. 3.36) shows a moist layer from approximately 950–750 hPa, with a shallow inversion layer near 900 hPa. There is an indication that surface winds may have decoupled from the rest of the column at this time, as shown by the reported northerly wind at the lowest reported level (Fig. 3.36). Gently backing winds from the surface to approximately 600 hPa indicate a layer of weak CAA (Fig. 3.36).

The vertical profile of horizontal temperature advection over KALB at 0000, 0600, and 1200/29 (shown in Fig. 3.37 and generated using 0-hour gridded, initialized data from the NARR) shows CAA at all times and for all levels below 500 hPa. Advection values below 850 hPa were modest, averaging approximately $-12°C \times 10^{-5}\ s^{-1}$. Vertical motions over KALB (shown in Fig. 3.38 and generated with the same model data used to compute the temperature advection values) were small (approximately +/− 2.0 μb s^{-1}) from the top to the bottom of the column at 0000, 0600, and 1200/29. Weak upward motion below 500 hPa at 0000/29 increased slightly by 0600/29, with a maximum upward motion of −2.0 μb s^{-1} shown in Fig. 3.38 between the surface and approximately 900 hPa. By 1200/29, downward vertical motion is shown at all levels above approximately 900 hPa, with weak upward motion (on the order of −0.3 μb s^{-1}) shown from 900 hPa to the surface.

An infrared image of the northeastern U.S. at 0845/29 is presented in Fig. 3.39 from the Geostationary Operational Environmental Satellite-12 (GOES-12) satellite. Shown are CTTs in the vicinity of KALB of approximately −20°C, which correspond to

an approximate pressure level of 775 hPa, inferred from the 1200/29 radiosonde sounding (see Fig. 3.36).

3.2.3 December 2002 Case Study

This MHC event occurred following the passage of an Alberta Clipper. Accumulating snowfall associated with this Alberta Clipper ended in most areas by mid morning (local time) on 16 December 2002. Patchy areas of light snow due to MHC effects continued in a localized area, however, into the early nighttime hours. Snowfall totals were light overall, with 7.1 cm of snow falling at KALB on 16 December (WRGB-TV, 2008).

3.2.3.1 SYNOPTIC SUMMARY

Radar imagery from the WSR-88D located at KENX are shown in Figs. 3.40a–f. At 1803/16 an expansive area of light and moderate snowfall covered eastern New York and western New England (Fig. 3.40a). The precipitation diminished in both coverage and intensity by 2101/16 and 2358/16, with two distinct areas of snow visible at these times: one over KALB and vicinity and the other over the Catskill Mountains (Figs. 3.40b,c). At 0302/17, as precipitation ended over the Catskills, a discrete area of light precipitation was seen over KALB and vicinity (Fig. 3.40d). Maximum reflectivity values at this time were approximately 13 dBZ. Through 0603/17 this area of precipitation diminished in intensity, ending by 0900/17 (Figs. 3.40e,f).

At the surface, Fig. 3.41a shows that a strong area of low pressure (979 hPa central pressure) was located over Newfoundland at 0000/16, while a weaker low

(1004 hPa central pressure) was located over western Lake Ontario. High pressure centered over southern Hudson Bay at this time changed very little in position and intensity during the following 24 h (Figs. 3.41a–e). As the low over Newfoundland slowly weakened, a low over western New York intensified and moved to southeast of Cape Cod by 1800/16 (Figs. 3.41b–d). Figure 3.41d shows a "reverse-S" pattern to the surface isobars over eastern New York and western New England at 1800/16. The area of low pressure centered southeast of Cape Cod at 1800/16 had tracked over 40°N, 70°W (a benchmark point commonly used for forecasting the track of Nor'easter-type storms), deepening 3 hPa in the preceding 6 h. The low center tracked due east and continued to intensify to a minimum central pressure of 987 hPa by 0600/17 (Figs. 3.41e,f). Increasing surface baroclinicity was associated with this storm as it tracked out of western New York and over the eastern Atlantic Ocean, with a well-developed frontal structure evident by 0000/17 (Fig. 3.41a–e).

At 700 hPa, diffuse, weak model-diagnosed ascent was located over the northeastern U.S. from 0000 to 0600/16 (Figs. 3.42a,b). A stronger and more coherent center of ascent (-6.0 μb s^{-1}) developed over western Massachusetts by 1200/16 as the surface low center moved offshore (Fig. 3.42c). Ascent increased to -16.0 μb s^{-1} in the following 18 h as the surface low deepened and moved southeast of Nova Scotia (Figs. 3.42d–f). During this time, no significant vertical motions were present over eastern New York or over western New England.

Figures 3.43a,b show that eastern New York and western New England were located under an area of diffluent 300-hPa winds from 0000 to 0600/16. This region was also located under the left-front quadrant of a 65 m s^{-1} jet streak at that time, a region

supportive of ascent, as a closed 300-hPa low crossed New York and Pennsylvania at that time. By 1800/16 and continuing through 0600/17, a strongly confluent wind conjunction had moved to a position over eastern New York and western New England (Figs. 3.43c–f). At both 0000 and 0600/17, this region was also under the left-rear quadrant of a weakening 65 m s^{-1} jet streak, a region associated with sinking air (Figs. 3.43e,f).

3.2.3.2 MESOSCALE SUMMARY

A regional view of surface weather features in eastern New York and western New England at 0300/17 is presented in Fig. 3.44 (with missing station data for winds, sky cover, and SLP, all of which were also unavailable for surrounding times). At 0300/17, an inverted surface pressure trough ran from central Connecticut west-northwest to the Catskill Mountains, with a zone of higher pressure located across northern New York.

Surface meteograms show a strongly confluent wind signature between KUCA and KGFL at 2000 and 2100/16 (Figs. 3.45a,b). Several hourly surface wind observations are missing from the KGFL data set from 0100 to 0600/17, making wind signatures difficult to analyze during the aforementioned time period.

An analysis of SLP, presented in Fig. 3.46, shows that the SLP at KUCA was greater than that at KALB and KPSF through the entire period from 1800/16 to 0800/17. Pressures at KGFL were greater than those at KPOU and at KALB during this period as well; however the pressure differences between KALB and KGFL were negligible (less than 1 hPa).

Atmospheric soundings from KALB at 1200/16 and 0000/17 (Figs. 3.47a,b) were generated using GFS-based 0-hour, gridded analysis data, to compensate for missing radiosonde data. A deep saturated layer is seen at 1200/16 from the surface to nearly 500 hPa, with near-moist moist adiabatic lapse rates present from 750 hPa to the surface (Fig. 3.47a). Backing winds present from the surface to approximately 550 hPa indicate CAA was occurring (Fig. 3.47a). By 0000/17, a shallow mixed layer was present from the surface to approximately 900 hPa (Fig. 3.47b) with an isothermal layer present above that level. The moist layer had become shallower, but still extended from the surface to approximately 700 hPa.

Infrared satellite imagery from GOES-8 (Fig. 3.48) at 2345/16 showed the impressive "comma-head" cloud structure associated with the developing low pressure system southeast of Cape Cod, and the lingering low clouds left in its wake over the northeastern U.S. The satellite-diagnosed CTT of approximately −18°C corresponds to a pressure level of 650 hPa, as inferred from the 0000/17 sounding (see Fig. 3.48b).

3.2.4 January 2003 Case Study

Several of the synoptic features that were present in eastern New York and western New England during the MHC event of 23–24 January 2003 are unique among the case studies included in this thesis; namely, the presence of weak WAA driven by northerly winds at 850 hPa, a corresponding surface trough that moved from north-to-south across the region, and an accompanying area of initially light precipitation that increased in areal coverage and intensity as it passed through the MHC domain. Thus, while synoptic-scale forcing was provided by the WAA at 850 hPa and the surface

trough, the January 2003 event is useful in examining how MHC effects might act to enhance preexisting precipitation.

3.2.4.1 Synoptic Summary

Radar imagery from the KENX WSR-88D at 1600/23 showed scattered weak precipitation (snow) echoes from KGFL extending north and west over the southern Adirondacks and upper Hudson valley (Fig. 3.49a). The echoes translated south-southeastward through 1958/23, increasing in coverage and intensity (Figs. 3.49b,c). By 2202/23 (Fig. 3.49d), a large area of enhanced echoes was present from the Hudson Valley in the vicinity of KALB on westward. Maximum reflectivity values of approximately 25 dBZ were detected at this time. Precipitation ended quickly thereafter, with no echoes were present near KALB at 0004/24, and only isolated weak echoes seen well south of KALB at 0159/24 (Figs. 3.49e,f). The total snowfall amount at KALB for this event was 2.0 cm, with up to 2.5 cm of snow reported by the weather watchers of WRGB-TV (2008).

At the surface, an inverted trough was apparent at 1200/23 from central Massachusetts westward to southeastern lower Michigan (Fig. 3.50a). A low-pressure center was also present at this time well off of the South Carolina coast, in an area of strong baroclinicity (Fig. 3.50a). As this surface low advanced northeastward away from the South Carolina coast and deepened to 991 hPa by 1800/23 (Fig. 3.50b), the surface features over the northeastern U.S. remained unchanged from 6 h earlier. A “reverse-S” isobar pattern (Fig. 3.50b) revealed a ridge axis oriented from west-northwest to east-southeast over northern New York, and an inverted surface trough over the southern tier

of the state. Close inspection of surface winds (see Figs. 3.54a–d) and the 1000–500-hPa thickness (see Figs. 3.50a–d) suggests that the surface trough is in response to weak WAA occurring from the north, as a core of exceptionally cold air (diagnosed by 1000–500-hPa thickness values below 500 dam) moves away from the region. Six-hourly analyses of 850-hPa wind and temperature (not shown) indicate that WAA is occurring at 850 hPa over eastern New York and western New England from 1200/23 to 0600/24, with warmer air (initially located poleward of KALB) being transported equatorward over KALB. Compared to 1200/23, surface features over the northeastern U.S. remained essentially unchanged from 1800/23 to 0600/24, as the low pressure center off the East Coast passed well south and east of 40°N, 70°W (Figs. 3.50b–d). This low reached a minimum central pressure of 970 hPa at 0600/24, representing a decrease in central pressure of 21 hPa in the preceding 12 h.

As the surface low deepened explosively over the Gulf Stream region of the western Atlantic Ocean, vertical motions at 700 hPa were quite vigorous. At 1200/23, the maximum ascent value associated with the surface low was −20.0 μb s^{-1}; by 0600/24, −40.0 μb s^{-1} of ascent is shown (Figs. 3.51a,d). These ascent maxima remain well off-shore throughout the MHC event, however, and have no direct impact over eastern New York or western New England. Weak upward motion (−2.0 μb s^{-1}) was seen over parts of New York and western New England at 1200 and 1800/23 (Figs. 3.51a,b). No ascent is shown at 0000 or 0600/24 (Figs. 3.51c,d) over eastern New York and western New England.

A cyclonic shear zone at 300 hPa was located over eastern New York and western New England at 1200 and 1800/23, and the region was also under the influence of the

left-rear quadrant of a 55 m s^{-1} jet streak (Figs. 3.52a,b). As this jet streak moved away from the region, winds at 300 hPa became slightly more confluent by 0000 and 0600/24 (Figs. 3.52c,d).

3.2.4.2 Mesoscale Summary

In the regional surface analysis shown in Fig. 3.53, an inverted surface trough is evident at 2100/23, running from the southern New England coast west-northwestward into central New York. Higher SLP was located over northern New York, shown as a pressure ridge oriented from west-to-east across the eastern shores of Lake Ontario and into the Adirondacks. Surface CAA is apparent across eastern New York and western New England. A strongly confluent wind signature is seen between KGFL (with an east-northeast wind) and KUCA and KALB (both with northwest winds). The confluence between KUCA and KGFL is also evident from 1800/23 to 0100/24 on the surface meteograms presented in Figs. 3.54a,b. The difference in wind direction between the two stations is as much as 180° during this period.

A meteogram analysis of SLP, shown in Fig. 3.55, indicates higher pressures from 1500/23 to 0600/24 at KUCA as compared to KALB and KPSF. Also, SLP was greater at KGFL than at KALB and KPOU during the MHC event, however the relative difference between KGFL and KALB was quite small (less than 1 hPa) at times. The meteogram reveals decreasing SLP values at all stations prior to 1900/23, and rising SLP values at all stations thereafter. The passage of a surface trough likely occurred at all stations around 1900/23, several hours prior to the appearance on radar of the most intense precipitation echoes (shown in Figs. 3.49c,d).

The radiosonde sounding from KALB at 1200/23 (Fig. 3.56a) showed a moist layer from 850 to 750 hPa. At that time, the mixed layer was shallow, extending only up to approximately 950 hPa, with an isothermal layer present between approximately 950 and 750 hPa. By 0000/24 (Fig. 3.56b), the depth of the moist layer had increased, with moisture present from the surface to approximately 500 hPa. A strong temperature inversion was present at this time from 850 to 750 hPa. A veering wind signature indicated WAA in the column above KALB between approximately 925 and 700 hPa (Fig. 3.56b), consistent with WAA from the north implied by 1000–500 hPa-thickness pattern at 0000/24 shown in Fig. 3.50c.

The exceptionally high and cold cloud tops associated with the deep ocean low, and shown by the GOES-8 satellite image in Fig. 3.57, had reached no farther west than coastal New England at 2045/23. Satellite-derived CTTs over eastern New York and western New England were approximately −22°C at this time, which correspond to lower clouds with tops around 675 hPa, as inferred from the radiosonde sounding over KALB at 0000/24 (Fig. 3.56b).

3.2.5 January 2005 Case Study

3.2.5.1 SYNOPTIC SUMMARY

At 1003 UTC 17 January 2005, a large area of light precipitation covered much of eastern New York and western New England, as shown on the KENX radar in Fig. 3.58a. The precipitation diminished in coverage through 1359/17 (Figs. 3.58b,c), at which time a small area of light precipitation (maximum reflectivities of approximately 15 dB*Z*) was located over and just south of KALB. This area of precipitation remained quasi-

stationary but varied in coverage and intensity through 2001/17, with reflectivities as low as 5 dBZ and as high as 25 dBZ (Figs. 3.58d–f). Total snowfall at KALB on 17 January 2005 was 8.6 cm (WRGB-TV 2008). Weather-watcher reports indicated that areas immediately surrounding KALB in the zone of MHC received 7.6–12.7 cm of snow that day; areas outside of the MHC zone received only a trace–7.6 cm of snow (WRGB-TV 2008). Subtracting the highest weather-watcher snowfall total measured outside of the MHC zone (7.6 cm) from the highest weather-watcher snowfall total measured within the MHC zone (12.7 cm) produces a difference of 5.1 cm. Thus, up to an additional 5.1 cm of snow may have fallen on 17 January 2005 as a direct result of MHC effects.

At the surface, from 0000 to 1200/17 (Figs. 3.59a–c), a quasi-stationary area of high pressure remained over south-central Quebec province. A 1006-hPa low, centered several hundred kilometers due east of Cape Hatteras, North Carolina at 0000/17 (Fig. 3.59a), deepened to 994 hPa and moved northeastward toward Nova Scotia through 1200/17 (Figs. 3.59b,c). This storm passed southeast of the 40°N, 70°W benchmark used in forecasting East Coast snowstorms. Cyclonically curved isobars were present over eastern New York and western New England from 0000 to 1200/17, as seen in Figs. 3.59a–c. An inverted trough was present within this region of cyclonic curvature, and moved from central Pennsylvania and the mid-Atlantic coast at 0000/17 (Fig. 3.59a) to near the Mohawk Valley at 1200/17 (Fig. 3.59c).

At 700 hPa, the storm had a well-defined area of upward vertical motion throughout the period 0000–1200/17 (Figs. 3.60a–c). This area of upward vertical motion was located well offshore, and ascent over eastern New York and western New England was weak (less than -2.0 μb s^{-1}) during the period.

At 0000/17 a 300-hPa jet streak was located over southern Vermont, as seen in Fig. 3.61a. By 0600 and 1200/17, the jet streak had translated away from this area, putting eastern New York and western New England under confluent flow and the left-rear quadrant of the departing jet streak, an area frequently associated with sinking air (Figs. 3.61b,c).

3.2.5.2 MESOSCALE SUMMARY

Examination of surface features across the MHC domain at 1200/17 reveals a familiar configuration (Fig. 3.62). An inverted surface trough ran from coastal New England to the southern tier of New York, with higher pressure and a weak ridge oriented along a west-northwest to east-southeast axis across northern New York. Weak CAA was present at the surface in eastern New York and New England. The wind directions at KGFL and KALB (both with northeast winds) and KUCA (west-northwest winds) at 1200/17 oppose each other at an approximate angle of 110°, indicating strongly confluent flow (Fig. 3.62). Surface meteograms suggest that this strongly confluent wind signature existed between KUCA and KGFL throughout the entire period, from 1000 to 1800/17 (Figs. 3.63a,b). During this period, 100° or more of difference in surface wind direction existed between KUCA and KGFL.

Throughout the event, SLP at KUCA remained higher than at KALB and KPSF, as seen in Fig. 3.64. SLP was also higher at KGFL than at KALB and KPOU, but the relative difference in the former was negligible at times (Fig. 3.64). Overall, the change in SLP at any one station throughout the period was small, on the order of 2 hPa.

A deep moist layer, which extended from the surface to 500 hPa, was shown on the radiosonde sounding from KALY at 1200/17 (Fig. 3.65a). Cold advection was also made evident by a backing wind profile at this time, and was maximized from 800 to 600 hPa. By 0000/18 a unidirectional wind profile from the surface to approximately 650 hPa indicated that CAA had ended, and the stability of the 700–600 hPa layer had increased (Fig. 3.65b). The sounding at this time also indicated that the atmosphere was unsaturated throughout its entire depth.

Satellite-estimated CTTs over eastern New York and western New England (shown in Fig. 3.66) are approximately −28°C at 1145/17. As inferred from the 1200/17 radiosonde sounding (Fig. 3.65a), this value corresponds to cloud tops at approximately 600 hPa.

3.2.6 March 2006 Case Study

An area of surface low pressure passed to the south of New York and New England during the daytime hours (local time) of 2 March 2006, bringing synoptic-scale snowfall to parts of the MHC domain. Accumulating snowfall was reported in areas equatorward of a line which ran through the Mohawk Valley, to KALB, to the border between Vermont and Massachusetts (WRGB-TV, 2008). Approximately 7.6–22.9 cm of snow fell south of that line, as reported by the volunteer weather watchers of WRGB-TV (2008). Precipitation related to MHC developed following the end of this synoptic-level snowfall across eastern New York and western New England into the nighttime hours of 2 March 2006 (local time; 3 March 2006, UTC).

3.2.6.1 SYNOPTIC SUMMARY

The departure of synoptic-scale snowfall from north-to-south across the MHC domain is seen at 0000 and 0202/03 in Figs. 3.67a,b. At 0359/03, a sizeable area of moderate and locally heavy snowfall had developed in the vicinity of KALB, with maximum reflectivity values approaching 25 dBZ (Fig. 3.67c). This snowfall maintained its intensity through 0601/03 (Fig. 3.67d), but decreased in coverage. Snowfall appeared to end completely over the region by 0757/03 (Fig. 3.67e) only to reappear, at a much-diminished intensity, briefly at 0901/03 (Fig. 3.67f).

A surface low (central pressure: 996 hPa) was present at 0000/03 on a baroclinic zone centered over the western Atlantic Ocean, southeast of 40°N, 70°W (Fig. 3.68a). The storm intensified and moved rapidly toward the east-northeast, and began to merge with another low centered over Newfoundland by 1200/03 (Figs. 3.68b,c). The SLP pattern over eastern New York and western New England exhibited an inverted surface trough that ran from central Rhode Island northwestward to approximately KALB at 0000/03 (Fig. 3.68a). This trough pivoted south of KALB by 0600/03, ending up along a line from the southern New England coast to western New York by 1200/03 (Figs. 3.68b,c). Decreasing 1000-500 hPa thickness values were observed across eastern New York and western New England between 0000 and 1200/03, suggesting that CAA was occurring over the region (Figs. 3.68a–c).

Upward vertical motion at 700 hPa (associated with the aforementioned surface low located over the eastern Atlantic Ocean) increased from a maximum of −12.0 μb s^{-1} at 0000/03 to −16.0 μb s^{-1} by 1200/03 (Figs. 3.69a–c). This upward motion remained largely offshore at 0000/03 and completely offshore thereafter. Weak ascent was

diagnosed over eastern New York and western New England at 0000/03 (−2.0 μb s^{-1}), with little or no ascent evident after that time (Figs. 3.69a–c). At 300 hPa, a coupled jet structure existed south and east of KALB at 0000/03 (Fig. 3.70a), with weakly confluent flow over KALB from 0000 to 1200/03 (Figs. 3.70a–c).

3.2.6.2 MESOSCALE SUMMARY

A close inspection of surface weather features over eastern New York and western New England at 0300/03 (Fig. 3.71) shows a "reverse-S" isobar pattern over the region, with a ridge of high pressure oriented along a west-northwest to east-southeast axis over northern New York, and an inverted trough located along the border between New York and Pennsylvania. A strongly confluent wind signature existed at 0300/03 between KGFL and KALB (both with northeast winds) and KUCA (with a northwest wind). Some of the strongest surface winds during any MHC case study were recorded at this time at KGFL, which was experiencing wind speeds of 7.5 m s^{-1}.

The confluent wind signature between KGFL and KUCA is evident on surface meteograms (Figs. 3.72a,b) during the period 0000–0700/03. Winds at KALB gradually shifted from northeast to northwest from 0200 to 1000/03 (Fig. 3.72c). Interestingly, calm winds were reported at KPOU for 9 h during the 12 h period ending 1200/03 (Fig. 3.72d). An analysis of SLP at these stations (Fig. 3.73) shows higher pressures at KUCA than at KALB and KSPF throughout the period from 0000 to 1200/03. Likewise, SLP was higher at KGFL than at KPOU during the period, with less than 1 hPa of pressure difference between KGFL and KALB after 0400/03.

The radiosonde sounding from KALY at 0000/03 (Fig. 3.74a) showed the top of the mixed layer was at approximately 780 hPa, with an inversion/isothermal layer between 780 and 625 hPa. By 1200/03 (Fig. 3.74b), the top of the mixed layer had fallen to approximately 950 hPa, with a strong inversion present between approximately 850 and 800 hPa. A deep moist layer was present at both 0000/03 and 1200/03 (Figs. 3.74a,b). Infrared satellite estimates of CTTs over eastern New York, made by GOES-12, were near −20°C at 0401/03 (Fig. 3.75). Such temperatures corresponded to approximately 575 hPa, as inferred from the KALY radiosonde soundings presented in Figs. 3.74a,b.

3.2.7 January 2008 Case Study

The 2 January 2008 MHC event began as an area of surface low pressure deepened in the Gulf of Maine, a low that earlier had brought brief periods of locally heavy snow to eastern New York and western New England. The MHC event that ensued was remarkable in both duration and intensity. Snowfall associated with MHC began in the region around 0600 UTC and continued until approximately 1800 UTC on 2 January 2008. Snowfall amounts which were attributed to MHC-induced precipitation varied widely (not shown) with 0.8 cm reported officially at KALB, and WRGB-TV (2008) weather watcher reports of 2.5–9.4 cm in various parts of Clifton Park, NY (located approximately 10 km north of KALB), to as much as 12.7 cm in North Colonie, NY (located approximately 3 km east of KALB).

While a detailed analysis of the January 2008 MHC event is not included in this thesis, this event would make an excellent benchmark case for further study. A cursory

examination of the key synoptic (mesoscale) weather features which contributed to the January 2008 MHC event follows in section 3.2.7.1 (3.2.7.2); pressure and wind data from this case are not included in the aggregate analyses discussed in section 3.1.

3.2.7.1 Synoptic Summary

Several discrete areas of moderate-to-heavy snow were evident on the KENX WSR-88D radar at 0757/02 (Fig. 3.76a), indicating the early stages of MHC. By 1004/02, only one large area of moderate-to-heavy (reflectivities up to 25 dBZ) snow remained (Fig. 3.76b). This area of snow consolidated between 1004 and 1357/02 (Figs. 3.76c,d), with maximum reflectivities up to 30 dBZ at 1357/02. From 1604 to 1801/02, precipitation continued in the same general area, however its coverage and intensity lessened (Figs. 3.76e,f).

At the surface at 0600/02 (Fig. 3.77a), a 992-hPa low was moving into the Bay of Fundy, and this low had passed slightly west (i.e., "inside") of 40°N, 70°W. At this time, an inverted trough ran from the low center west-southwestward to near KPOU, and then west across the southern tier of New York and over Lake Erie (Fig. 3.77a). Weak high pressure also lay across central Quebec. At 1200/02 (Fig. 3.77b), the storm had intensified to 989 hPa as it neared Prince Edward Island. The inverted trough had moved slightly southward by 1200/02, and was oriented in a "U"–shape from coastal Massachusetts, to southeastern Pennsylvania, to the shores of Lake Erie in northeast Ohio (Fig. 3.77b). At 1800/02 the surface low had intensified further, to 983 hPa, and had moved to near Newfoundland (Fig. 3.77c). The surface trough is shown at this time (Fig. 3.77c) off the southern New England coast and across southern Pennsylvania.

Surface features and ascent at 700 hPa are shown in Figs. 3.78a–c. Strong ascent (in excess of −16.0 μb s^{-1}) is seen on the north and east sides of the surface low, far from eastern New York and western New England, at 0600 and 1200/02 (Figs. 3.78a,b). Weaker ascent (approximately −2.0 μb s^{-1} or less) was diagnosed with the surface trough, located well south of the eastern New York/western New England region, from 0600 to 1800/02, with little or no ascent seen in the vicinity of KALB (Figs. 3.78a–c).

A core of 75 m s^{-1} winds at 300 hPa was located just southeast of eastern New York and western New England at 0600/02, as shown in Fig. 3.79a. As this core of maximum winds shifted southeastward, an area of confluent winds developed over KALB, seen at 1200 and 1800/02 (Figs. 3.79b,c).

3.2.7.2 Mesoscale Summary

By 2 January 2008, the ASOS at KRME was fully operational as the designated replacement for the ASOS at KUCA. Observations of SLP taken at KRME, however, were widely deemed unreliable by forecasters at this time. Indeed, SLP reductions reported at KRME (Fig. 3.80a) on 2 January 2008 show an approximate 5-hPa bias towards higher pressures than those reported at KSYR (Fig. 3.81a). The SLP reductions at KRME are outliers compared to surrounding stations and are not supported by the overall synoptic pattern. Thus, the wind analyses that follow were conducted using wind data from KRME; however pressure analyses were conducted using SLP data from KSYR.

A confluent wind signature is shown between KRME (Fig. 3.80a) and KGFL (Fig. 3.80b) throughout the MHC event, with the strongest confluence occurring around

1600/02. Surface winds are, overall, stronger in this case than in any other case study. Wind speeds at KRME and KALB consistently range between 5 and 7.5 m s^{-1}, while winds at KGFL are 5 m s^{-1} or less. The highest SLP was located on the western side of the domain during this MHC event, with higher SLP reported at KSYR than at KALB and KPSF from 0600 to 2300/02 (Fig. 3.82). Likewise, higher SLP was located on the northern side of the domain, with SLP at KGFL higher than that at KALB and KPOU from 0700 to 2300/02 (Fig. 3.82). SLP change at any one station from 0800 to 2000/02 is over 10 hPa, with over 20 hPa of change at KALB and KGFL, the largest increase in SLP of any case study.

The radiosonde sounding from KALY at 1200/02 (Fig. 3.83) shows a moist layer between the surface and approximately 750 hPa. A shallow mixed layer extends from the surface to approximately 950 hPa, with an isothermal layer above, to near 700 hPa.

3.3 Summary of Case Studies

Presented in Table V is a summary of the important synoptic and mesoscale parameters at the time of peak precipitation coverage and intensity for each of the six original MHC case studies. As shown in this table, weak CAA (values between −7.0 and -17.9×10^{-5} °C s^{-1}) was present at 925 hPa at the peak of all case studies. Similarly, weak CAA (values between −7.1 and -20.7×10^{-5} °C s^{-1}) were observed at 850 hPa in all but one case. This one exception occurred on 23 January 2003 as a warm front at 850 hPa moved from north-to-south across eastern New York and western New England, bringing WAA and an 850-hPa temperature advection value of 52.2×10^{-5} °C s^{-1} at 2100 UTC. CAA was also observed at 700 hPa in four of the six cases presented in Table V,

except for the January 2003 case (involving the passage of a warm front at 850 hPa) and a near-zero temperature advection value at 0000 UTC 17 December 2002. Advection of geostrophic absolute vorticity at 500 hPa and advection of 700-hPa geostrophic relative vorticity by the thermal wind were weak during the six case studies.

Ascent was maximized in five of the six case studies at 925 hPa, although ascent values were still very weak, between 0.0 and −2.2 μb s^{-1}. A maximum ascent value of −4.0 μb s^{-1} occurred at 700 hPa in the January 2003 case, consistent with the midlevel WAA present during that storm.

Radiosonde soundings show a moist PBL is present during MHC events, with the top of the moist layer located from 825–500 hPa during all cases. Infrared satellite imagery confirms the presence of low-topped clouds, with inferred pressure heights at approximately 840–600 hPa. Despite the moist atmosphere, PWAT values of 3.8–7.1 mm were present, representing 60–90% of the climatological normal values during each case. Regarding convection, the lower troposphere is statically stable during each case with mixed-layer convective available potential energy (MLCAPE) and most-unstable convective available potential energy (MUCAPE) values of zero. Likewise, lifted index (and most-unstable lifted index; MULI) values ranged from +4 to +26°C, well above zero and well within the stable categorization. Surface–2 km shear values were small as well, ranging from 3–10 m s^{-1}.

Subsequent to the completion of the writing of this thesis, an MHC event that occurred from approximately 2300 UTC March 28 to 0600 UTC 29 March 2008 generated 1.5 cm of snowfall at KALB (WRGB-TV 2008). Slippery travel persisted in the vicinity of KALB overnight, and lasted through the early morning hours (local time)

of 29 March 2008. The light snow generated by MHC in this event extended the impacts, in a localized area, of a synoptic-scale storm that had concluded nearly 12 h earlier. While further details of the March 2008 MHC event are not included in this thesis, the evolution of this event is in agreement with the benchmark cases of November 2002 and January 2007 (see sections 3.2.1 and 3.2.2). A detailed study of the March 2008 MHC is suggested for future research.

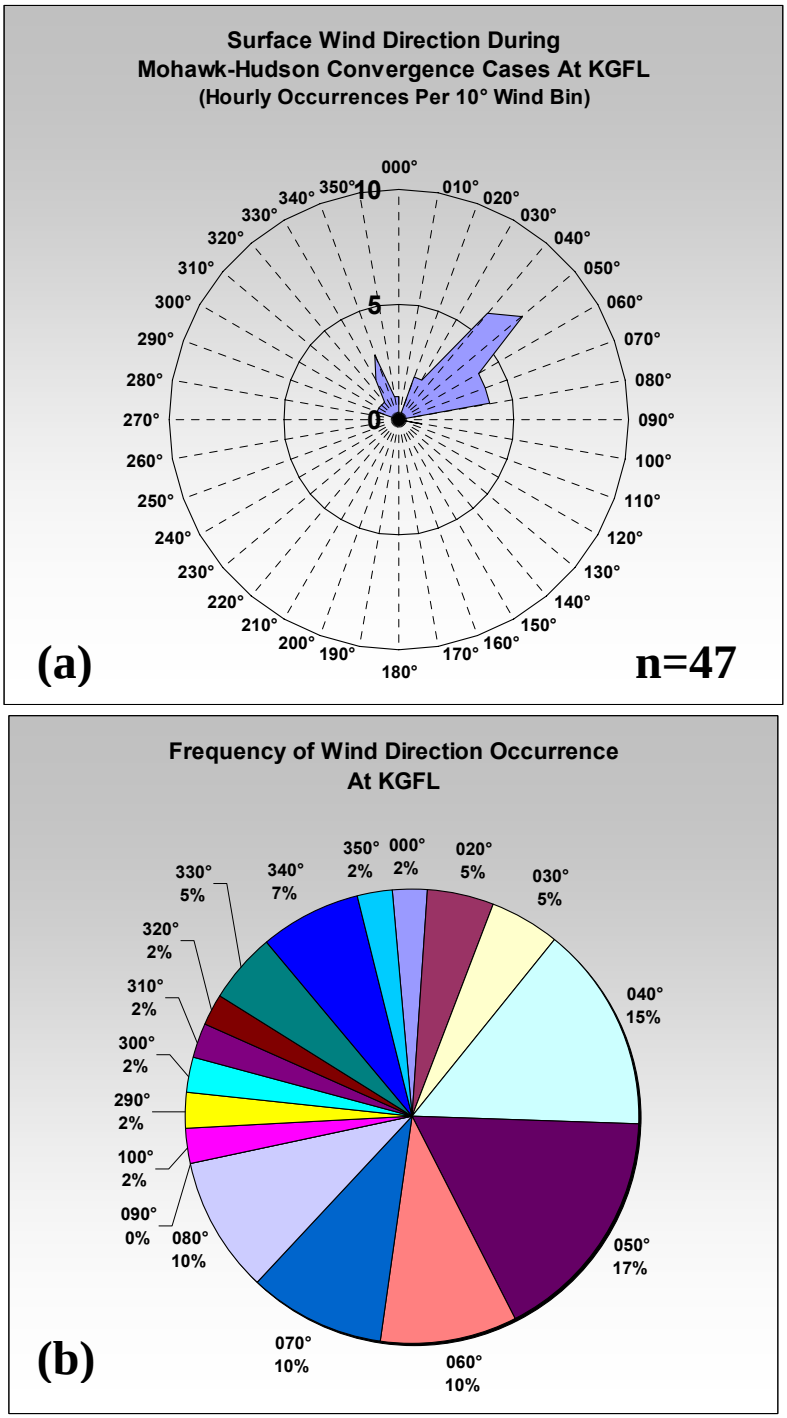

Figure 3.1: (a) Surface wind rose for KGFL during ongoing MHC events studied from November 2002 to January 2007, inclusive. Azimuthal axis represents wind direction in degrees, and radial axis represents number of hourly occurrences. (b) Frequency (in percent) with which each wind direction occurred at KGFL during the aforementioned case studies. Data source: University at Albany archive; supplemental data from the Historical Weather Data Archives of the National Severe Storms Laboratory (NSSL) in Norman, Oklahoma.

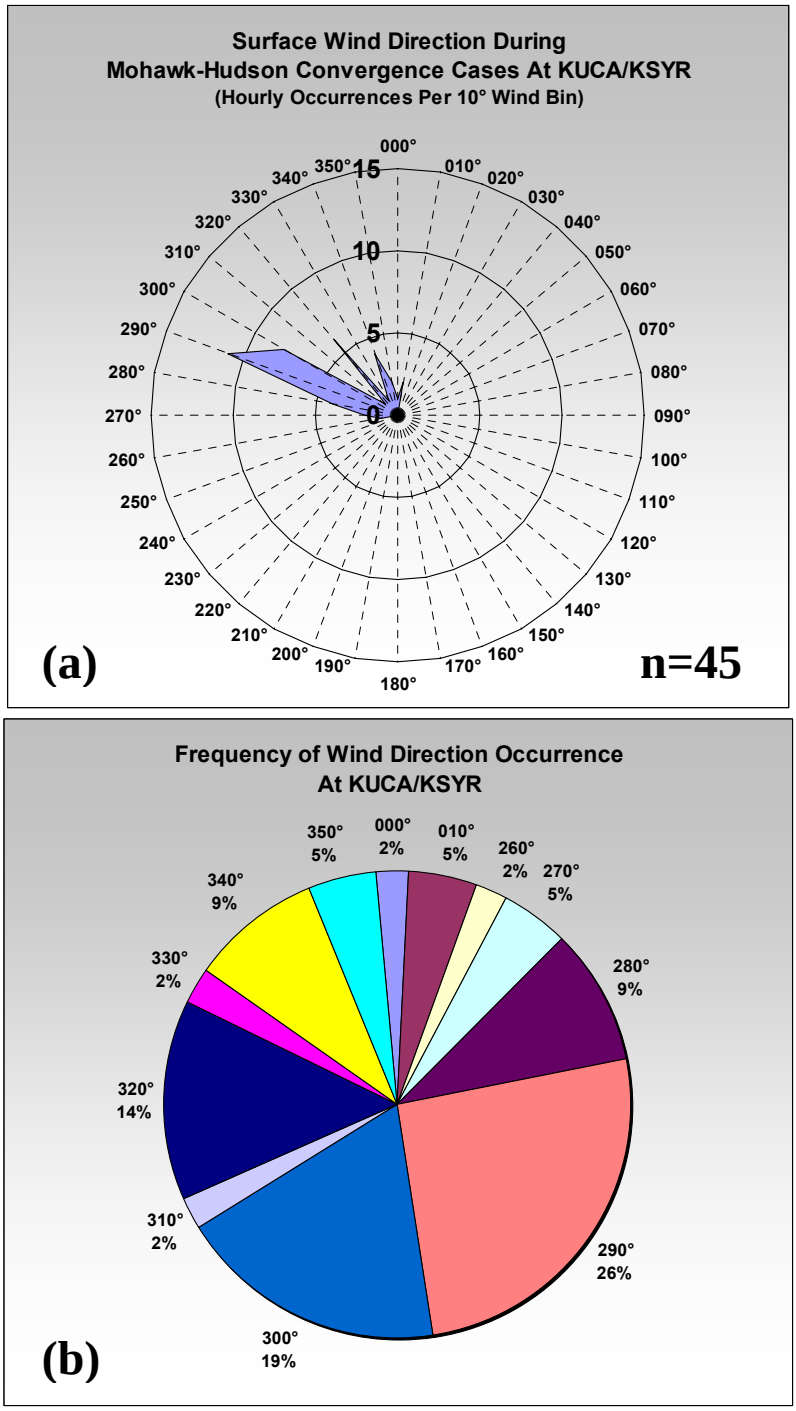

Figure 3.2: (a) Surface wind rose for KUCA (case studies spanning November 2002 – March 2006, inclusive) and KSYR (January 2007 case study) during ongoing MHC events. Azimuthal axis represents wind direction in degrees, and radial axis represents number of hourly occurrences. (b) Frequency (in percent) with which each wind direction occurred at KUCA and KSYR during the aforementioned case studies. Data source: University at Albany archive; supplemental data from the Historical Weather Data Archives of the National Severe Storms Laboratory (NSSL) in Norman, Oklahoma.

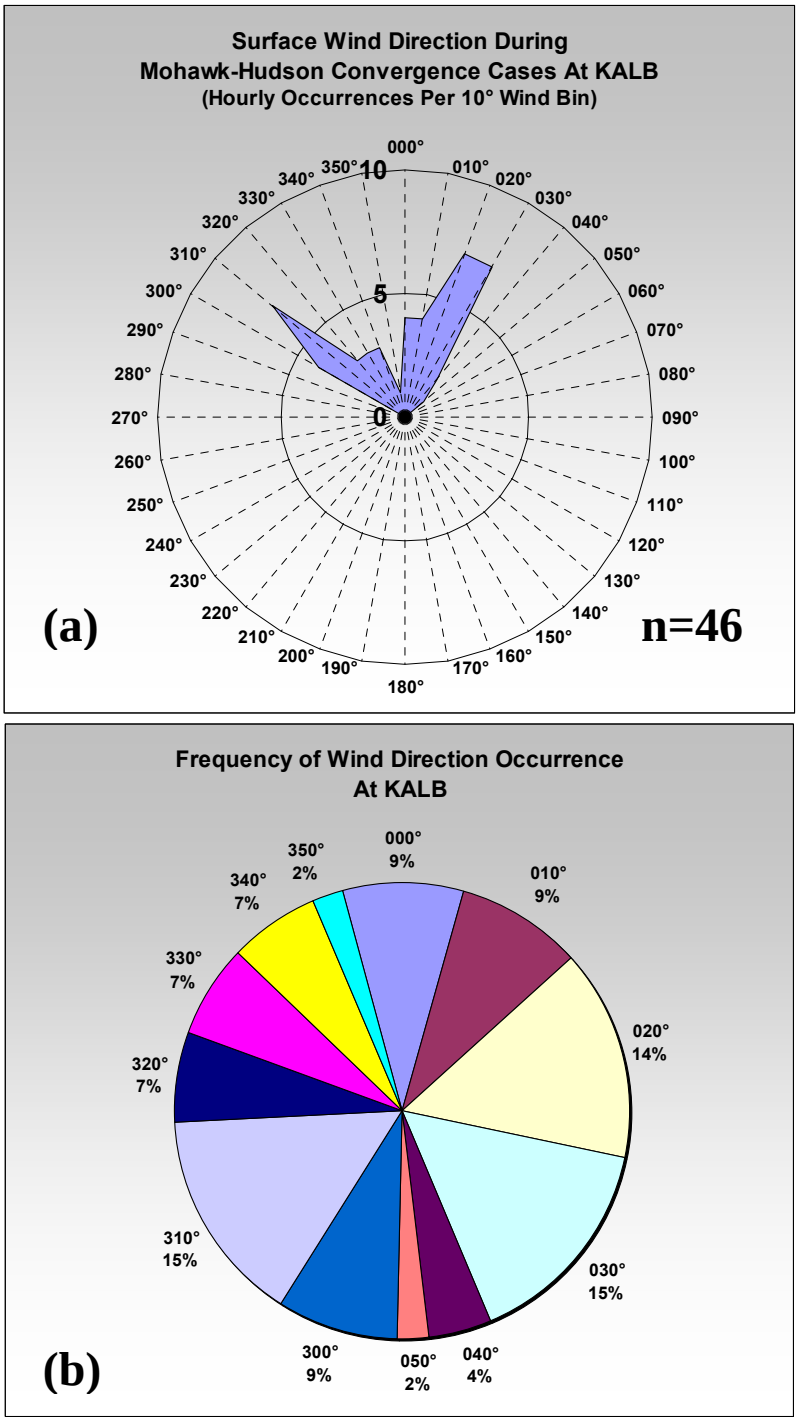

Figure 3.3: As in Fig. 3.1, except for KALB.

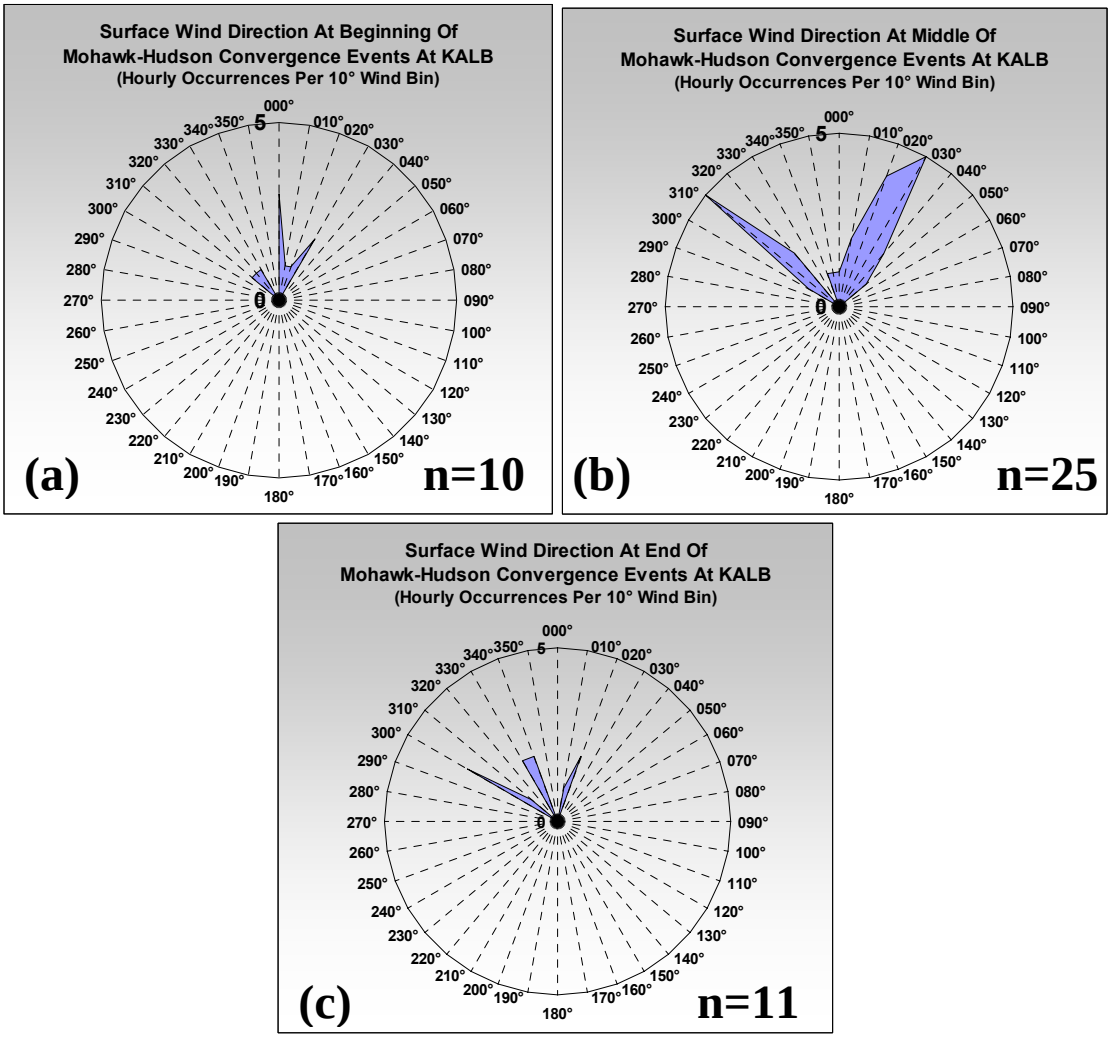

Figure 3.4: Surface wind rose for KALB at (a) beginning, (b) middle, and (c) end of MHC events studied from November 2002 to January 2007, inclusive. Azimuthal axis represents wind direction in degrees, and radial axis represents number of hourly occurrences. Data source: University at Albany archive; supplemental data from the Historical Weather Data Archives of the National Severe Storms Laboratory (NSSL) in Norman, Oklahoma.

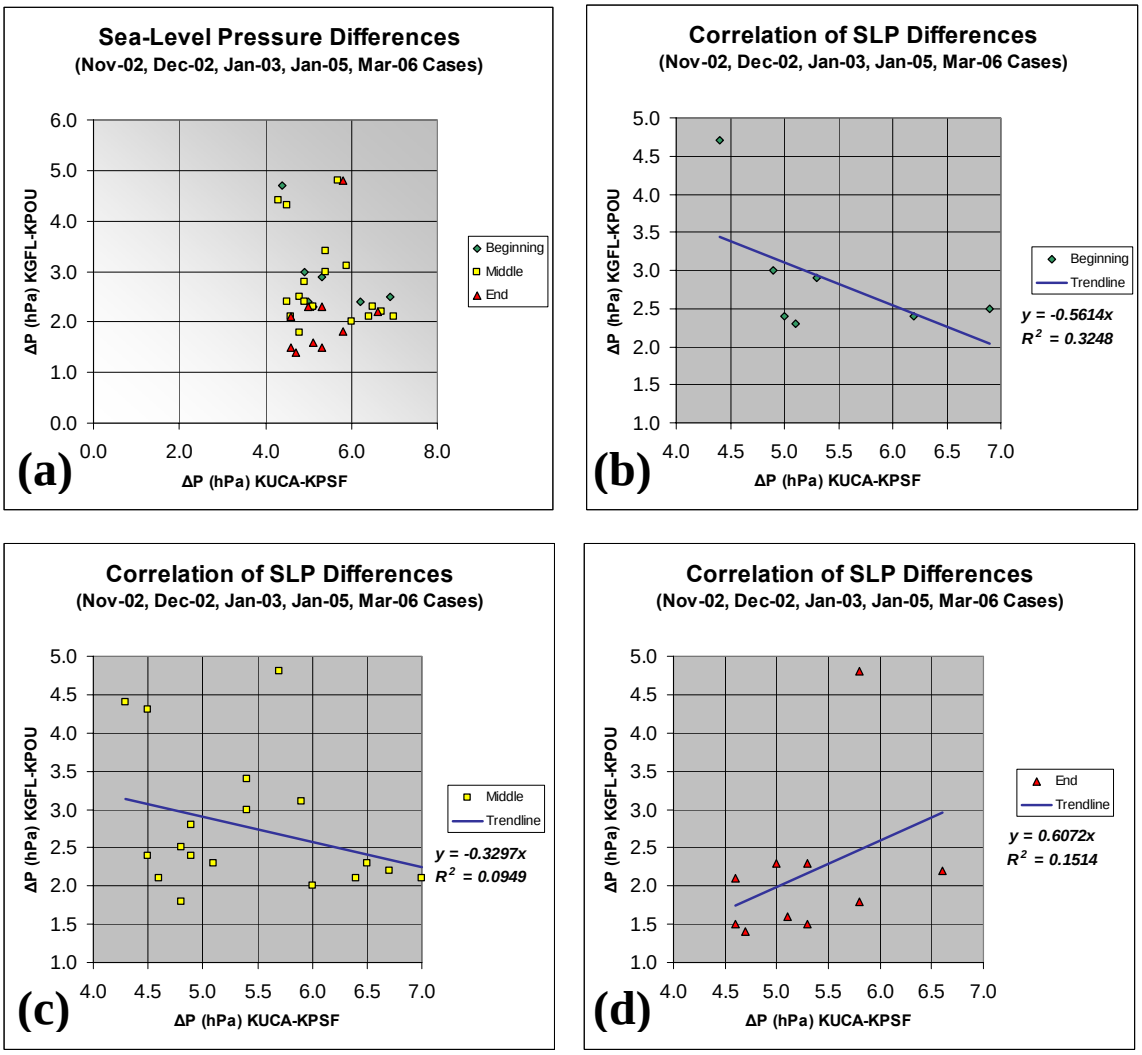

Figure 3.5: Scatterplot graph of SLP differences between KGFL and KPOU (KUCA and KPSF) during MHC case studies from November 2002 to March 2006, inclusive, where positive pressure differences indicate higher pressures to the north (west). (a) For all observations; (b) for observations taken during the "beginning" of MHC events, where the solid blue line indicates the best-fit linear regression between north-south and west-east pressure difference pairs; (c) as in (b), but for the "middle" of MHC events; (d) as in (b), but for the "end" of MHC events. Data source: University at Albany archive; supplemental data from the Historical Weather Data Archives of the National Severe Storms Laboratory (NSSL) in Norman, Oklahoma.

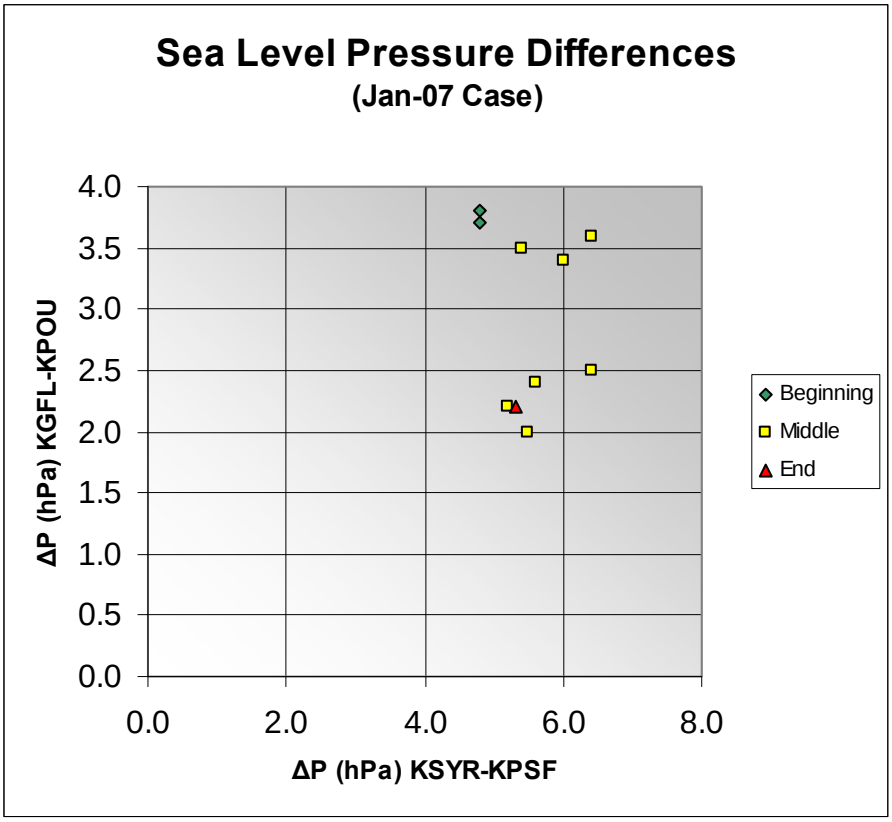

Figure 3.6: Scatterplot graph of SLP differences between KGFL and KPOU (KSYR and KPSF) during the January 2007 MHC case study, where positive pressure differences indicate higher pressures to the north (west). Data source: University at Albany archive; supplemental data from the Historical Weather Data Archives of the National Severe Storms Laboratory (NSSL) in Norman, Oklahoma.

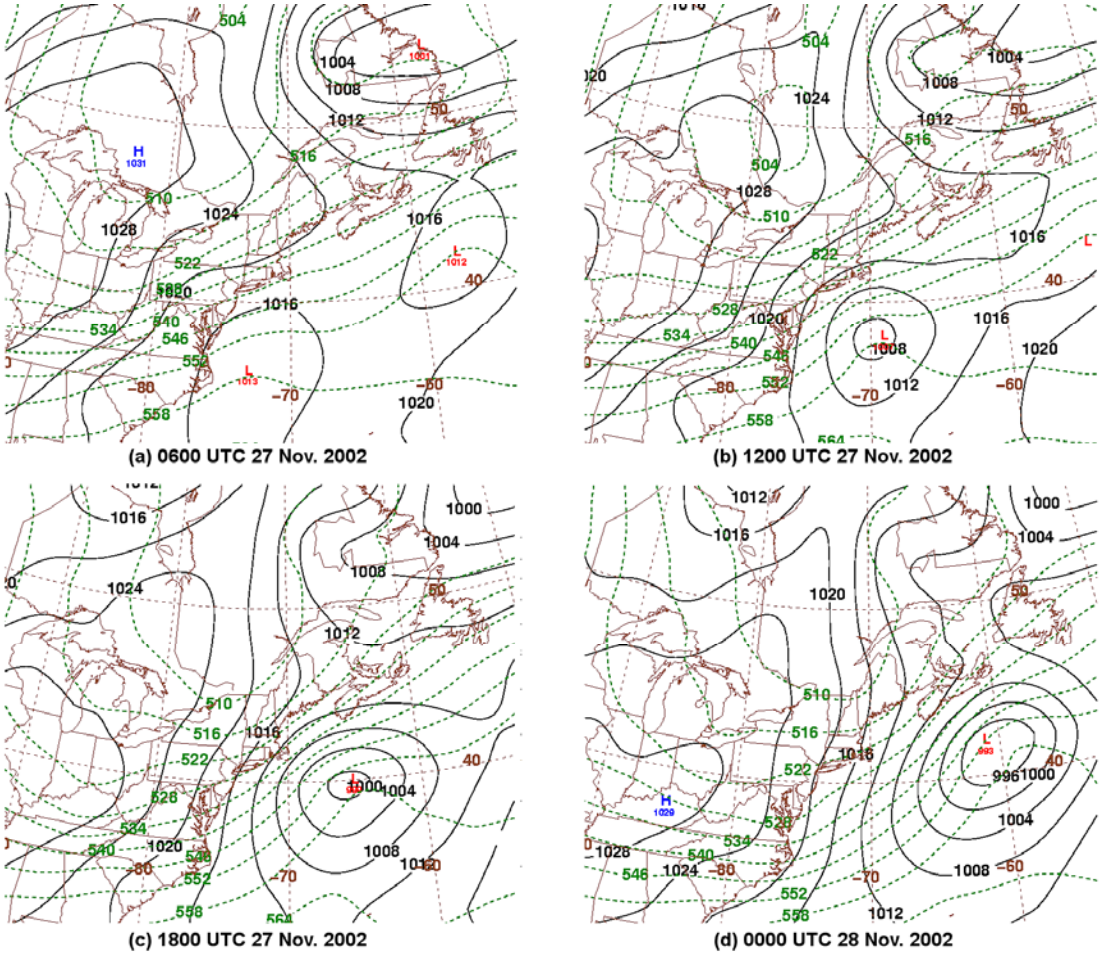

Figure 3.7: Sea level pressure (solid black lines every 4 hPa) with high- (low-) pressure centers labeled by a blue "H" (red "L"), and 1000–500-hPa thickness (dashed green lines every 6 dam) at (a) 0600, (b) 1200, and (c) 1800 UTC 27 November 2002, and at (d) 0000 UTC 28 November 2002. (Data source: 0-h gridded, initialized 1.0° NCEP GFS analyses).

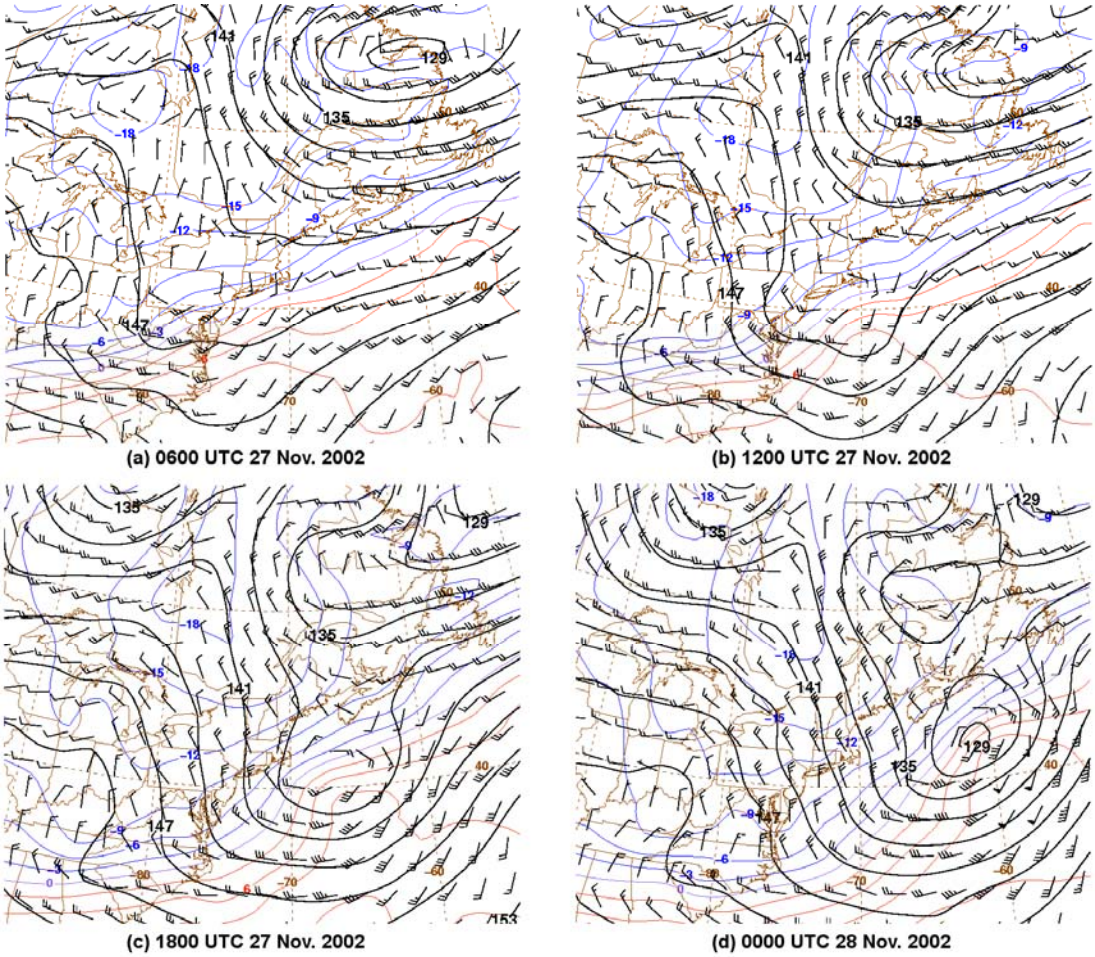

Figure 3.8: 850-hPa geopotential height (solid black lines, every 3 dam), temperatures (solid colored lines, every 3°C), and winds (m s^{-1}, with pennant, full barb, and half barb denoting 25, 5, and 2.5 m s^{-1}, respectively) at (a) 0600, (b) 1200, and (c) 1800 UTC 27 November 2002, and at (d) 0000 UTC 28 November 2002. (Data source: 0-h gridded, initialized 1.0° NCEP GFS analyses).

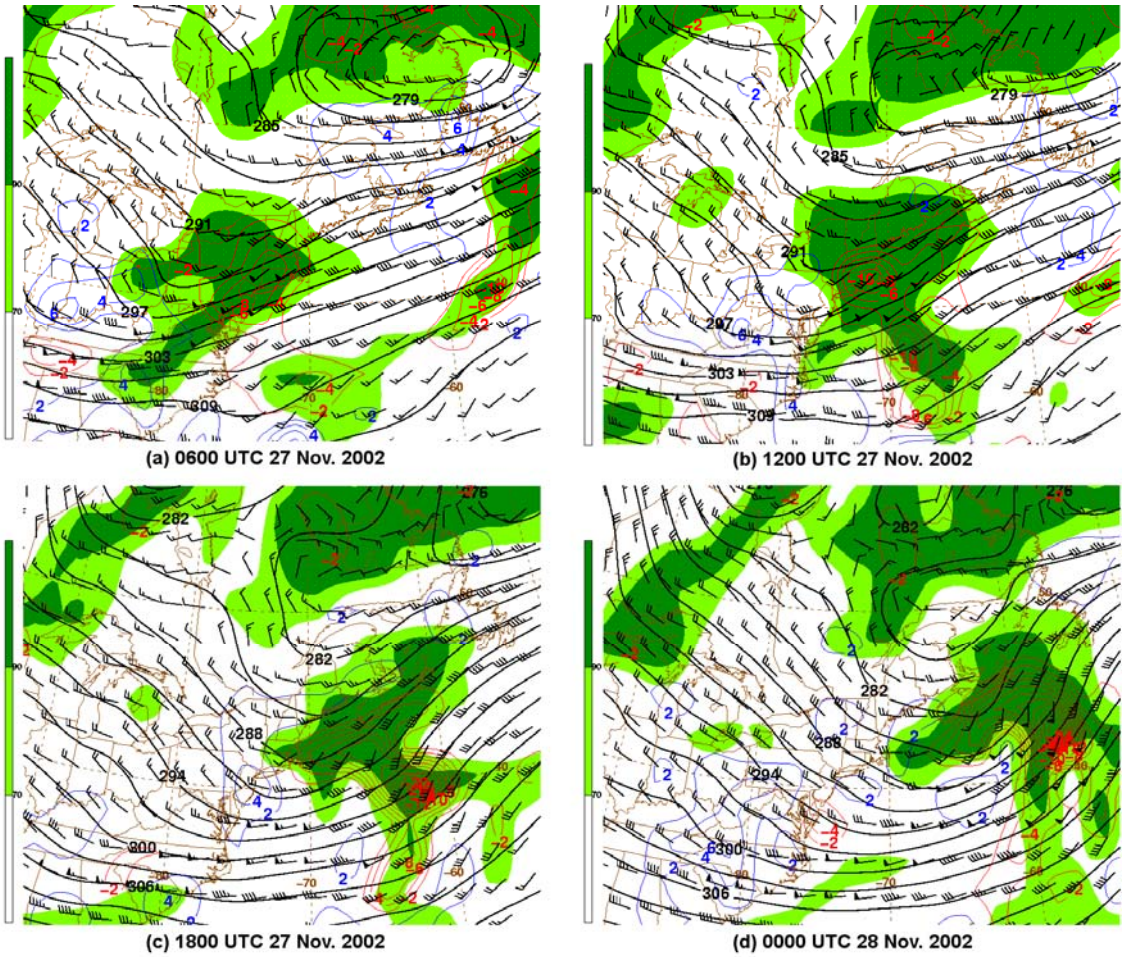

Figure 3.9: 700-hPa geopotential height (solid black lines, every 3 dam), relative humidity (shaded beginning at 70% according to the scale), vertical motion [solid red (blue) contours show ascent (descent), every 2×10^{-3} hPa s^{-1}], and winds (m s^{-1}, with pennant, full barb, and half barb denoting 25, 5, and 2.5 m s^{-1}, respectively) at (a) 0600, (b) 1200, and (c) 1800 UTC 27 November 2002, and at (d) 0000 UTC 28 November 2002. (Data source: 0-hour gridded, initialized 1.0° NCEP GFS analyses).

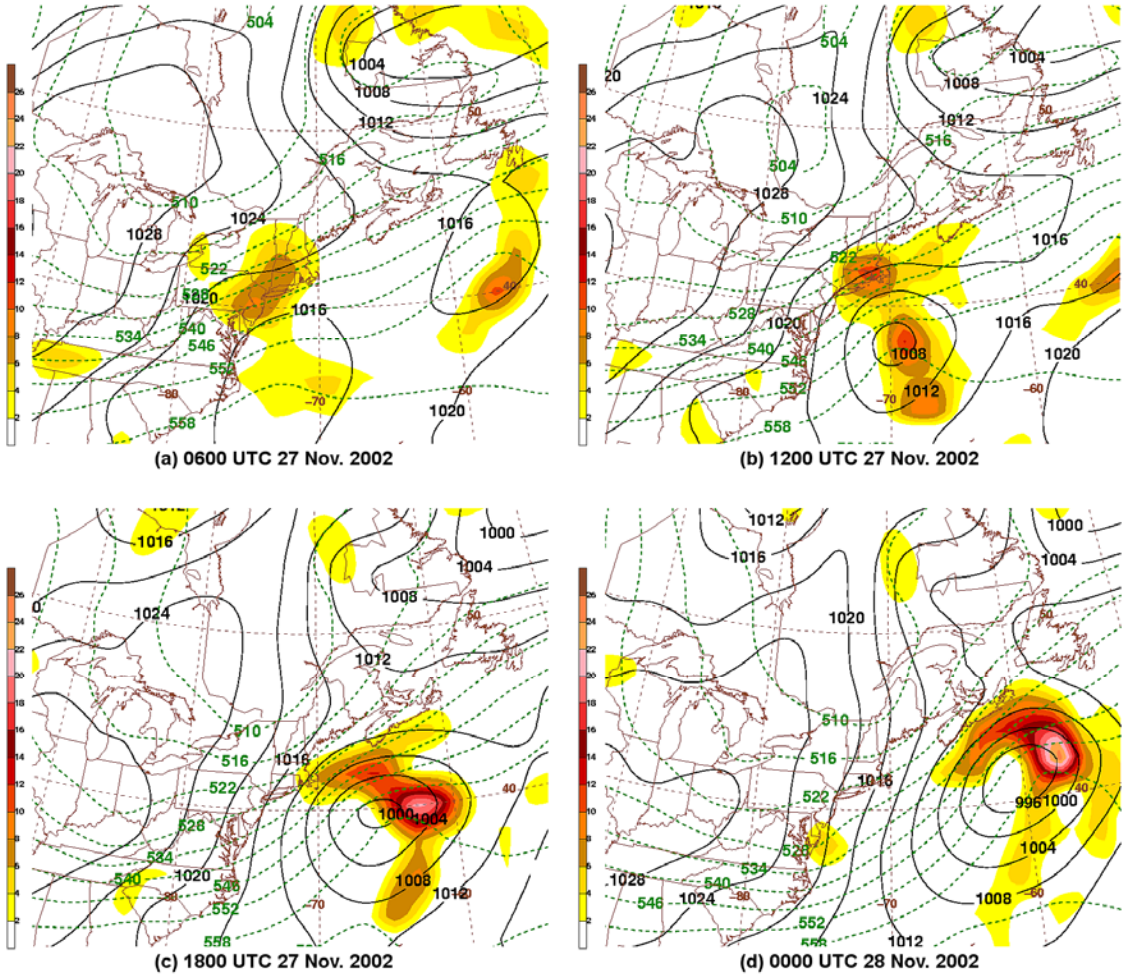

Figure 3.10: Sea level pressure (solid black lines every 4 hPa), 700-hPa vertical motion (ascent shaded beginning at -2×10^{-3} hPa s^{-1} according to the scale), and 1000–500-hPa thickness (dashed green lines every 6 dam) at (a) 0600, (b) 1200, and (c) 1800 UTC 27 November 2002, and at (d) 0000 UTC 28 November 2002. (Data source: 0-hour gridded, initialized 1.0° NCEP GFS analyses).

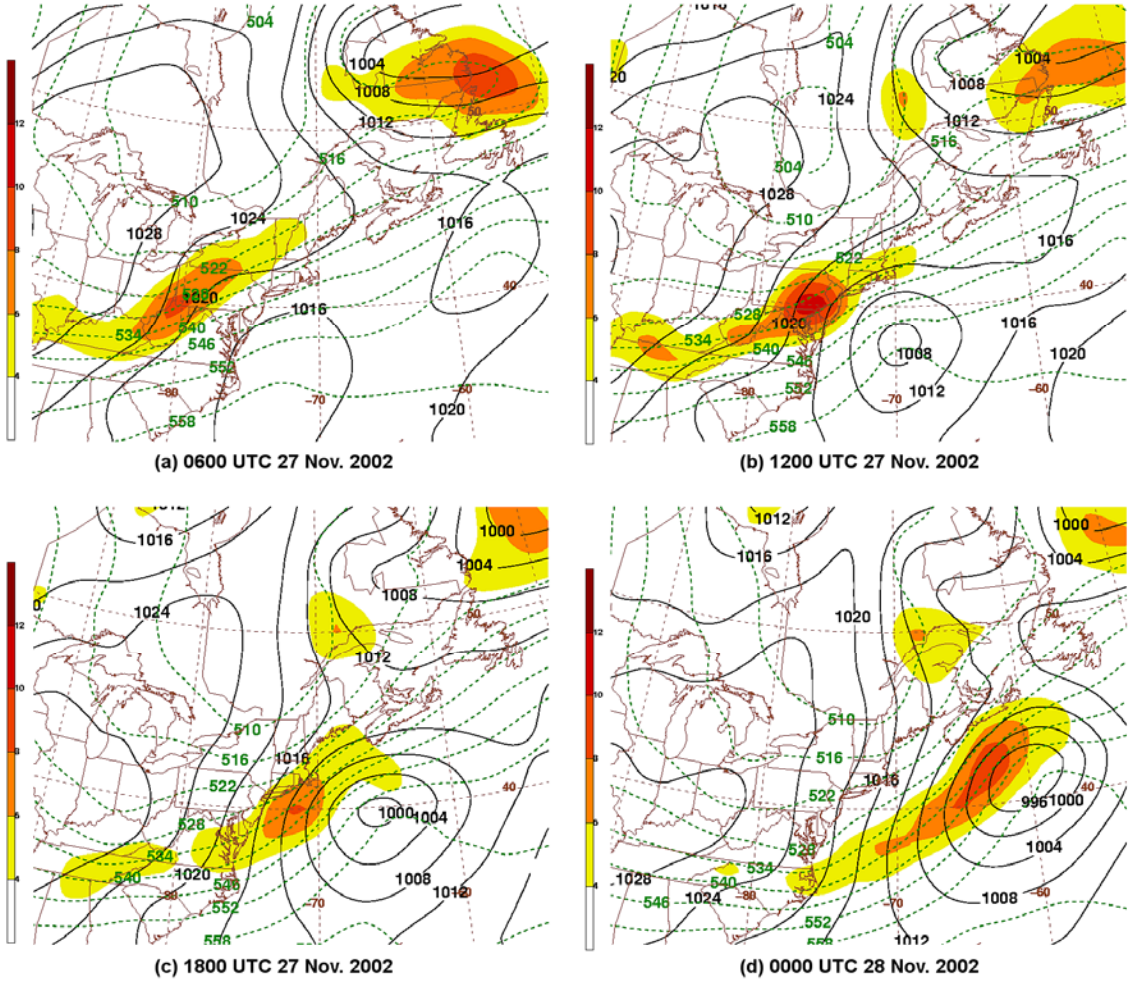

Figure 3.11: Sea level pressure (solid black lines every 4 hPa), 700-hPa geostrophic relative vorticity (shaded beginning at 4×10^{-5} s^{-1} according to the scale), and 1000–500-hPa thickness (dashed green lines every 6 dam) at (a) 0600, (b) 1200, and (c) 1800 UTC 27 November 2002, and at (d) 0000 UTC 28 November 2002. (Data source: 0-hour gridded, initialized 1.0° NCEP GFS analyses).

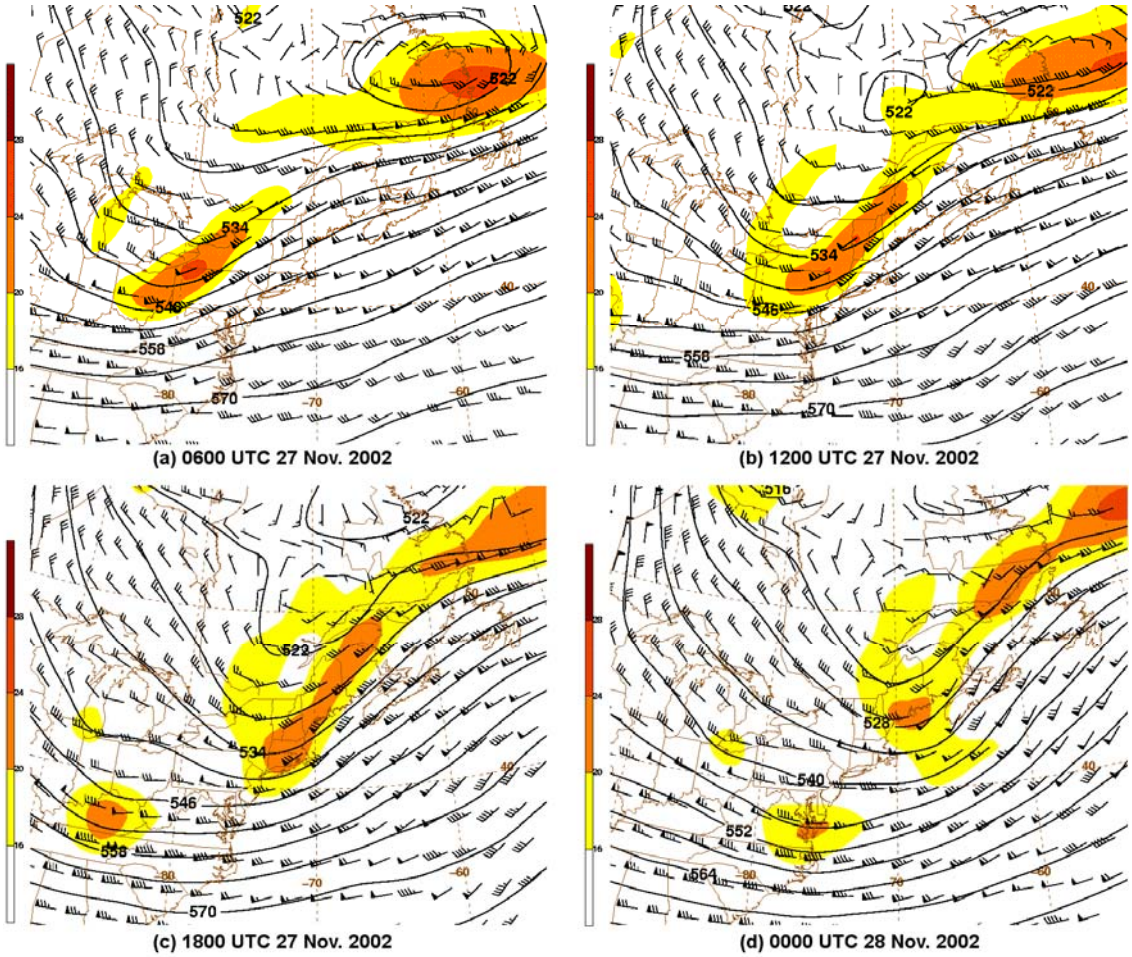

Figure 3.12: 500-hPa geopotential height (solid black lines, every 6 dam), absolute vorticity (shaded beginning at 16×10^{-5} s^{-1} according to the scale), and winds (m s^{-1}, with pennant, full barb, and half barb denoting 25, 5, and 2.5 m s^{-1}, respectively) at (a) 0600, (b) 1200, and (c) 1800 UTC 28 November 2002, and at (d) 0000 UTC 28 November 2002. (Data source: 0-hour gridded, initialized 1.0° NCEP GFS analyses).

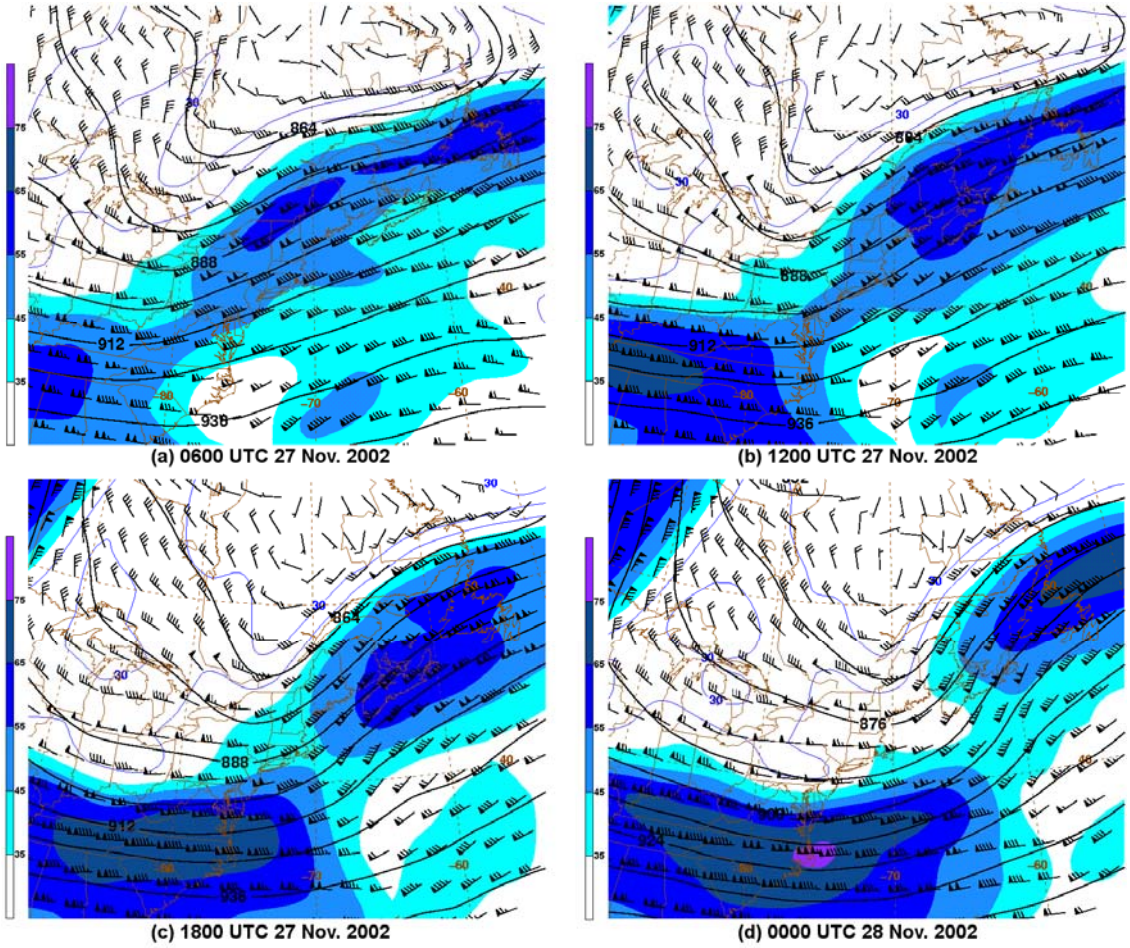

Figure 3.13: 300-hPa geopotential height (solid black lines, every 12 dam), winds (m s^{-1}, with pennant, full barb, and half barb denoting 25, 5, and 2.5 m s^{-1}, respectively), and wind speed (shaded beginning at 35 m s^{-1} according to the scale) at (a) 0600, (b) 1200, and (c) 1800 UTC 27 November 2002, and at (d) 0000 UTC 28 November 2002. (Data source: 0-hour gridded, initialized 1.0° NCEP GFS analyses).

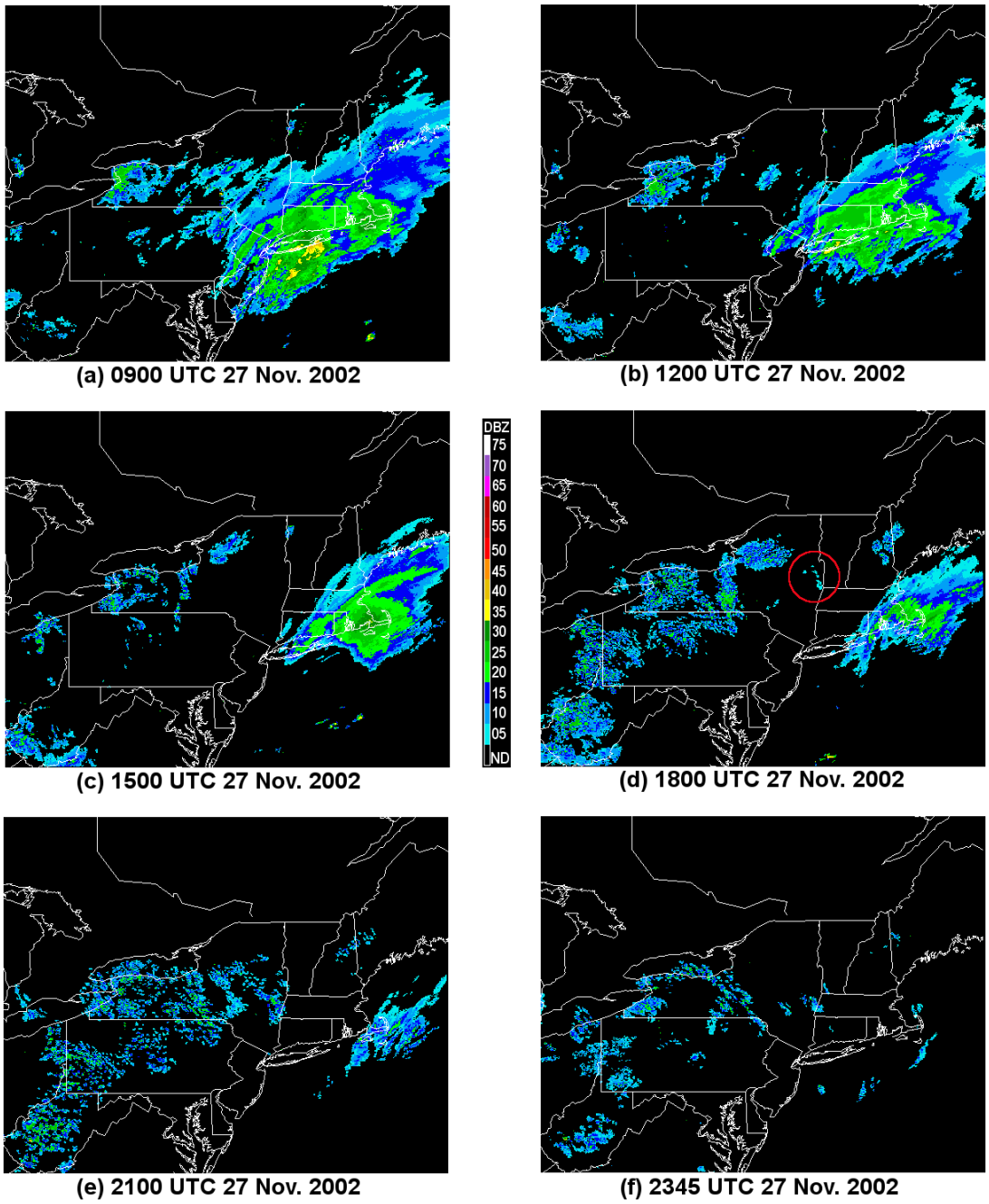

Figure 3.14: Weather Services International (WSI) NOWrad 2 km base reflectivity (dBZ shaded according to scale) mosaic at (a) 0900, (b) 1200, (c) 1500, (d) 1800, (e) 2100, and (f) 2345 UTC 27 November 2002. (Data source: WSI, via MMM/NCAR). Precipitation related to MHC is circled in red.

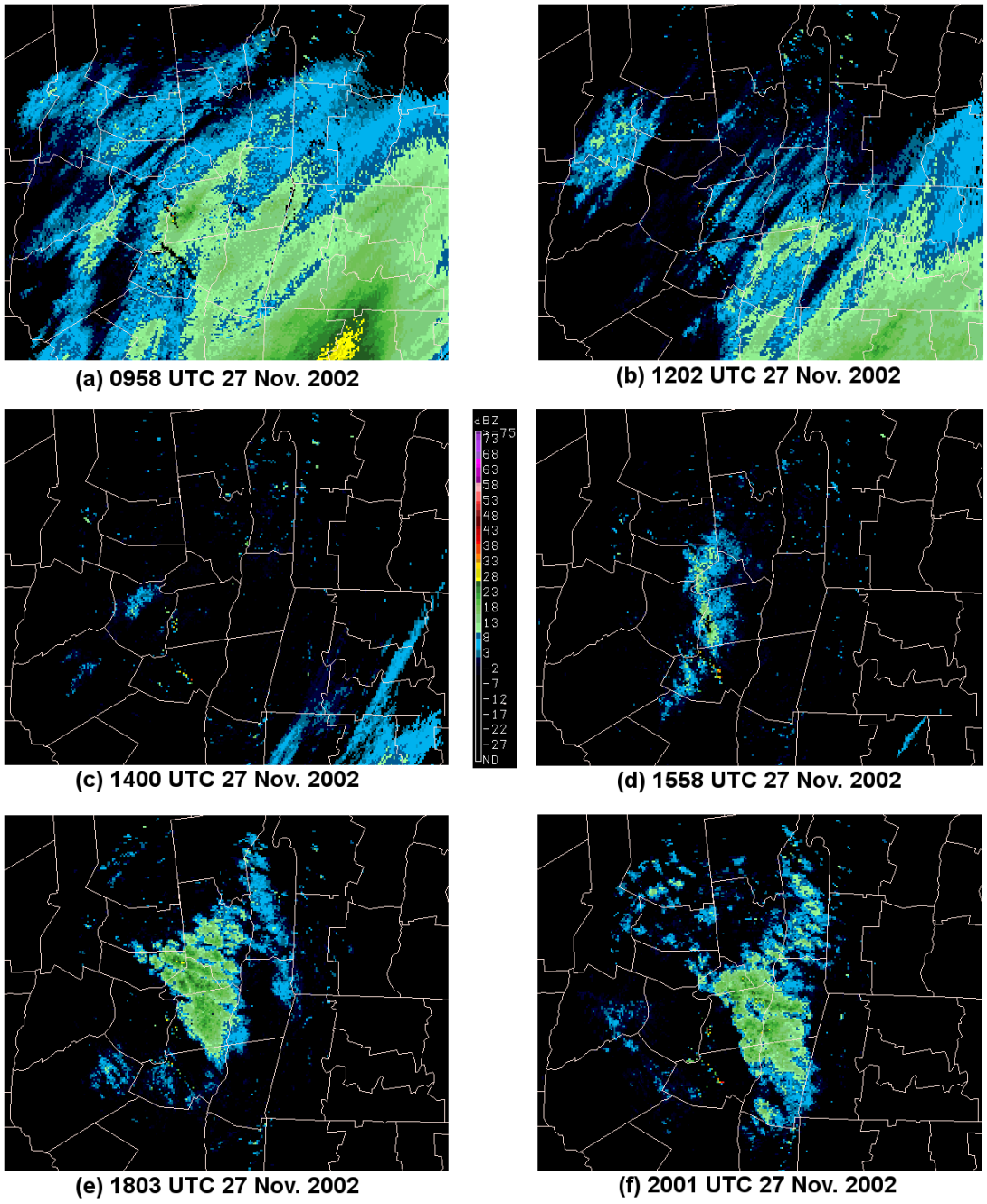

Figure 3.15: KENX 0.5° base reflectivity (dBZ shaded according to scale) at (a) 0958, (b) 1202, (c) 1400, (d) 1558, (e) 1803, and (f) 2001 UTC 27 November 2002. (Data source: NCDC).

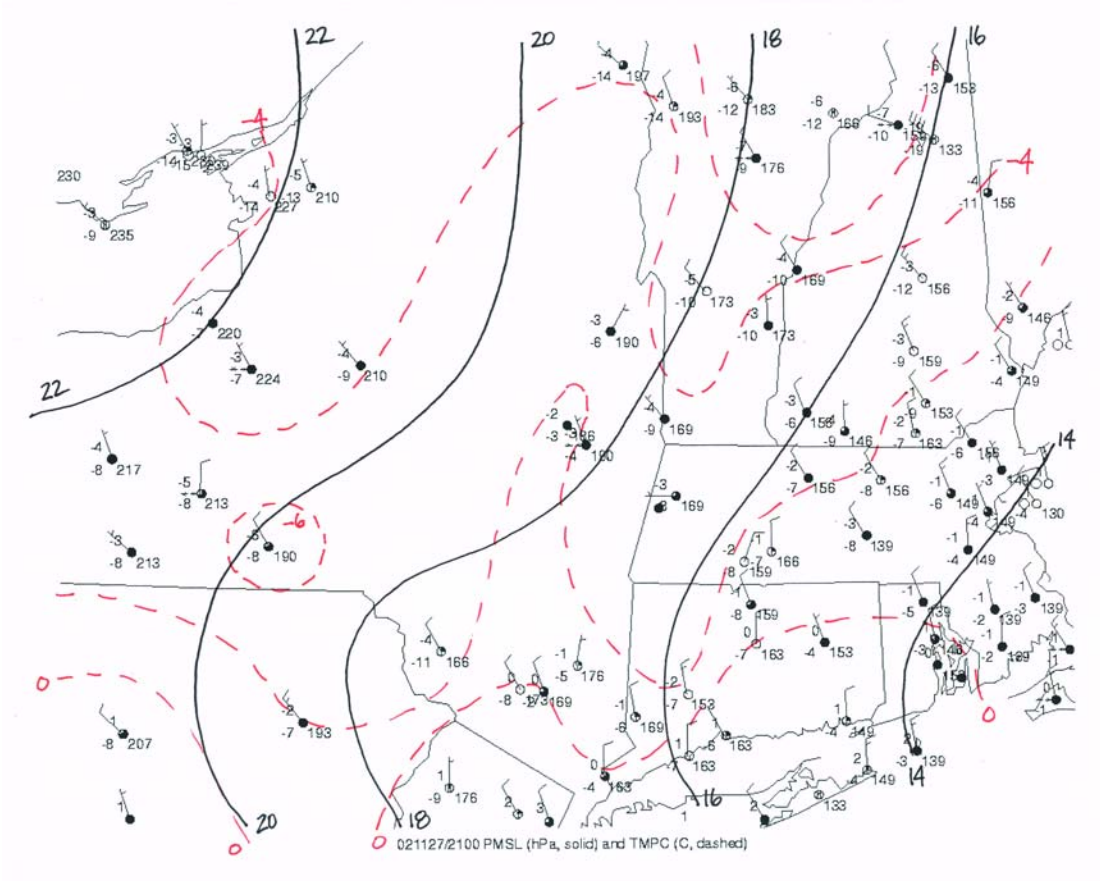

Figure 3.16: Manual regional surface analysis of eastern New York and New England at 2100 UTC 27 November 2002. Isobars (solid) every 2 hPa. Isotherms (dashed red lines) every 2°C. Surface observations are plotted conventionally and show wind speed (m s^{-1}, with full barb, and half barb denoting 5, and 2.5 m s^{-1}, respectively). (Data source: the University at Albany DEAS archives).

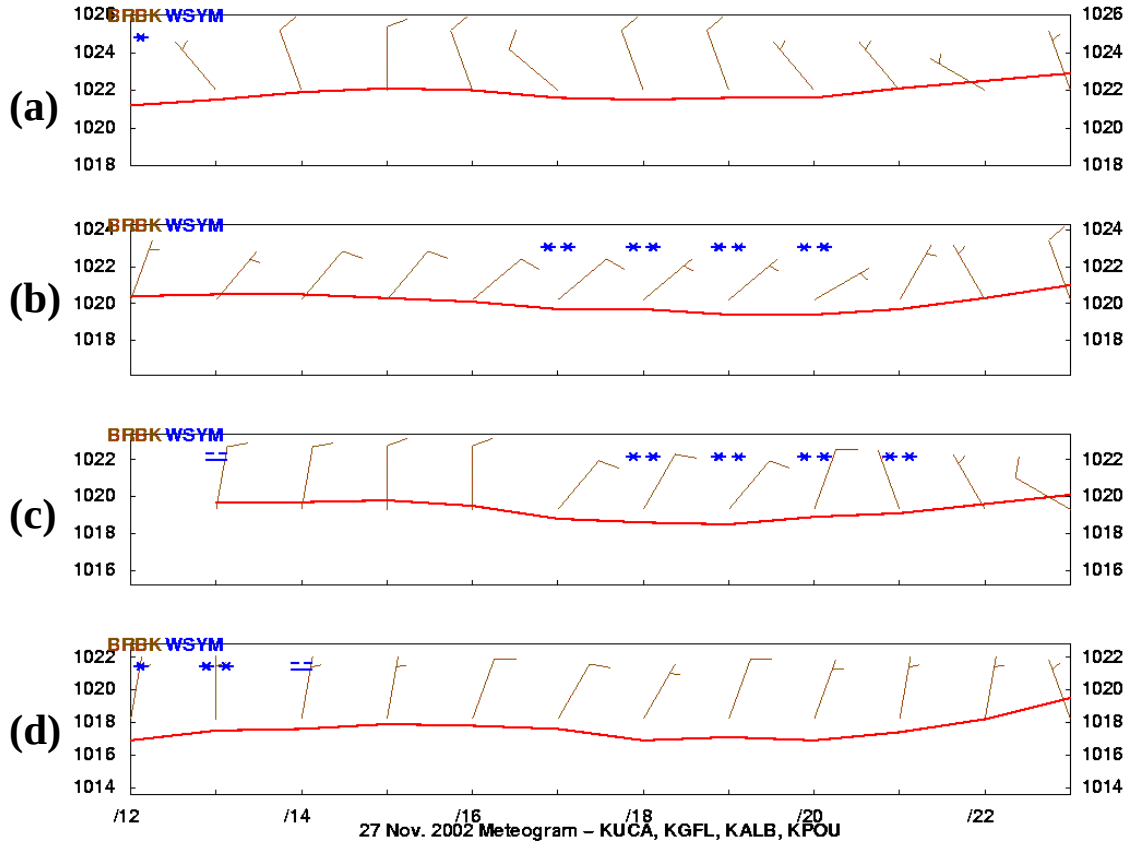

Figure 3.17: Meteograms of surface weather from 1200 to 2300 UTC 27 November 2002 for (a) KUCA, (b) KGFL, (c) KALB, and (d) KPOU. Plotted are sea level pressure (hPa), wind direction and speed (m s^{-1}, with full barb, and half barb denoting 5, and 2.5 m s^{-1}, respectively), and present weather. (Data source: the University at Albany DEAS archives).

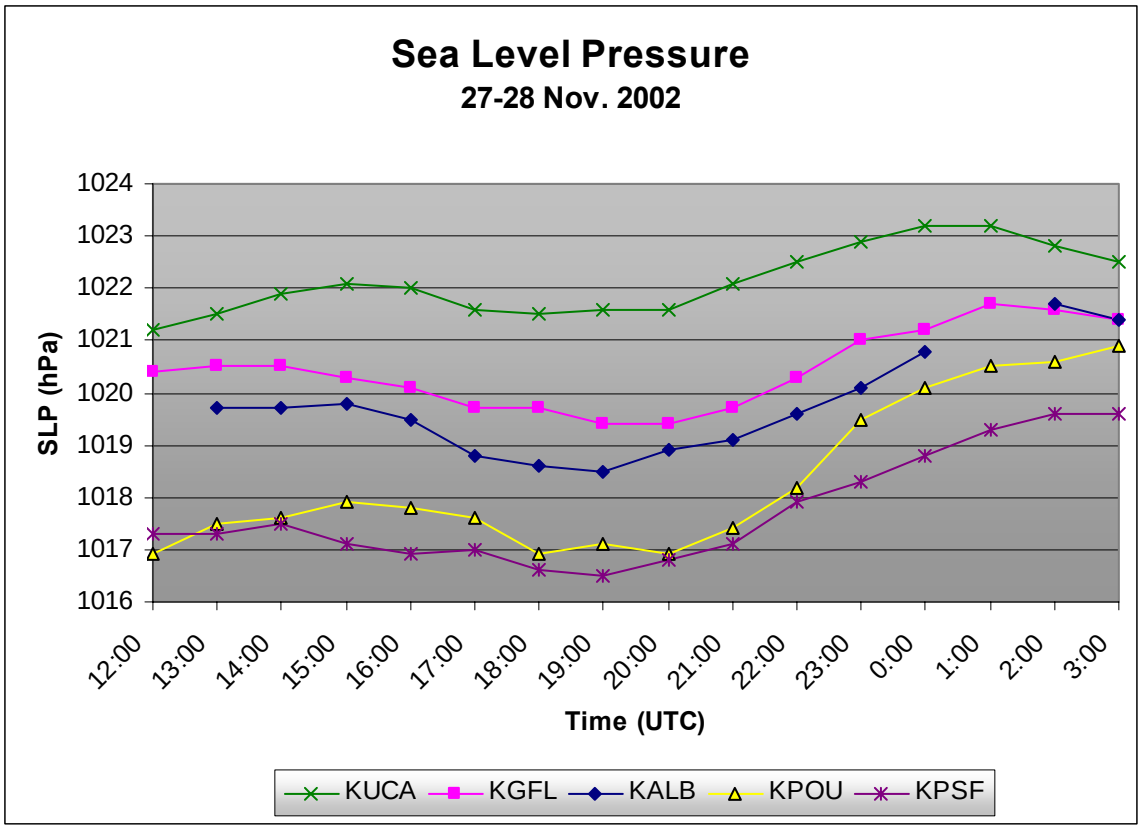

Figure 3.18: Sea level pressure time series (hPa) from 1200 UTC 27 November to 0300 UTC 28 November 2002 for KUCA, KGFL, KALB, KPOU, and KPSF (trace and data point markers according to the legend). (Data source: the University at Albany DEAS archives, with supplemental data provided by the Historical Weather Data Archives of NSSL).

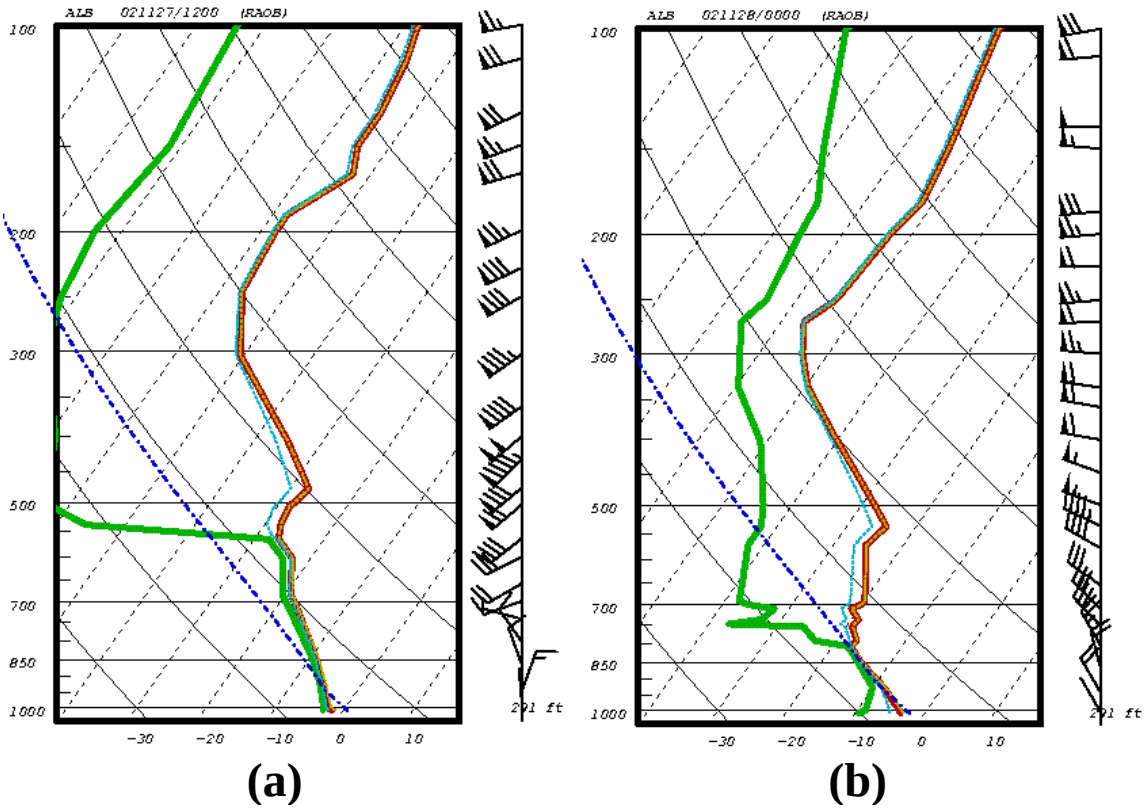

Figure 3.19: Skew *T*–log *p* radiosonde observations at KALY (72518) of air temperature (red line, in °C), dewpoint (green line, in °C), wet-bulb temperature (solid blue line, in °C), and wind (to the right of each sounding; m s^{-1}, with pennant, full barb, and half barb denoting 25, 5, and 2.5 m s^{-1}, respectively) for (a) 1200 UTC 27 November 2002, and (b) 0000 UTC 28 November 2002. (Data source: the University at Albany DEAS archives).

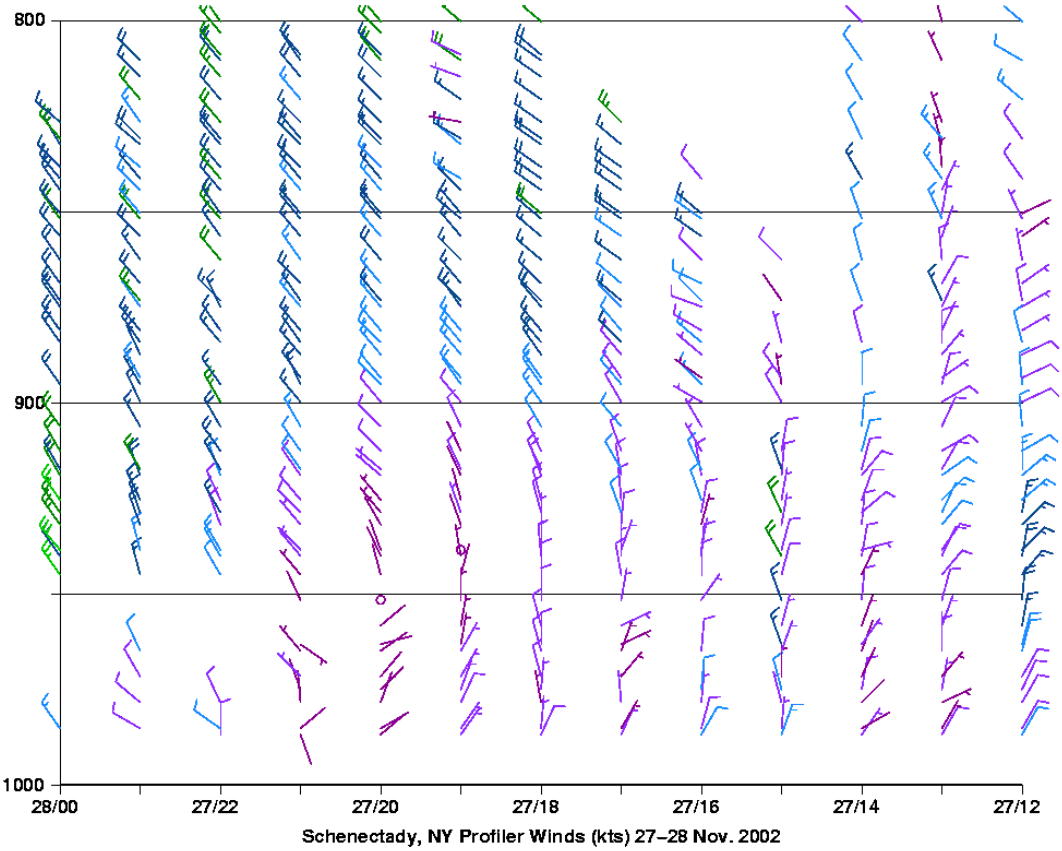

Figure 3.20: Time–height cross section from the Schenectady, NY (KSCH), wind profiler (now defunct; originally part of NPN, established by NOAA). Shown are wind direction and speed (m s^{-1}, with full barb, and half barb denoting 5, and 2.5 m s^{-1}, respectively; barb color proportional to wind speed) from 1200 UTC 27 November to 0000 UTC 28 November 2002. (Data source: NOAA/NPN).

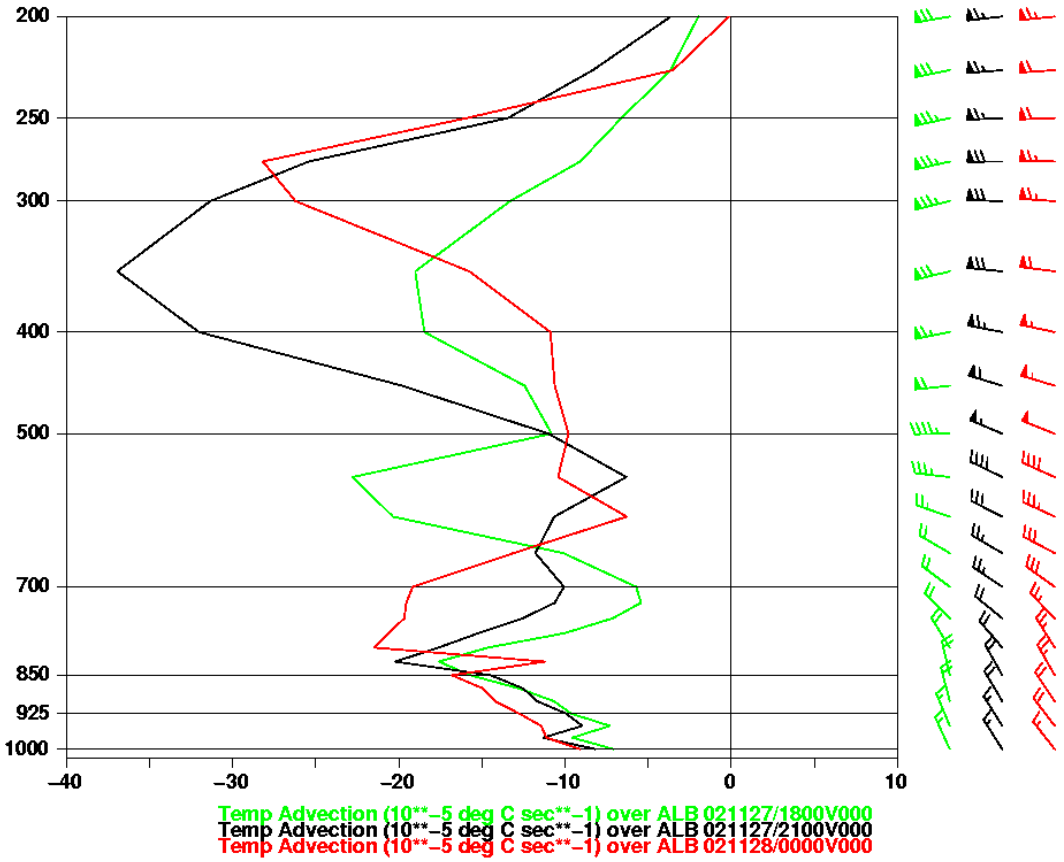

Figure 3.21: Vertical profile (log *p* format) over KALB of horizontal advection of temperature (in 10^{-5} °C s^{-1}) by the wind (m s^{-1}, with pennant, full barb, and half barb denoting 25, 5, and 2.5 m s^{-1}, respectively) at 1800 (green line and barbs), 2100 UTC 27 November 2002 (black line and barbs), and 0000 UTC 28 November 2002 (red line and barbs). (Data source: 0-h gridded, initialized analyses of the 32 km NCEP NARR).

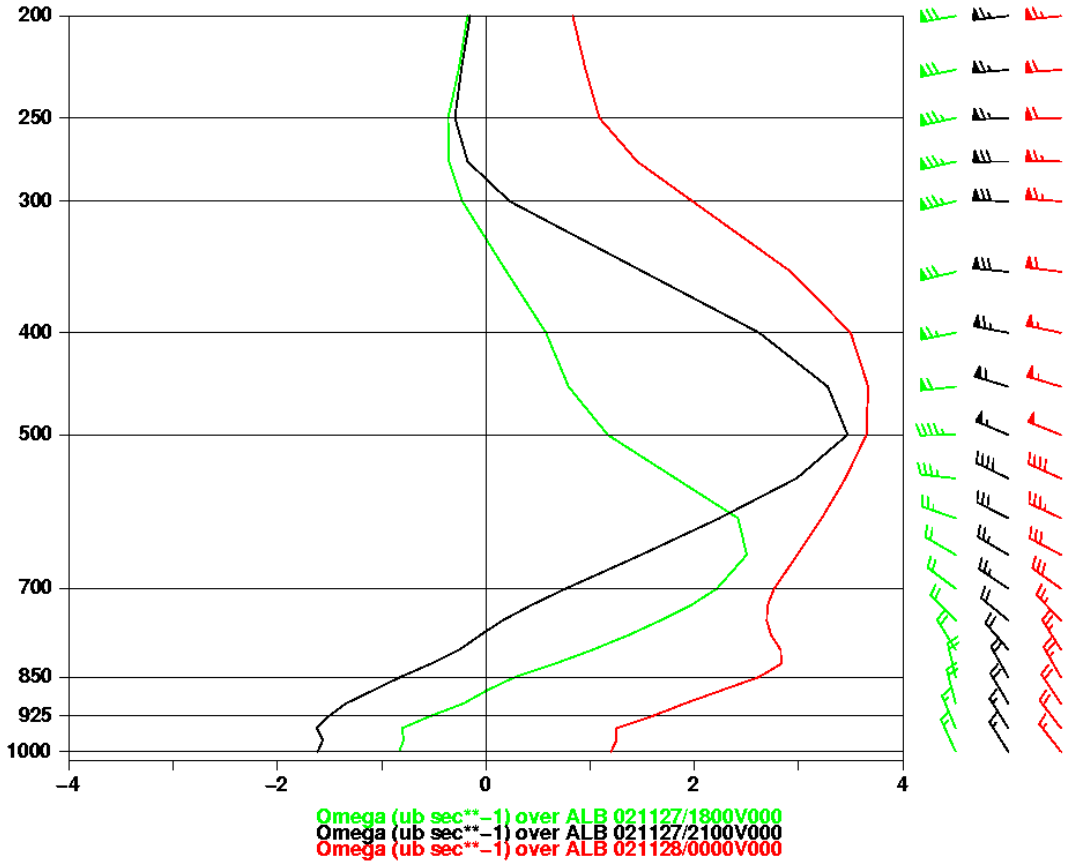

Figure 3.22: As in Fig. 3.21, except for vertical velocity (μb s^{-1}).

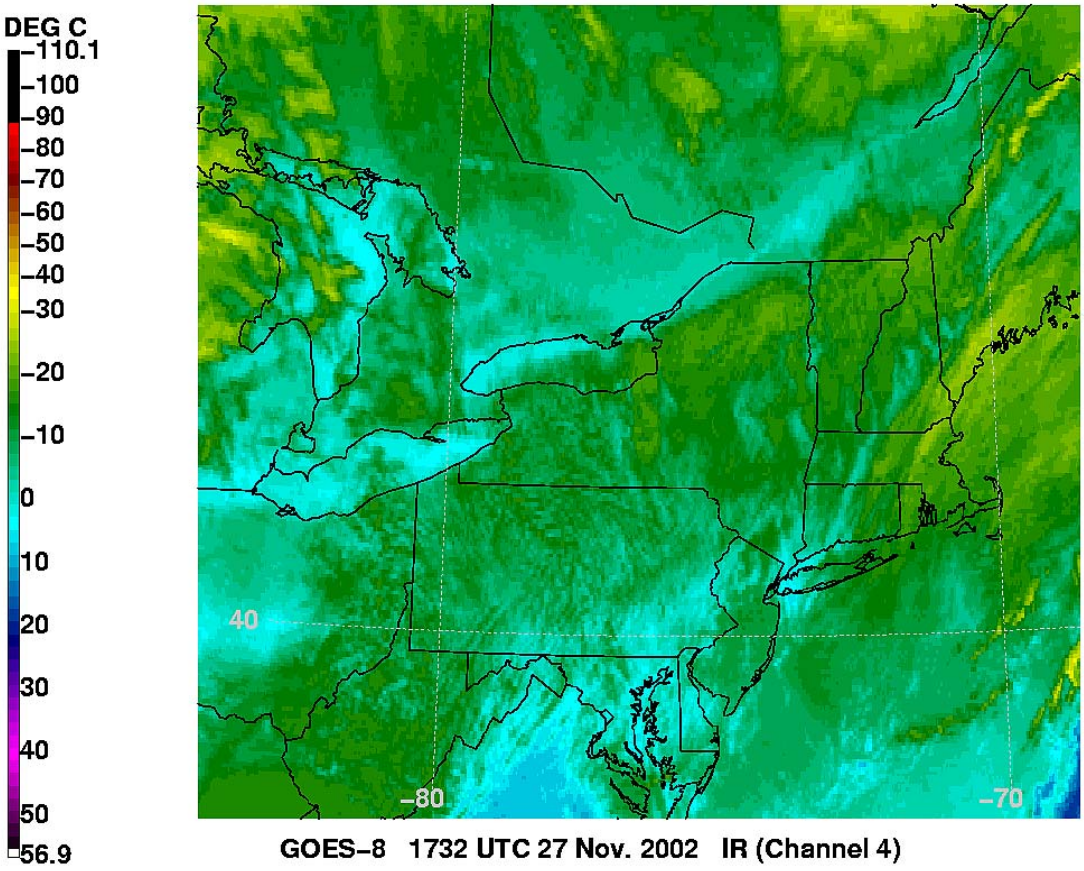

Figure 3.23: Infrared (Channel 4, wavelengths of 10.3–11.5 μm) satellite imagery from the Geostationary Operational Environmental Satellite-8 (GOES-8) at 1732 UTC 27 November 2002. Cloud top temperature (CTT) is shown (in °C shaded according to scale). (Data source: NOAA/CLASS).

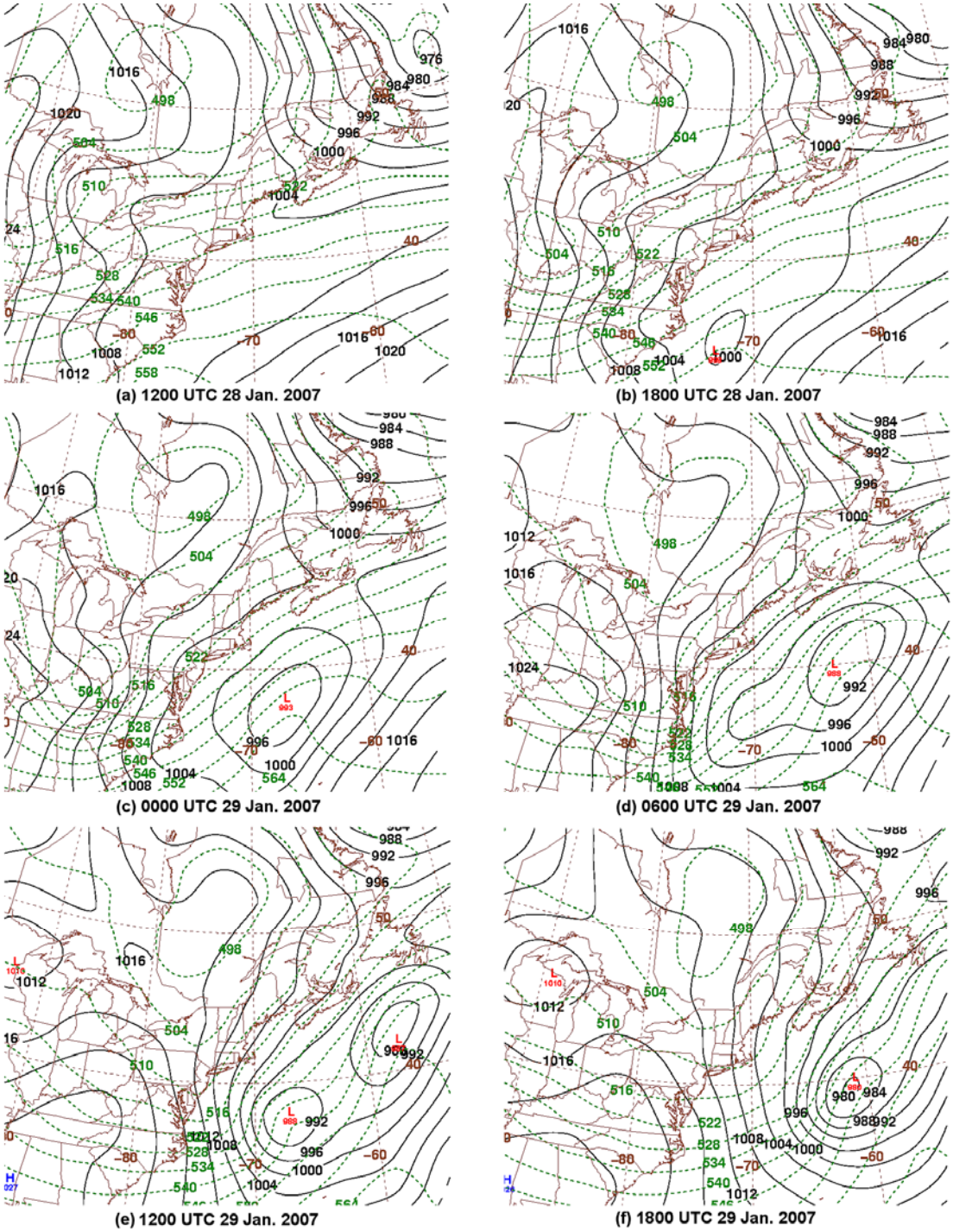

Figure 3.24: As in Fig. 3.7, except for (a) 1200, (b) 1800 UTC 28 January 2007, (c) 0000, (d) 0600, (e) 1200, and (f) 1800 UTC 29 January 2007.

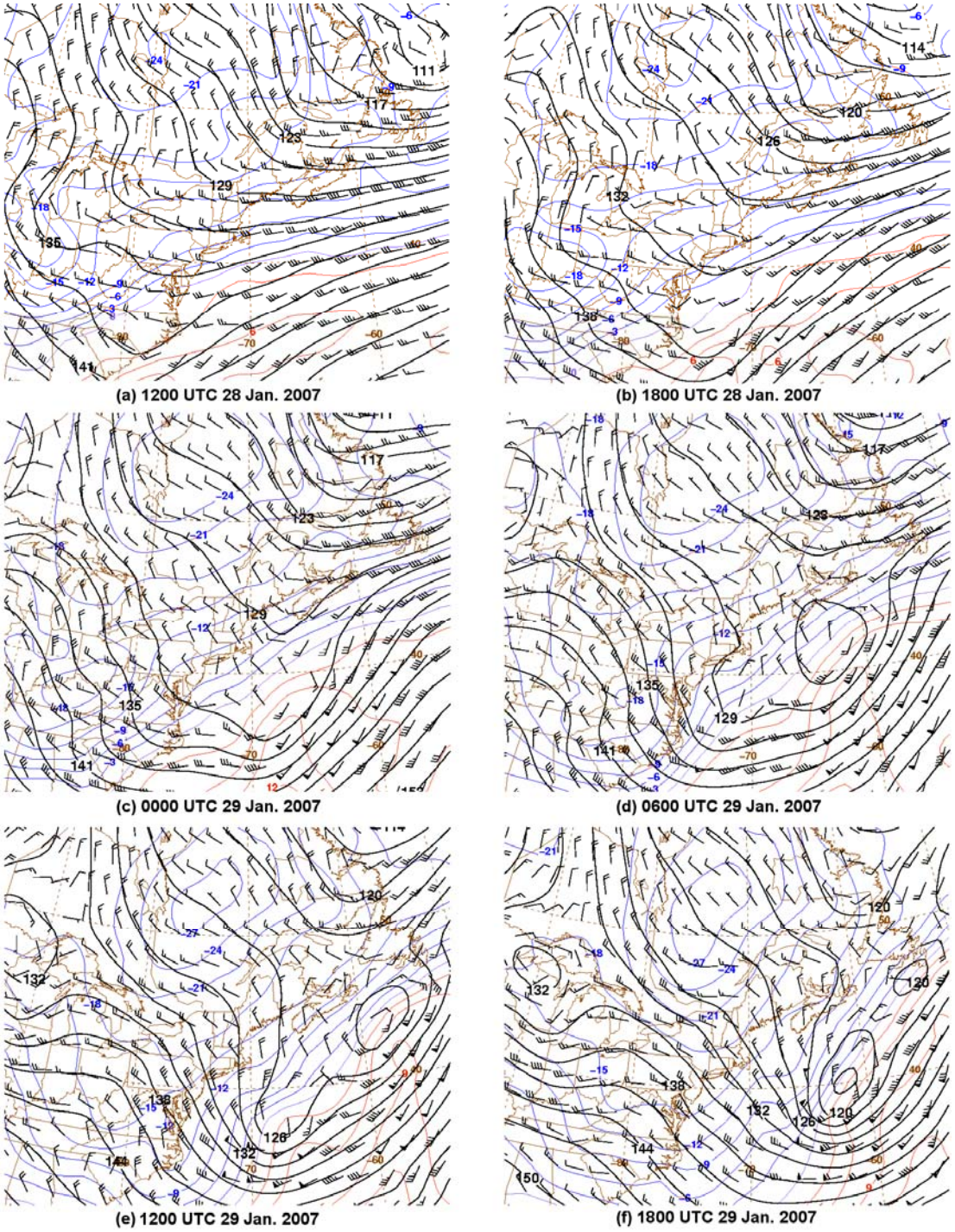

Figure 3.25: As in Fig. 3.8, except for (a) 1200, (b) 1800 UTC 28 January 2007, (c) 0000, (d) 0600, (e) 1200, and (f) 1800 UTC 29 January 2007.

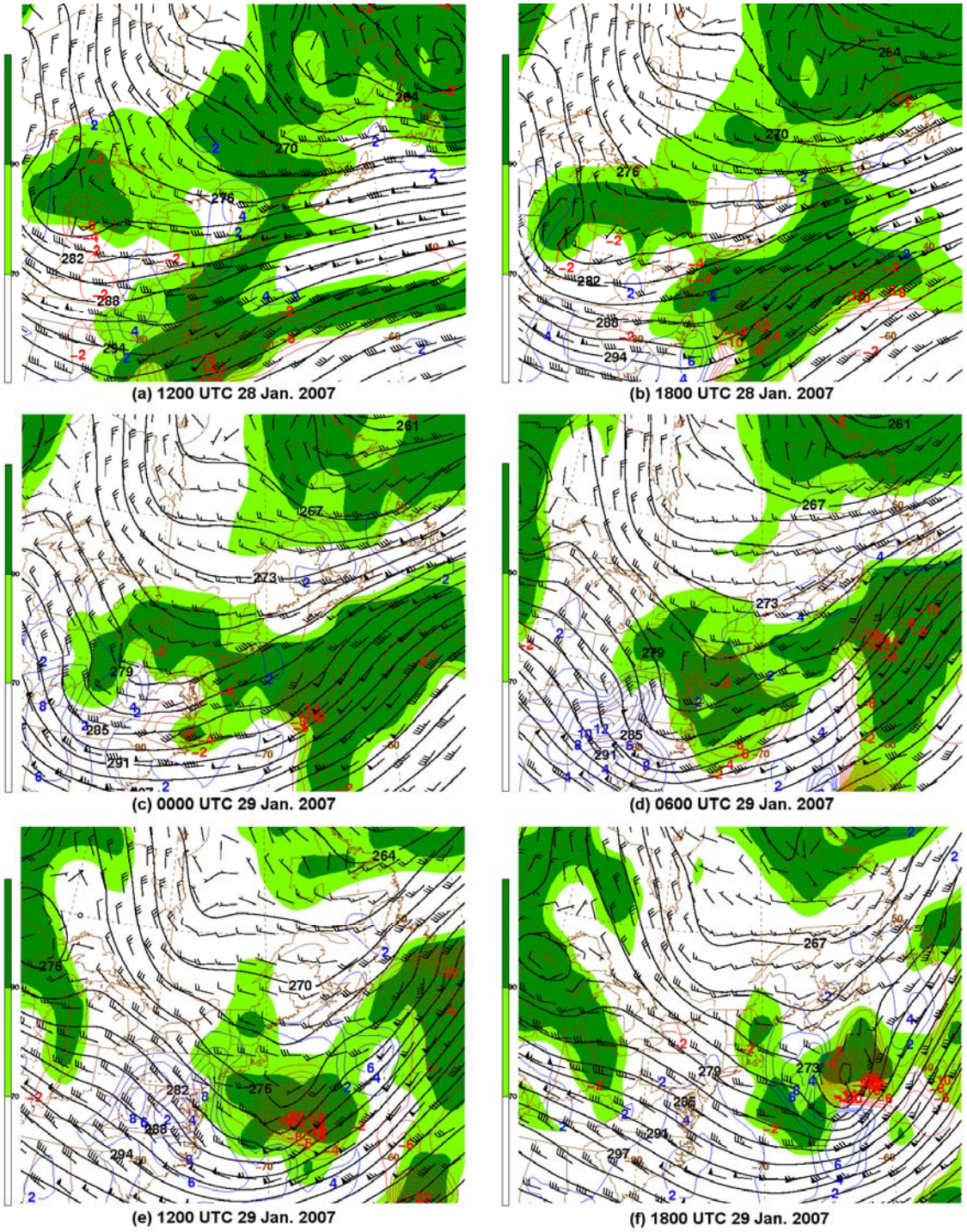

Figure 3.26: As in Fig. 3.9, except for (a) 1200, (b) 1800 UTC 28 January 2007, (c) 0000, (d) 0600, (e) 1200, and (f) 1800 UTC 29 January 2007.

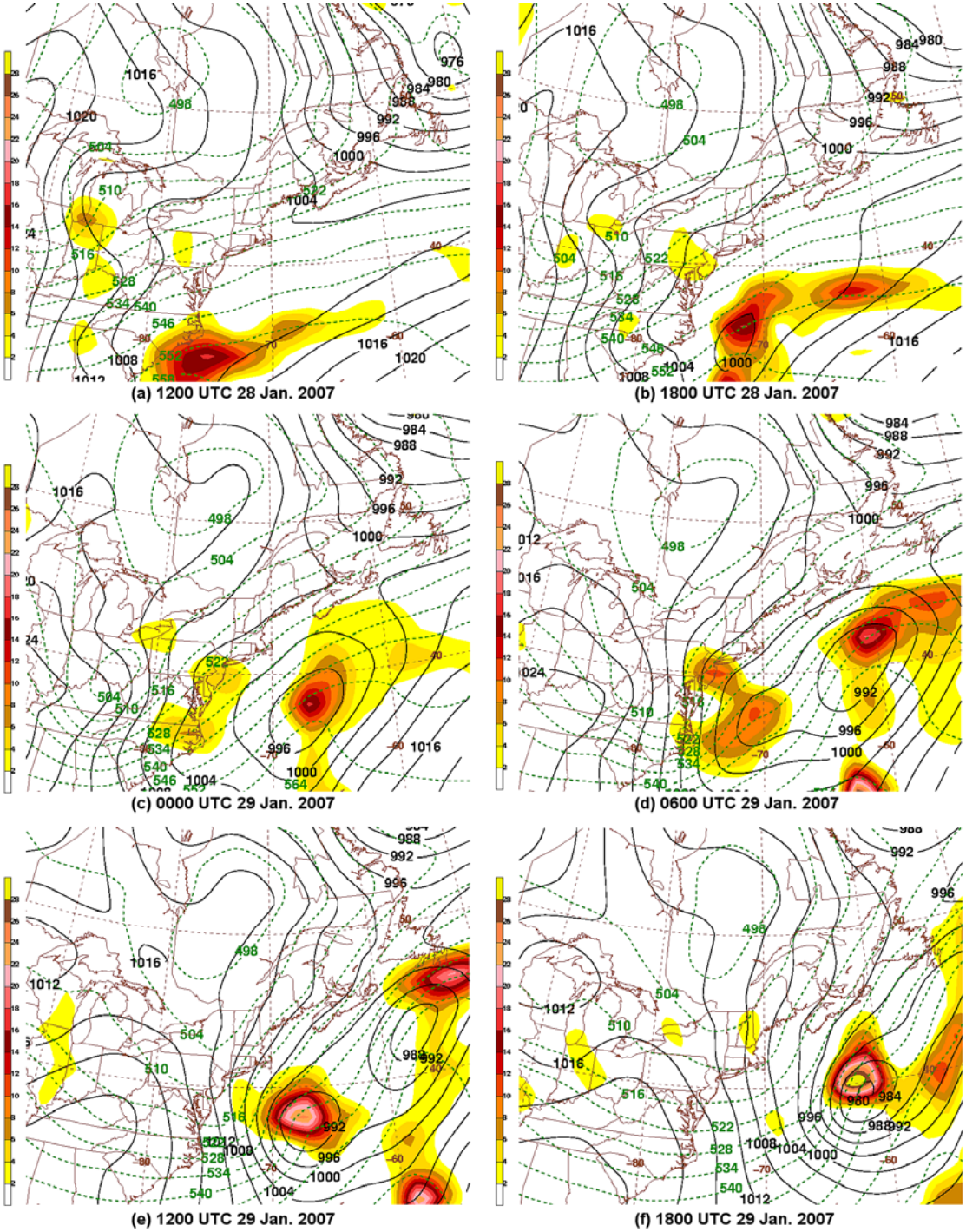

Figure 3.27: As in Fig. 3.10, except for (a) 1200, (b) 1800 UTC 28 January 2007, (c) 0000, (d) 0600, (e) 1200, and (f) 1800 UTC 29 January 2007.

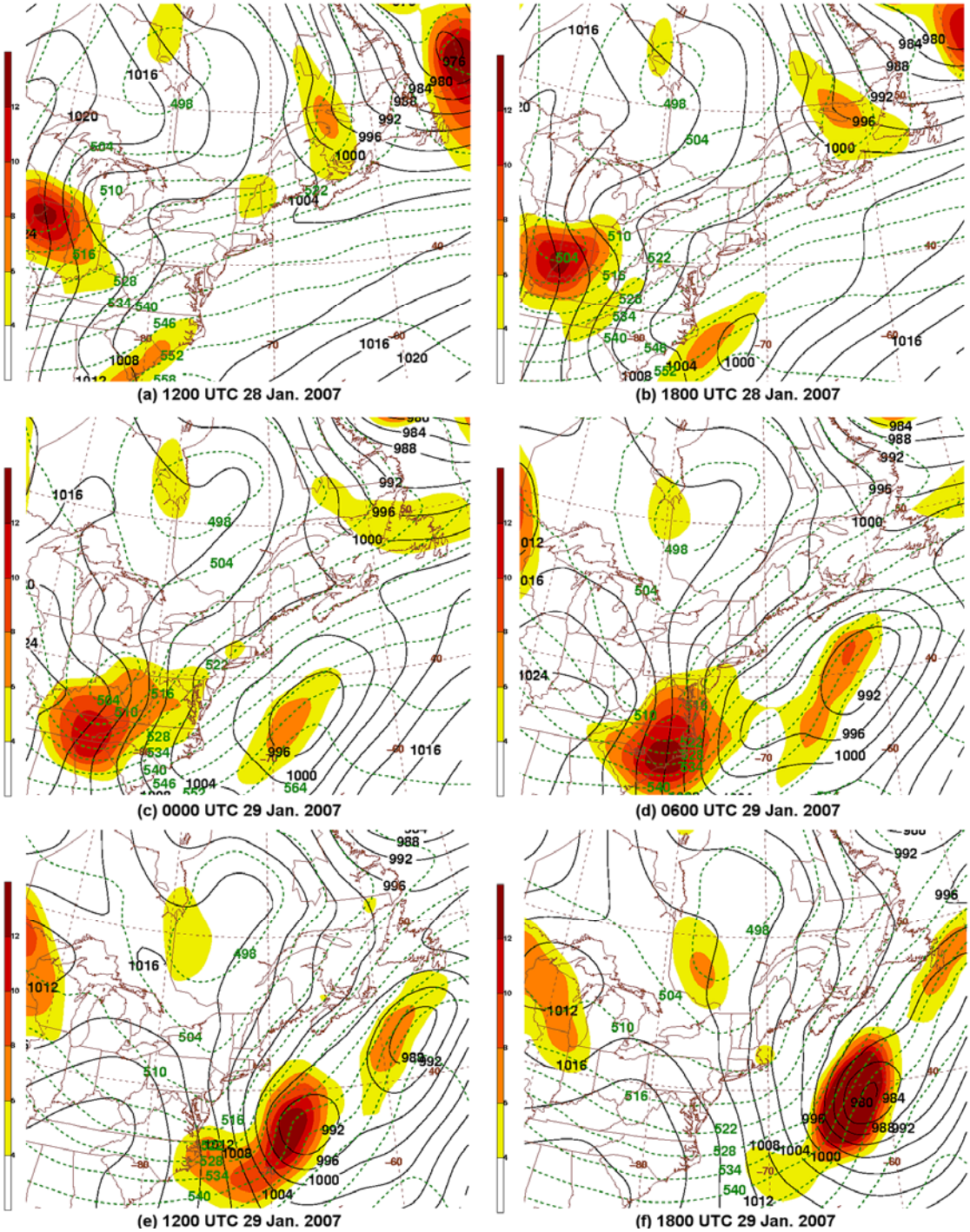

Figure 3.28: As in Fig. 3.11, except for (a) 1200, (b) 1800 UTC 28 January 2007, (c) 0000, (d) 0600, (e) 1200, and (f) 1800 UTC 29 January 2007.

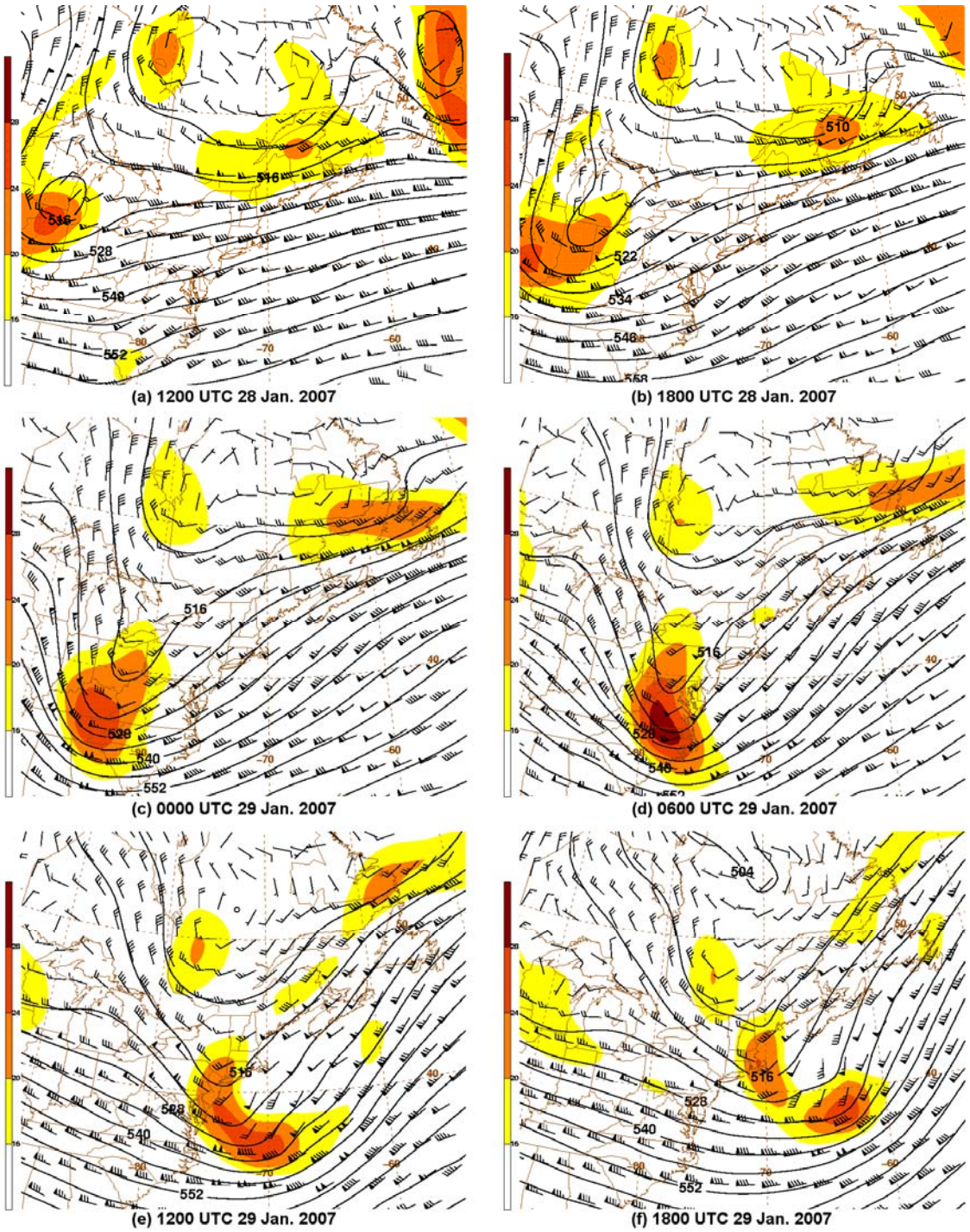

Figure 3.29: As in Fig. 3.12, except for (a) 1200, (b) 1800 UTC 28 January 2007, (c) 0000, (d) 0600, (e) 1200, and (f) 1800 UTC 29 January 2007.

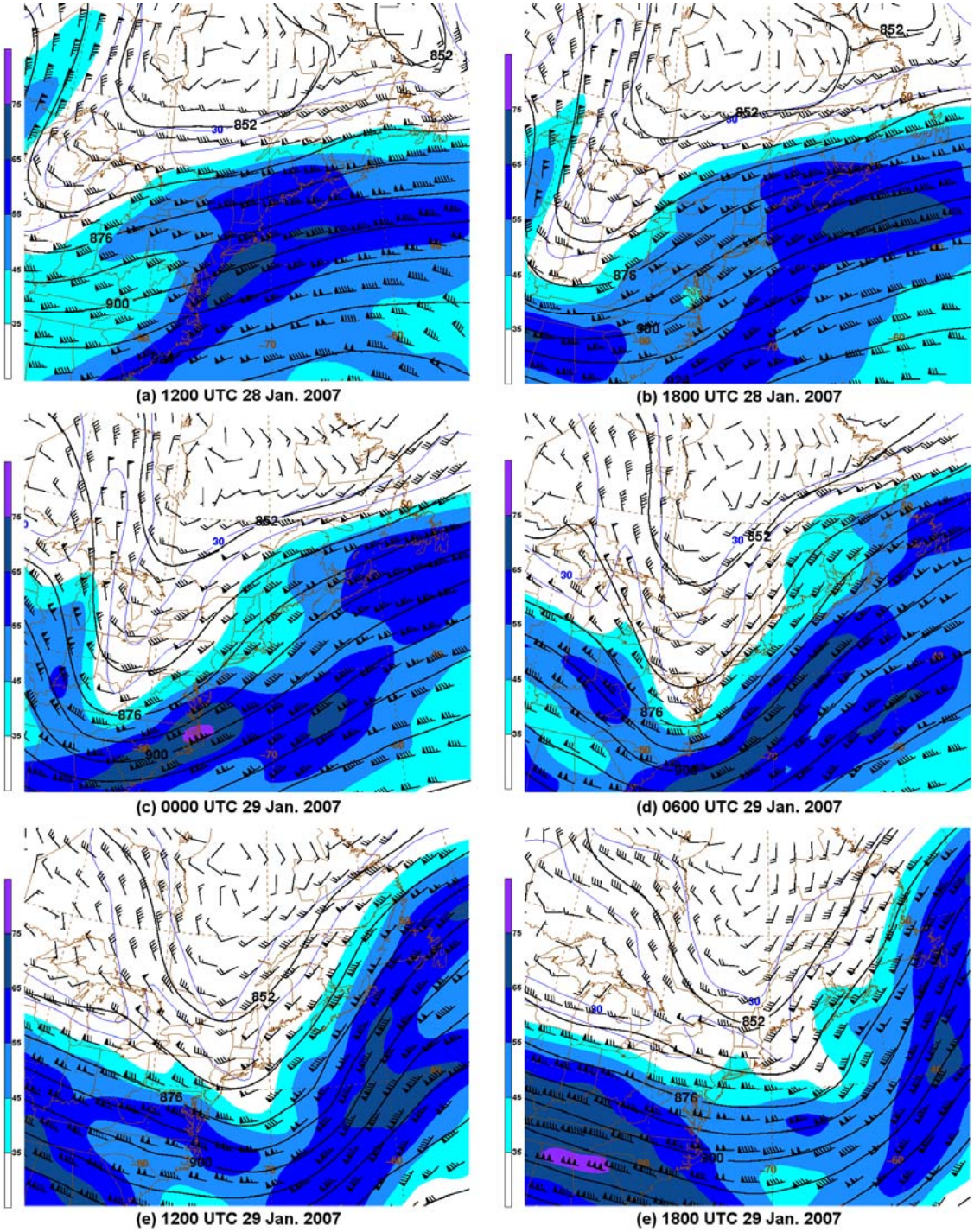

Figure 3.30: As in Fig. 3.13, except for (a) 1200, (b) 1800 UTC 28 January 2007, (c) 0000, (d) 0600, (e) 1200, and (f) 1800 UTC 29 January 2007.

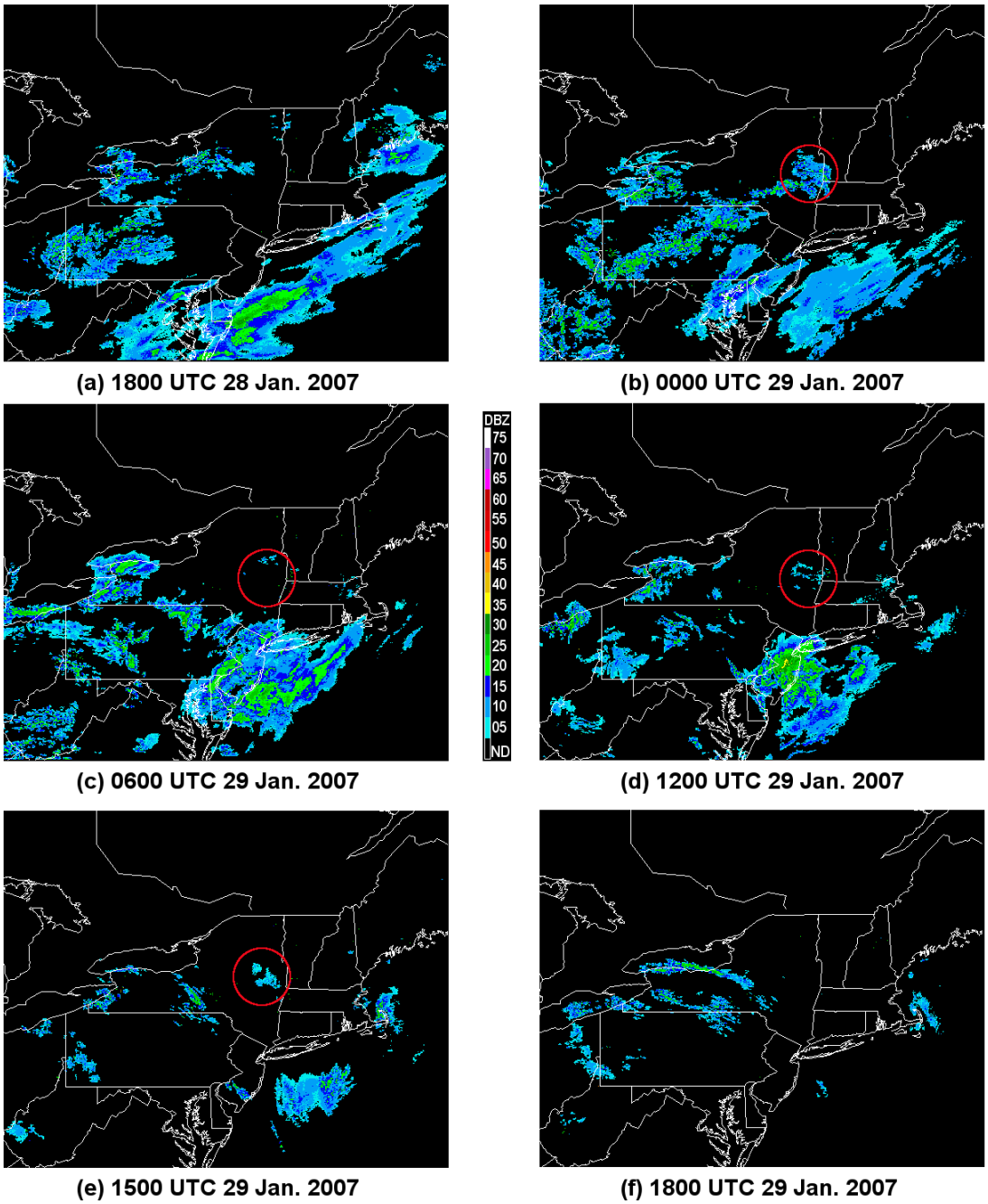

Figure 3.31: As in Fig. 3.14, except for (a) 1800 UTC 28 January 2007, (b) 0000, (c) 0600, (d) 1200, (e) 1500, and (f) 1800 UTC 29 January 2007. Precipitation related to MHC is circled in red.

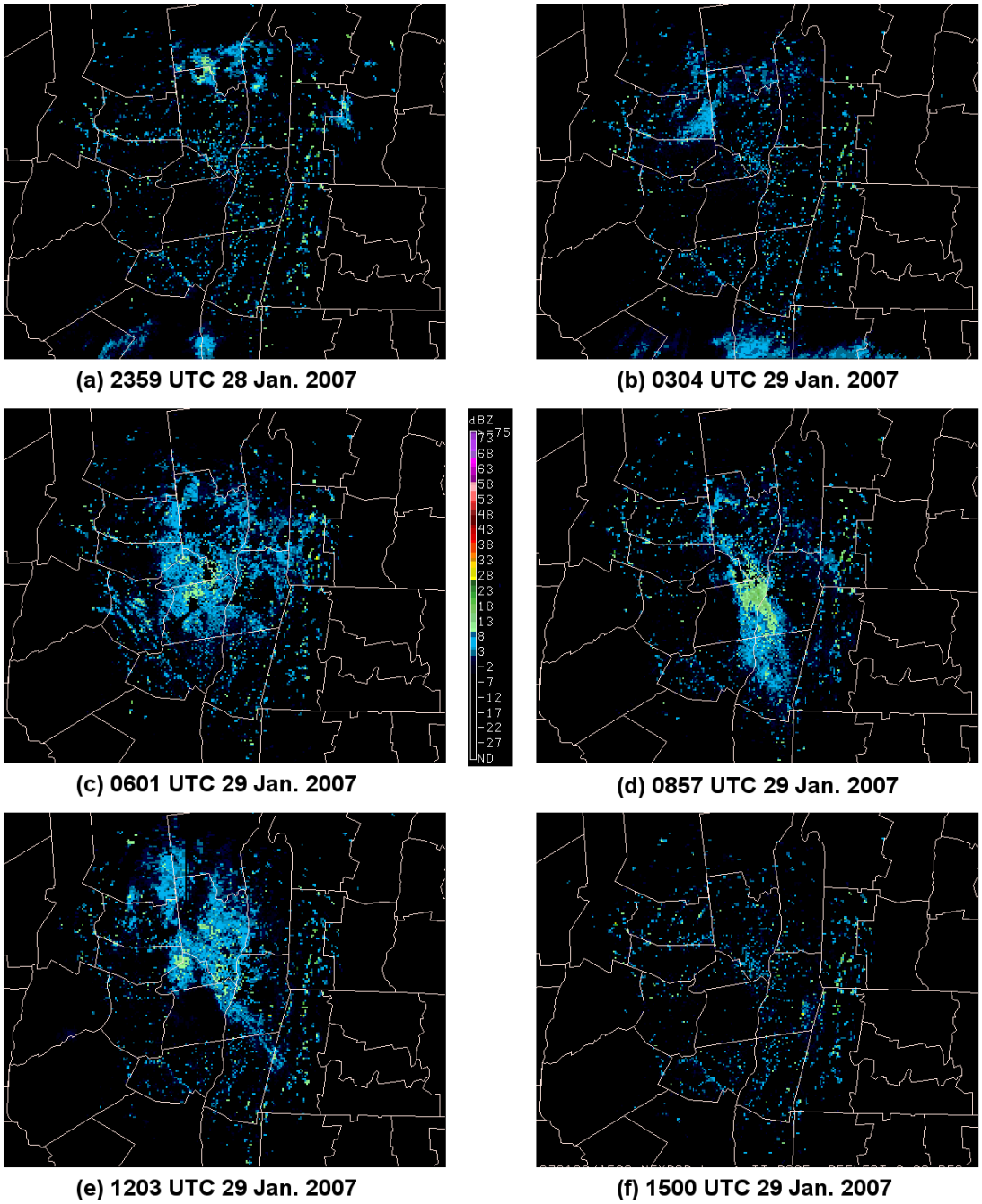

Figure 3.32: As in Fig. 3.15, except for (a) 2359 UTC 28 January 2007, (b) 0304, (c) 0601, (d), 0857, (e) 1203, and (f) 1500 UTC 29 January 2007.

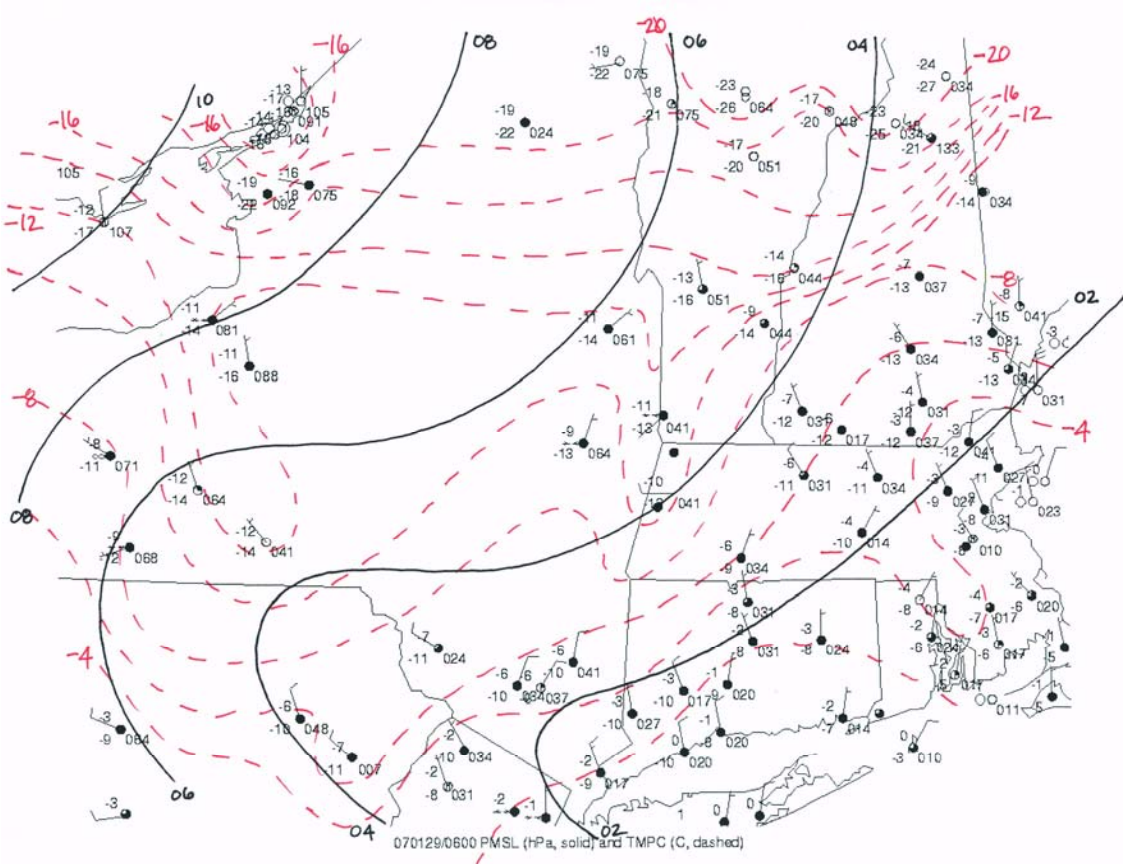

Figure 3.33: As in Fig. 3.16, except for 0600 UTC 29 January 2007.

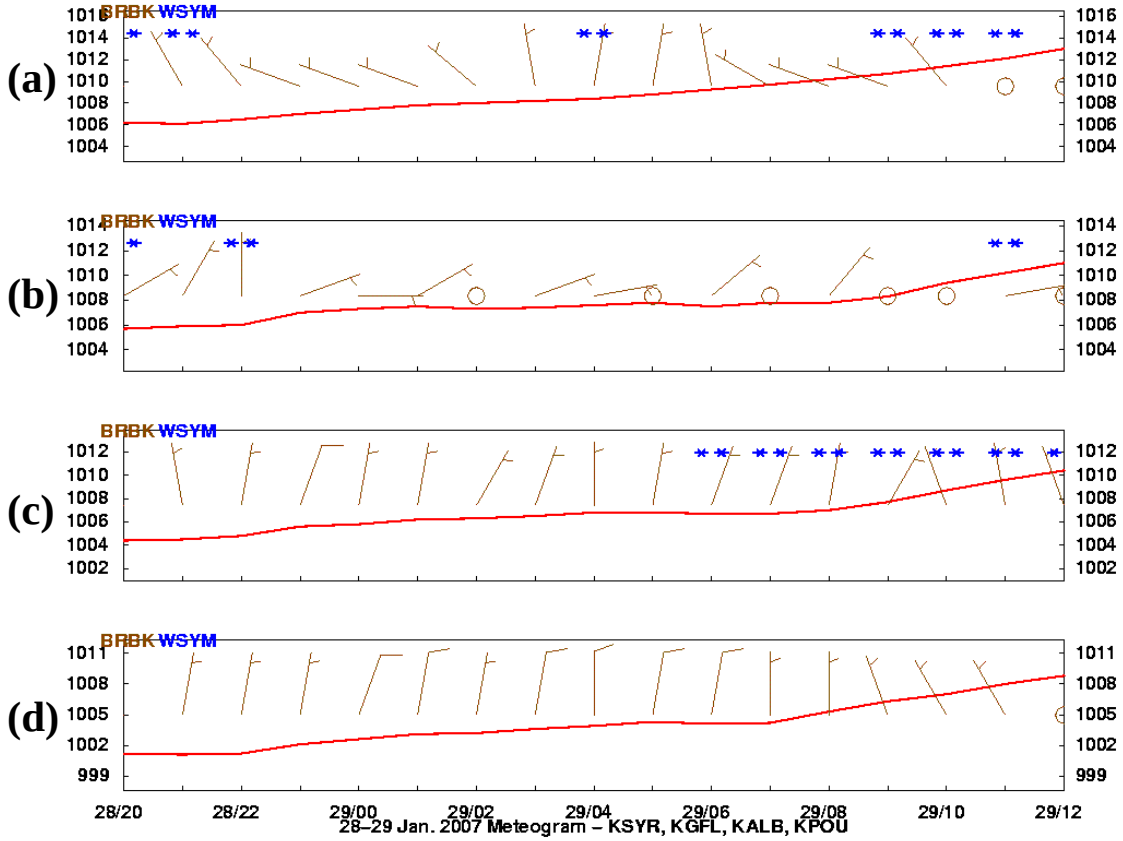

Figure 3.34: As in Fig. 3.17, except from 2000 UTC 28 January to 1200 UTC 29 January 2007 for (a) KSYR, (b) KGFL, (c) KALB and (d) KPOU.

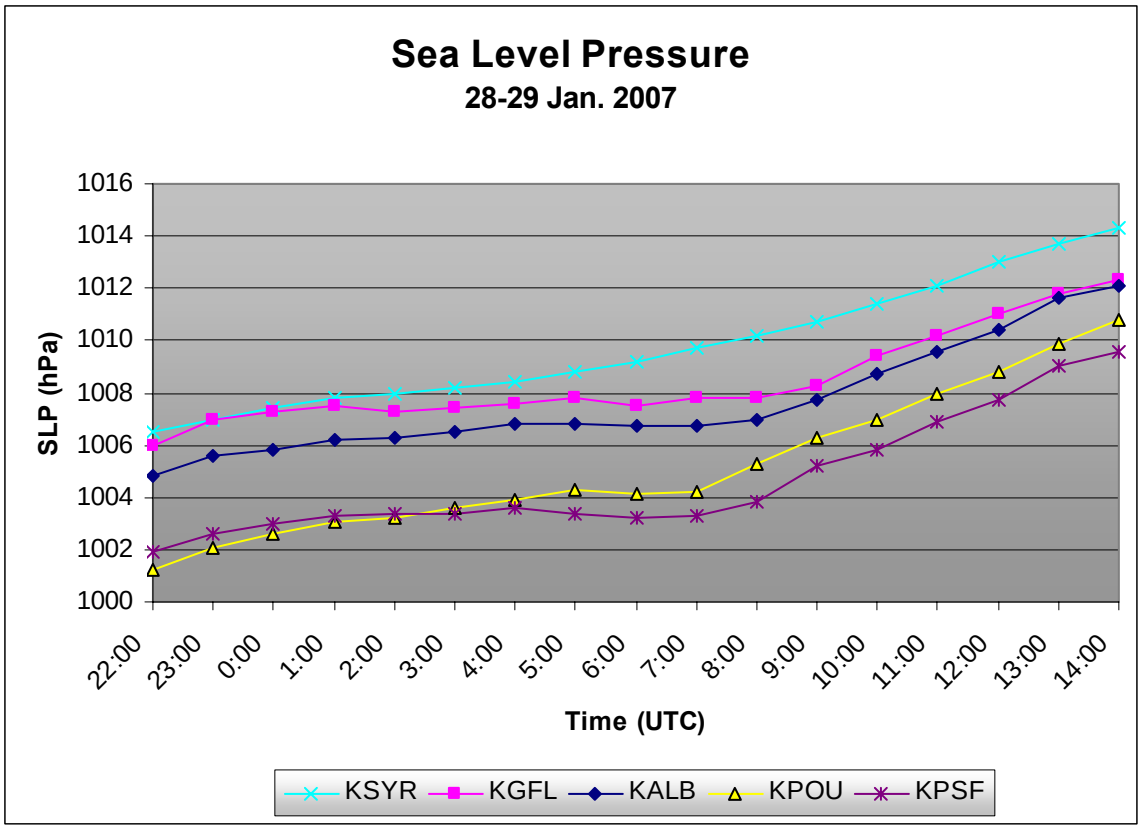

Figure 3.35: As in Fig. 3.18, except from 2200 UTC 28 January to 1400 UTC 29 January 2007 for KSYR, KGFL, KALB, KPOU, and KSPF. (Data source: University at Albany DEAS archives).

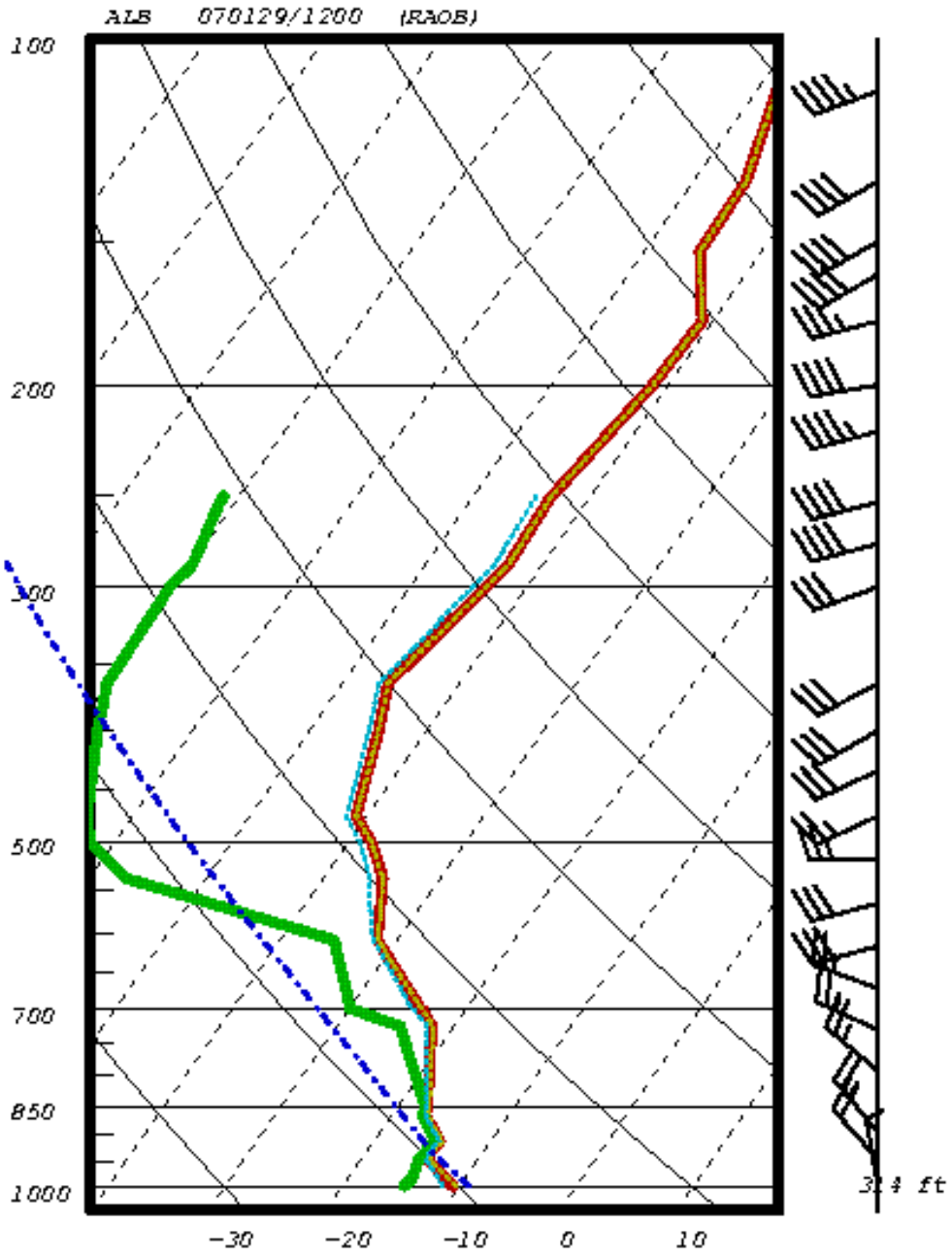

Figure 3.36: As in Fig. 3.19, except for 1200 UTC 29 January 2007.

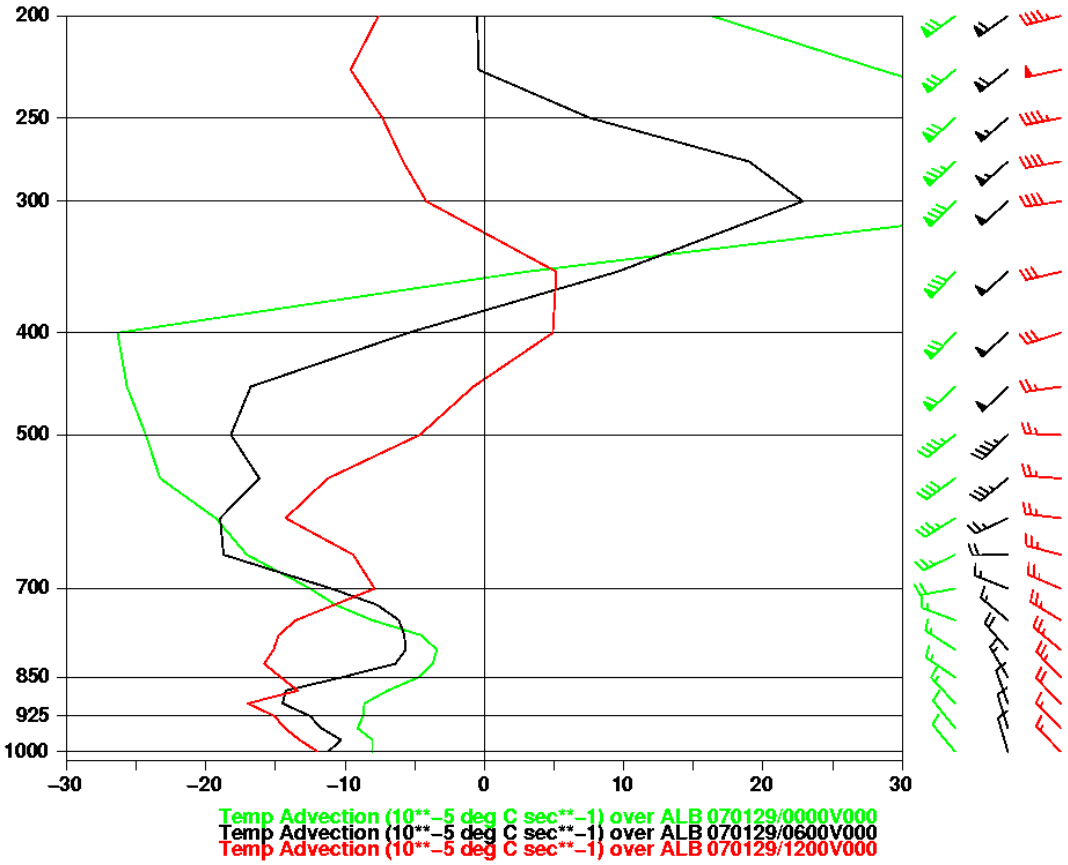

Figure 3.37: As in Fig. 3.21, except for 0000 (green line and barbs), 0600 (black line and barbs), and 1200 UTC 29 January 2007 (red line and barbs).

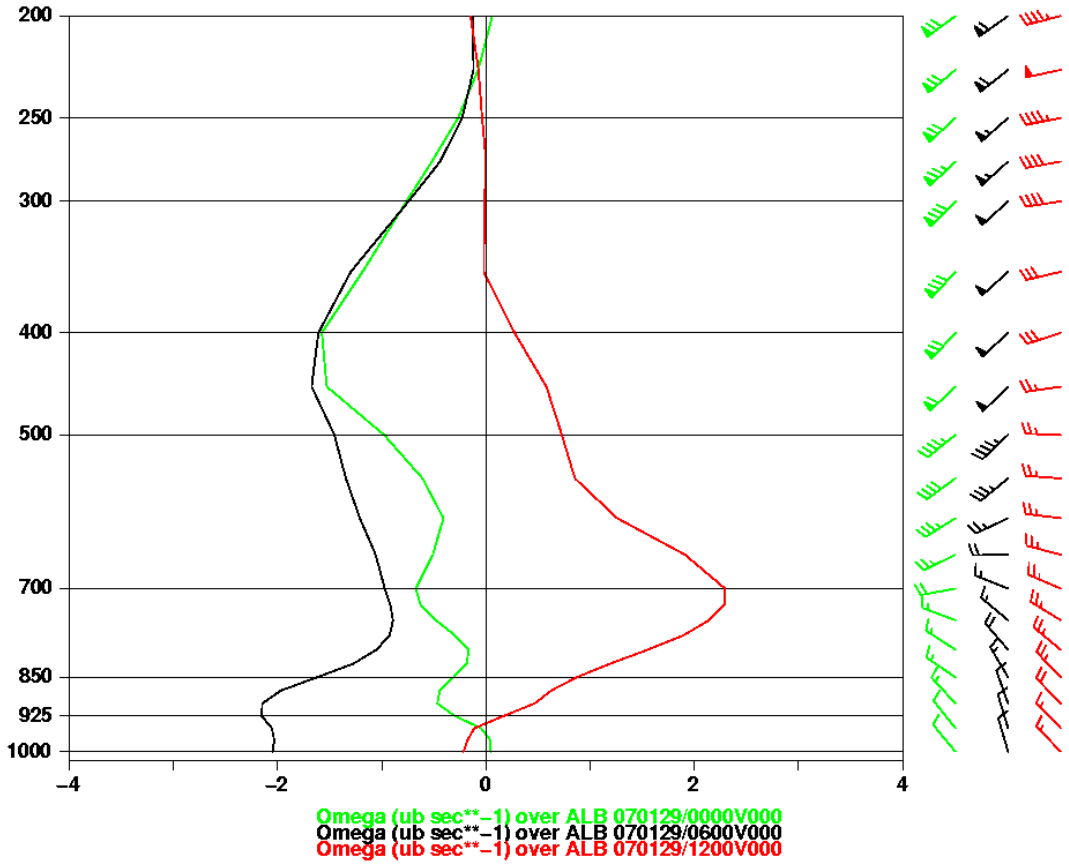

Figure 3.38: As in Fig. 3.22, except for 0000 (green line and barbs), 0600 (black line and barbs), and 1200 UTC 29 January 2007 (red line and barbs).

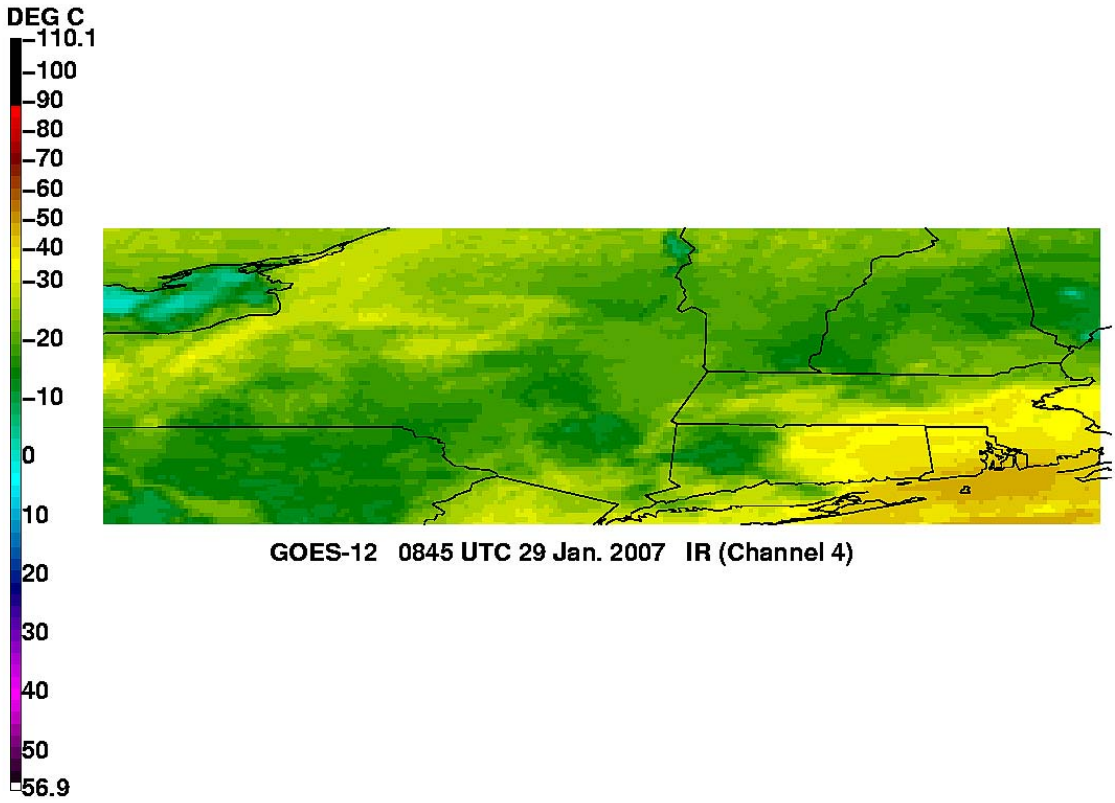

Figure 3.39: As in Fig. 3.23, except from GOES-12 at 0845 UTC 29 January 2007.

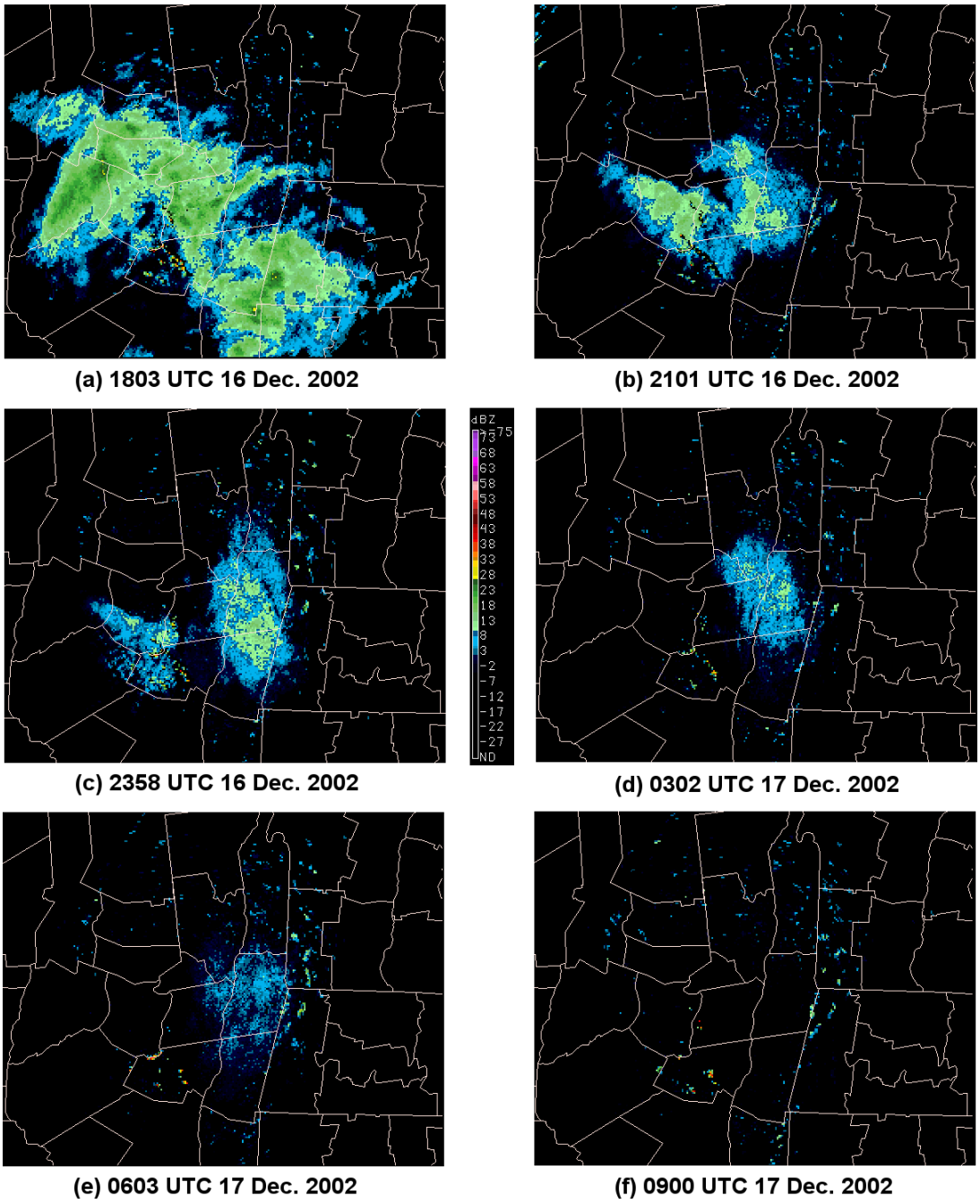

Figure 3.40: As in Fig. 3.15, except for (a) 1803, (b) 2101, (c) 2358 UTC 16 December 2002, (d) 0302, (e) 0603, and (f) 0900 UTC 17 December 2002.

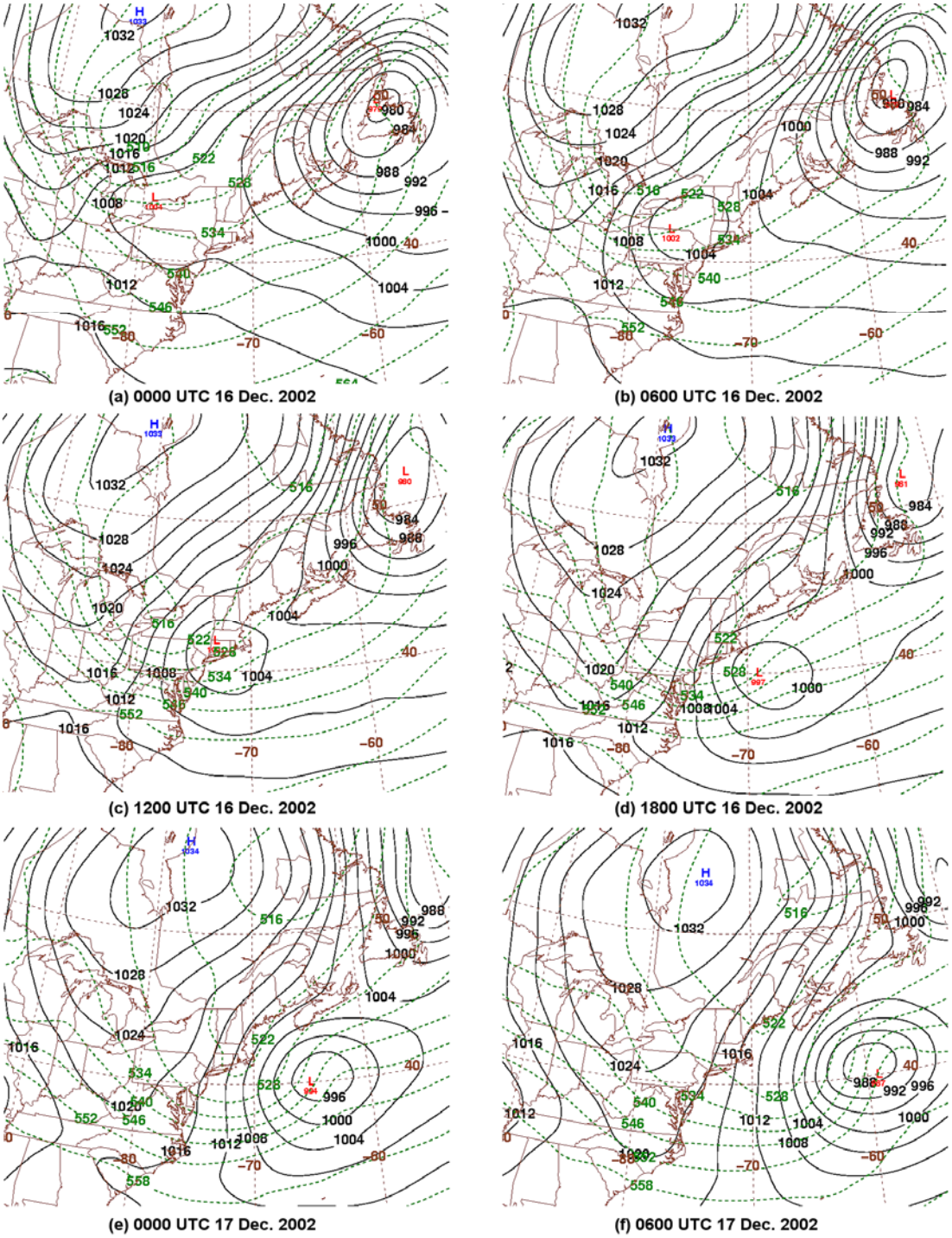

Figure 3.41: As in Fig. 3.7, except for (a) 0000, (b) 0600, (c) 1200, (d) 1800 UTC 16 December 2002, (e) 0000, and (f) 0600 UTC 17 December 2002.

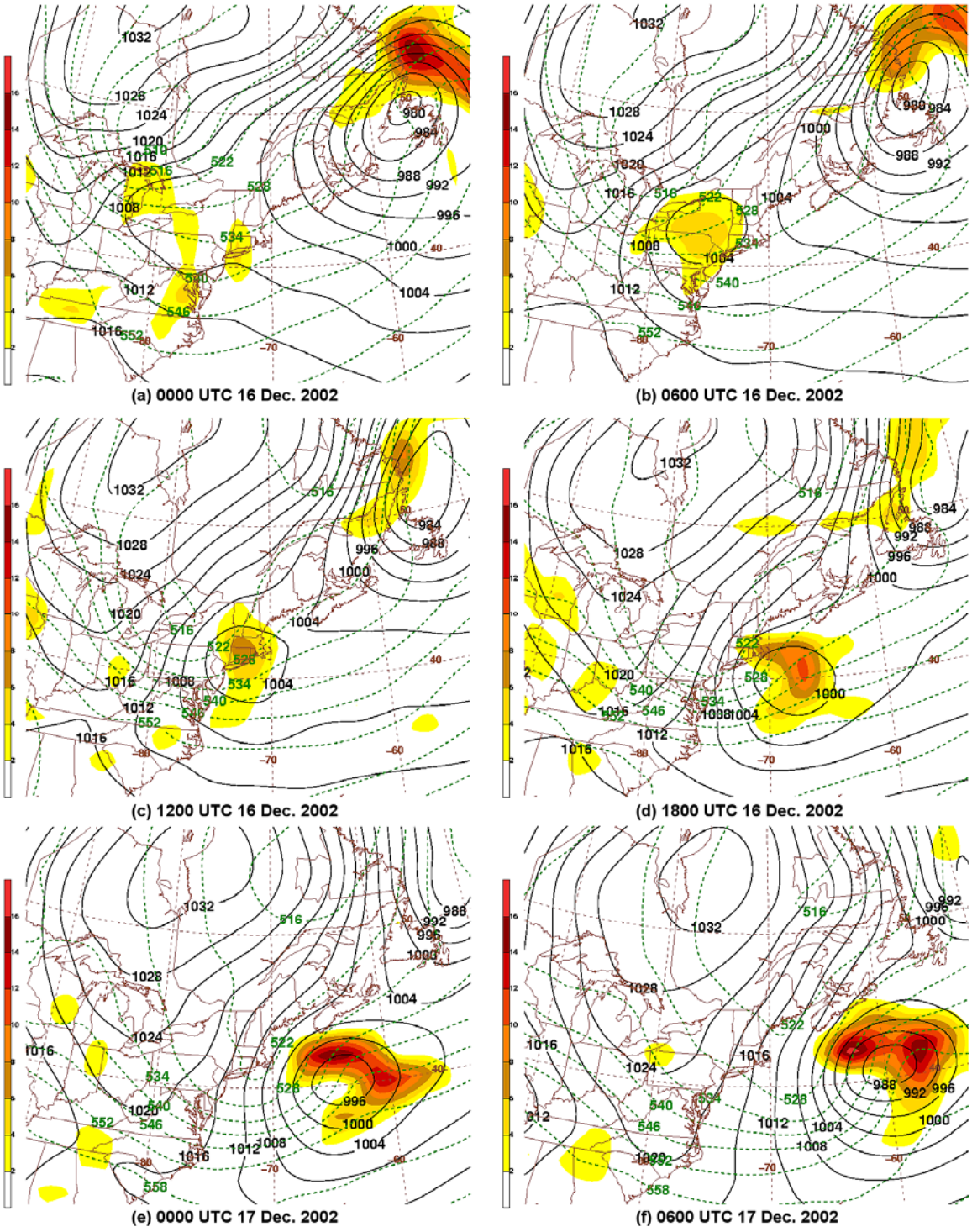

Figure 3.42: As in Fig. 3.10, except for (a) 0000, (b) 0600, (c) 1200, (d) 1800 UTC 16 December 2002, (e) 0000, and (f) 0600 UTC 17 December 2002.

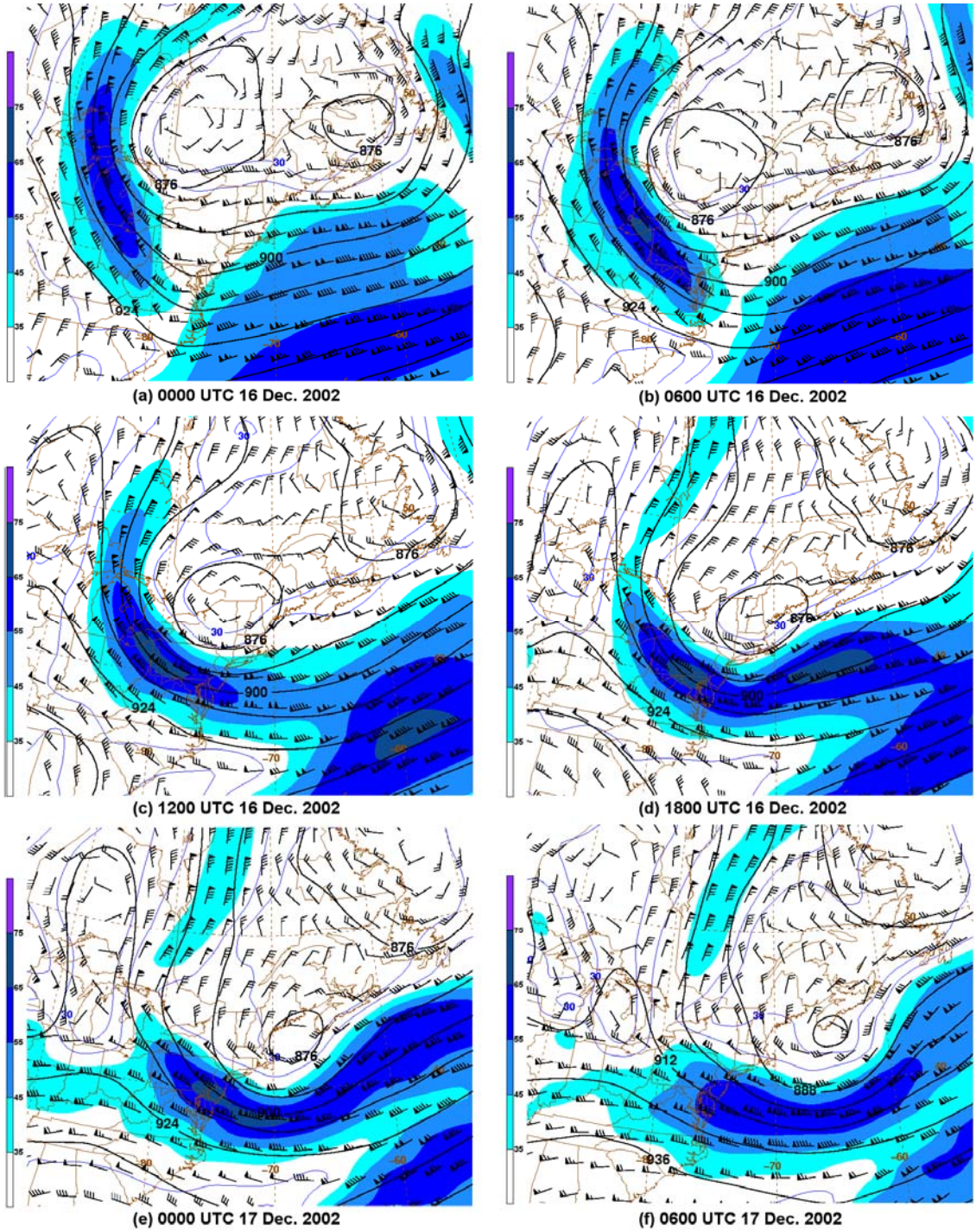

Figure 3.43: As in Fig. 3.13, except for (a) 0000, (b) 0600, (c) 1200, (d) 1800 UTC 16 December 2002, (e) 0000, and (f) 0600 UTC 17 December 2002.

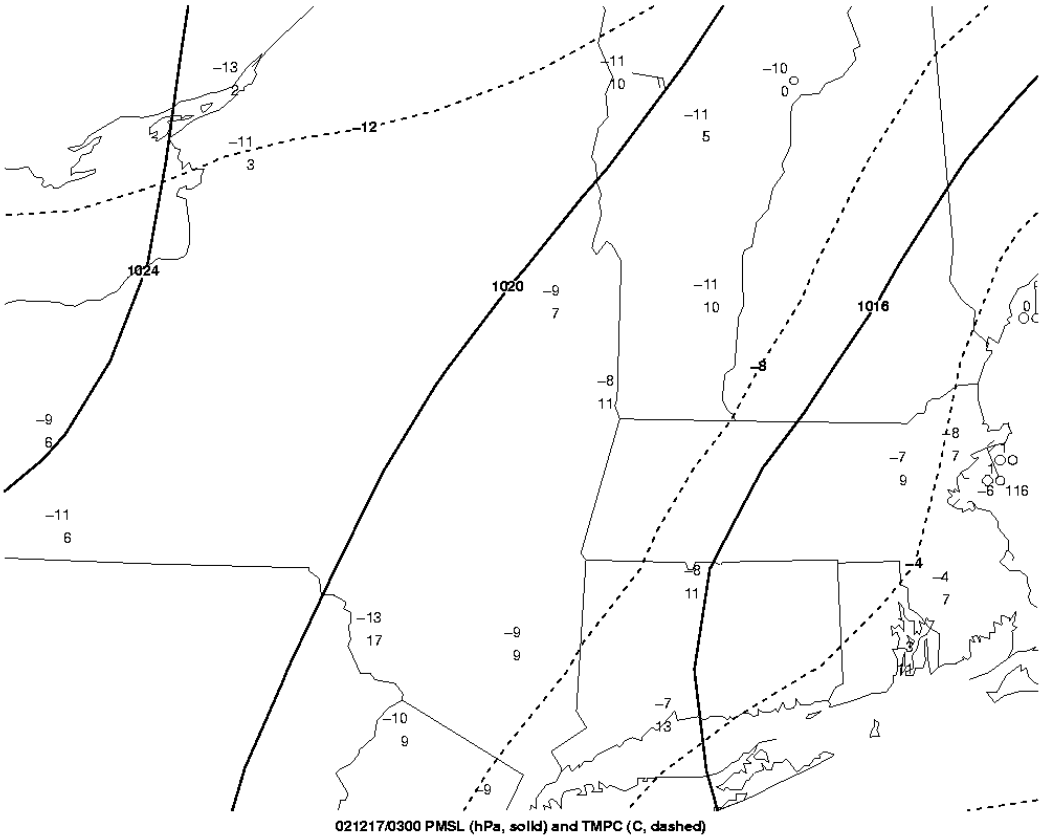

Figure 3.44: Regional surface analysis for eastern New York and New England at 0300 UTC 17 December 2002. Isobars (solid) every 4 hPa. Isotherms (dashed) every 4°C. Temperature (°C) is plotted above visibility at several stations; missing station data have been omitted. (Data source: the University at Albany DEAS archives, with supplemental data provided by the Historical Weather Data Archives of NSSL).

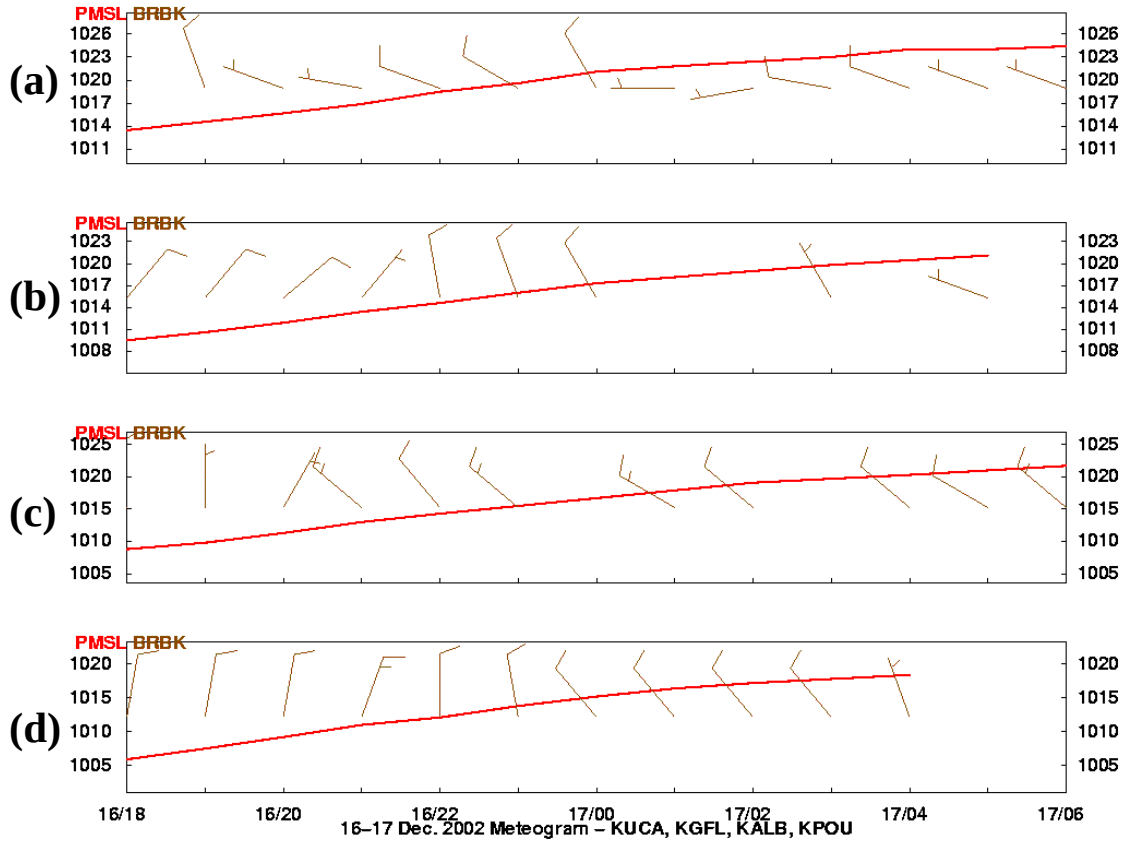

Figure 3.45: As in Fig. 3.17, except from 1800 UTC 16 December to 0600 UTC 17 December 2002. (Data source: the University at Albany DEAS archives, with supplemental data provided by the Historical Weather Data Archives of NSSL).

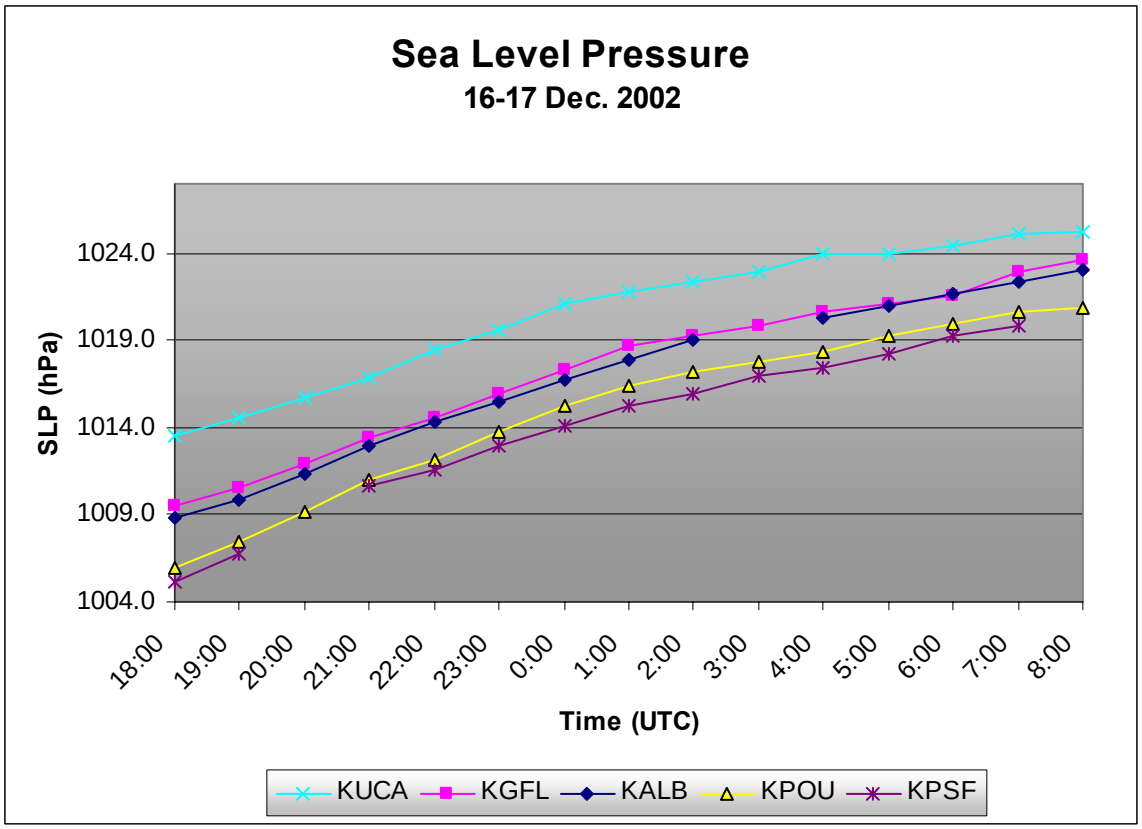

Figure 3.46: As in Fig. 3.18, except from 1800 UTC 16 December to 0800 UTC 17 December 2002).

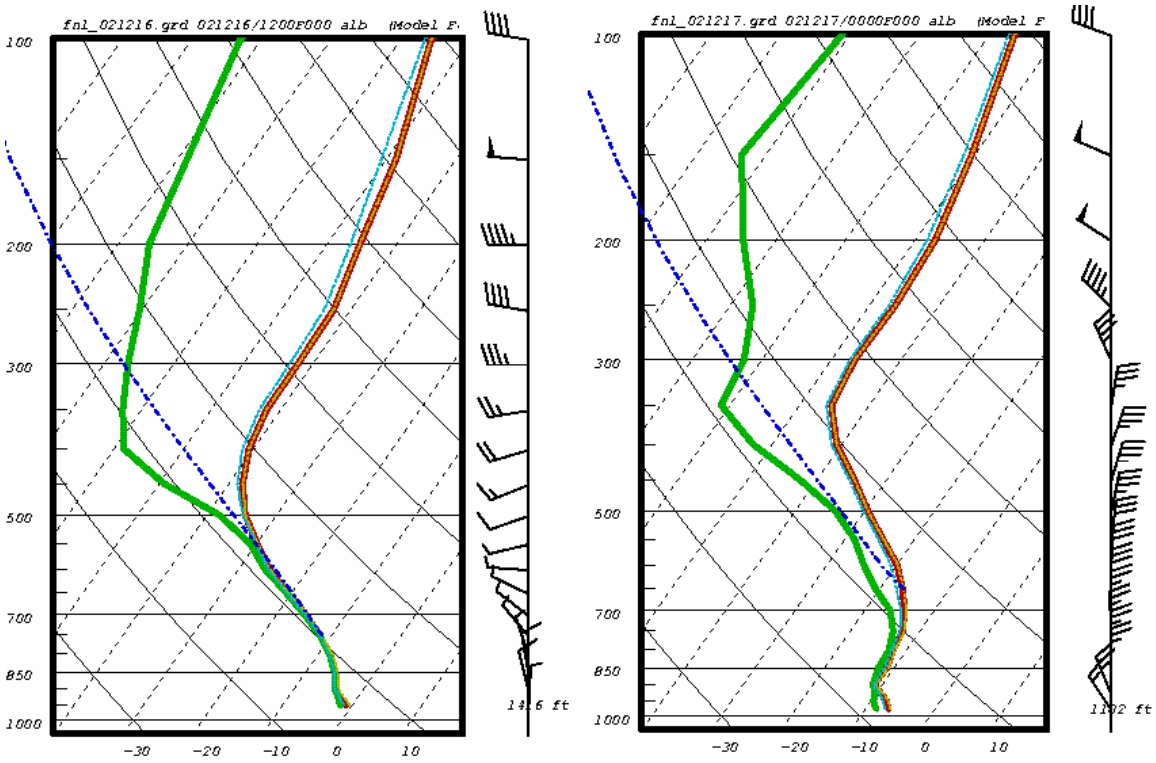

(a) **(b)**

Figure 3.47: As in Fig. 3.19, except for (a) 1200 UTC 16 December 2002 and (b) 0000 UTC 17 December 2002. (Data source: 0-h gridded, initialized 1.0° NCEP GFS analyses).

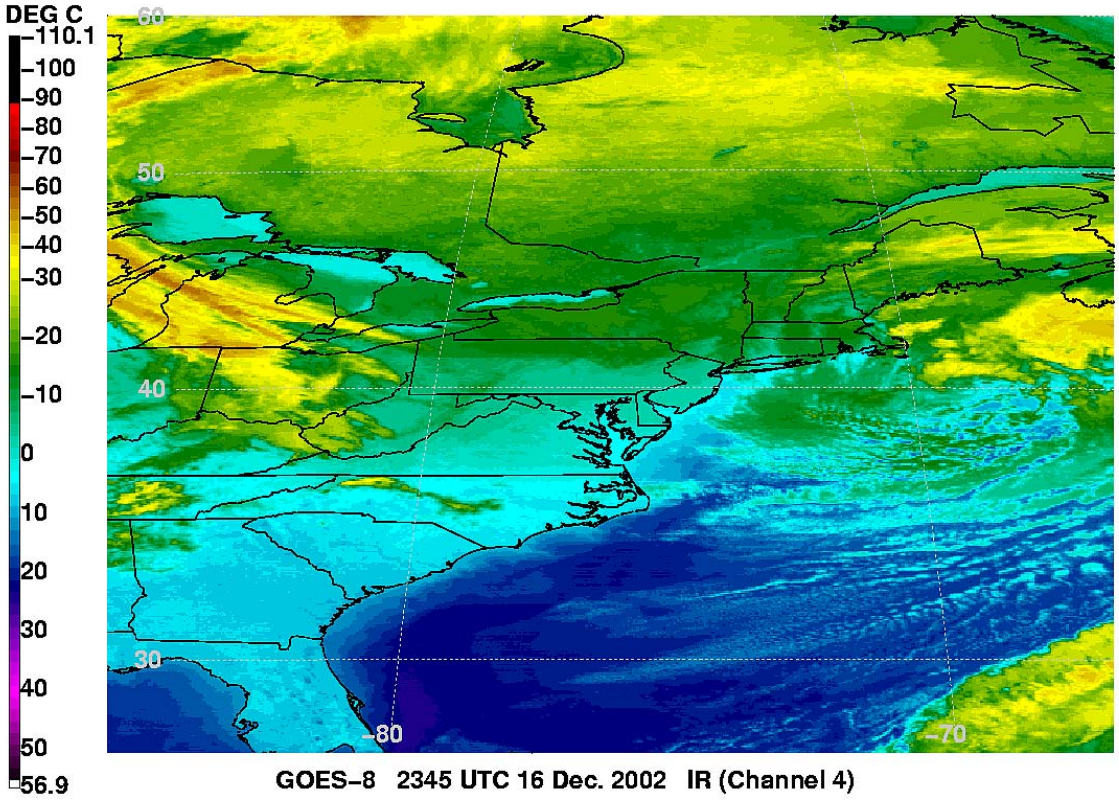

Figure 3.48: As in Fig. 3.23, except for 2345 UTC 16 December 2002.

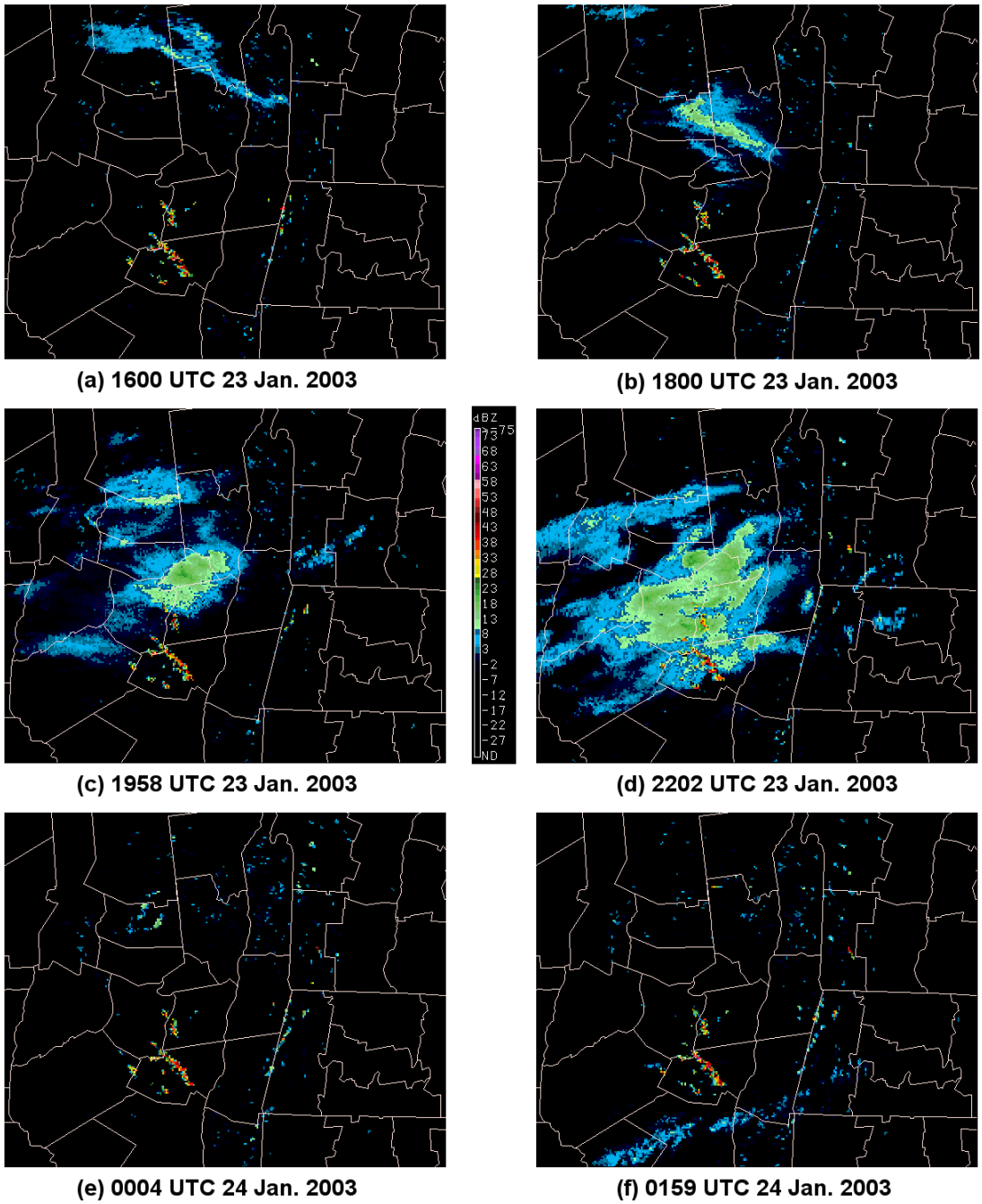

Figure 3.49: As in Fig. 3.15, except for (a) 1600, (b) 1800, (c) 1958, (d) 2202 UTC 23 January 2003, (e) 0004, and (f) 0159 UTC 24 January 2003.

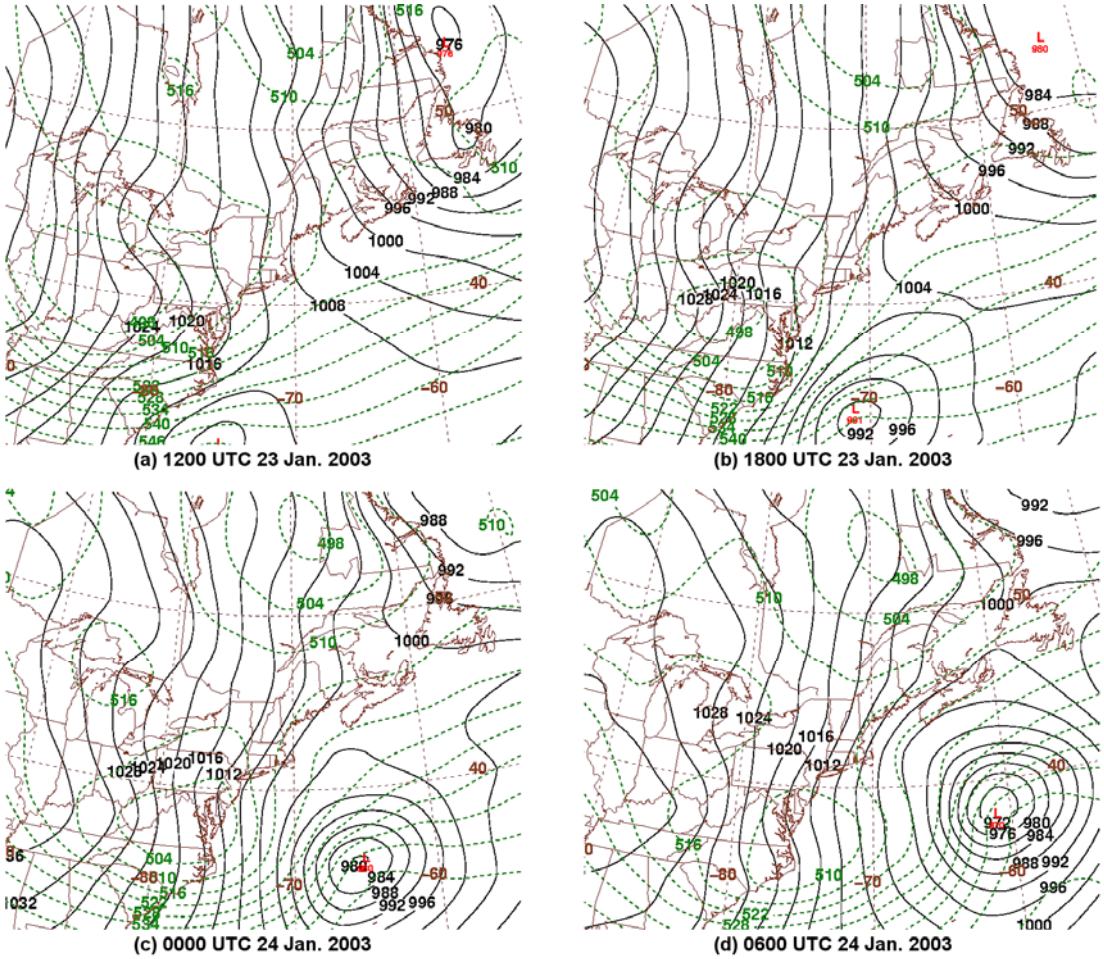

Figure 3.50: As in Fig. 3.7, except for (a) 1200, (b) 1800 UTC 23 January 2003, (c) 0000, and (d) 0600 UTC 24 January 2003.

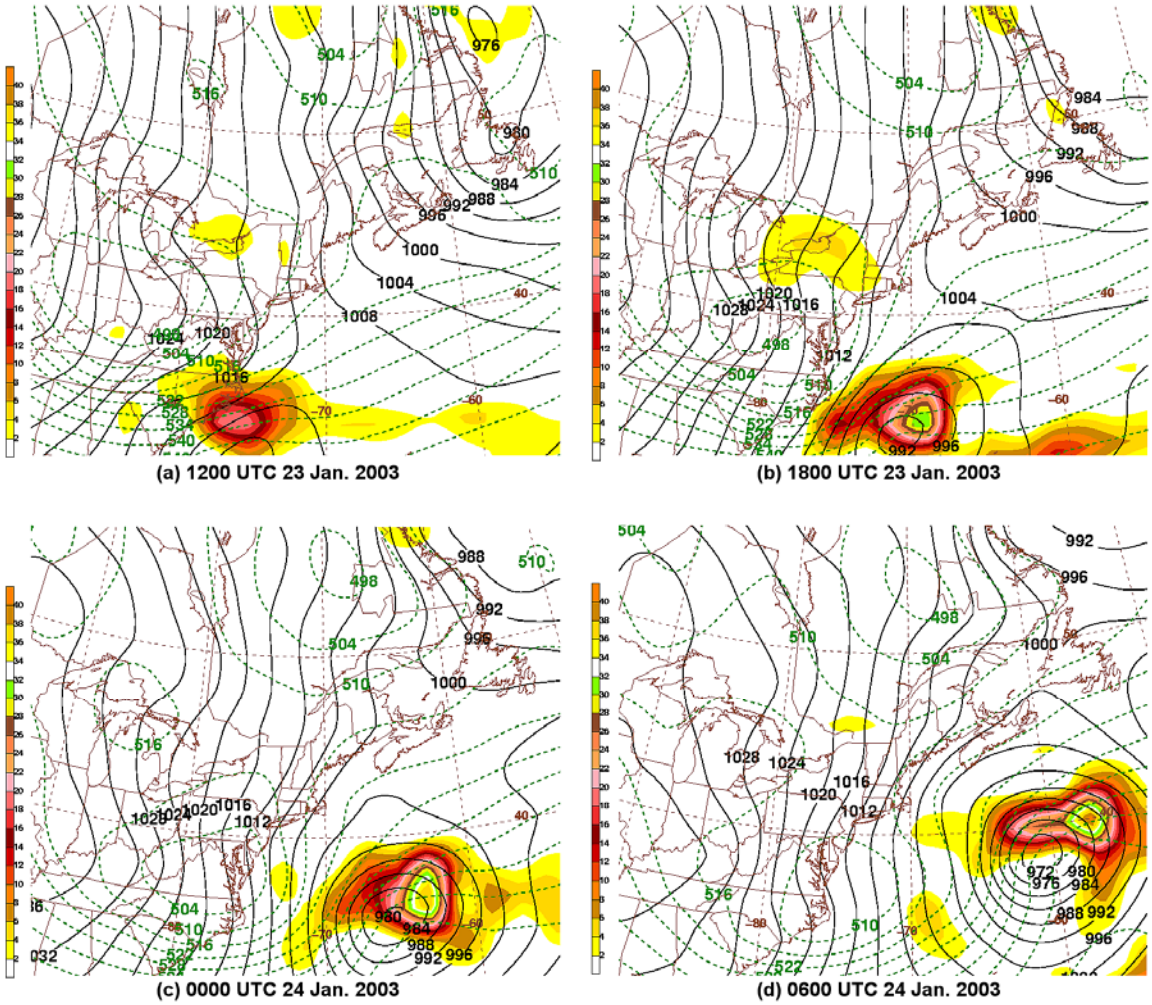

Figure 3.51: As in Fig. 3.10, except for (a) 1200, (b) 1800 UTC 23 January 2003, (c) 0000, and (d) 0600 UTC 24 January 2003.

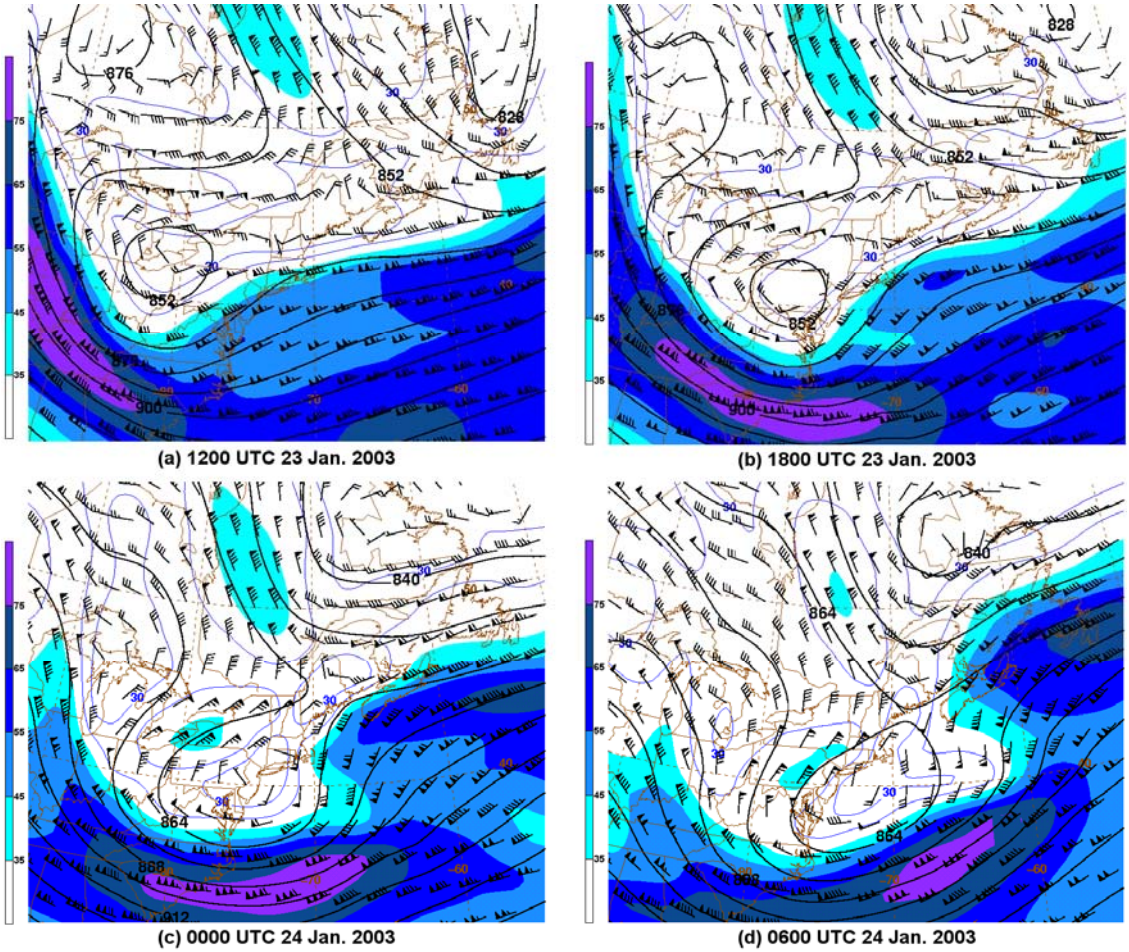

Figure 3.52: As in Fig. 3.13, except for (a) 1200, (b) 1800 UTC 23 January 2003, (c) 0000, and (d) 0600 UTC 24 January 2003.

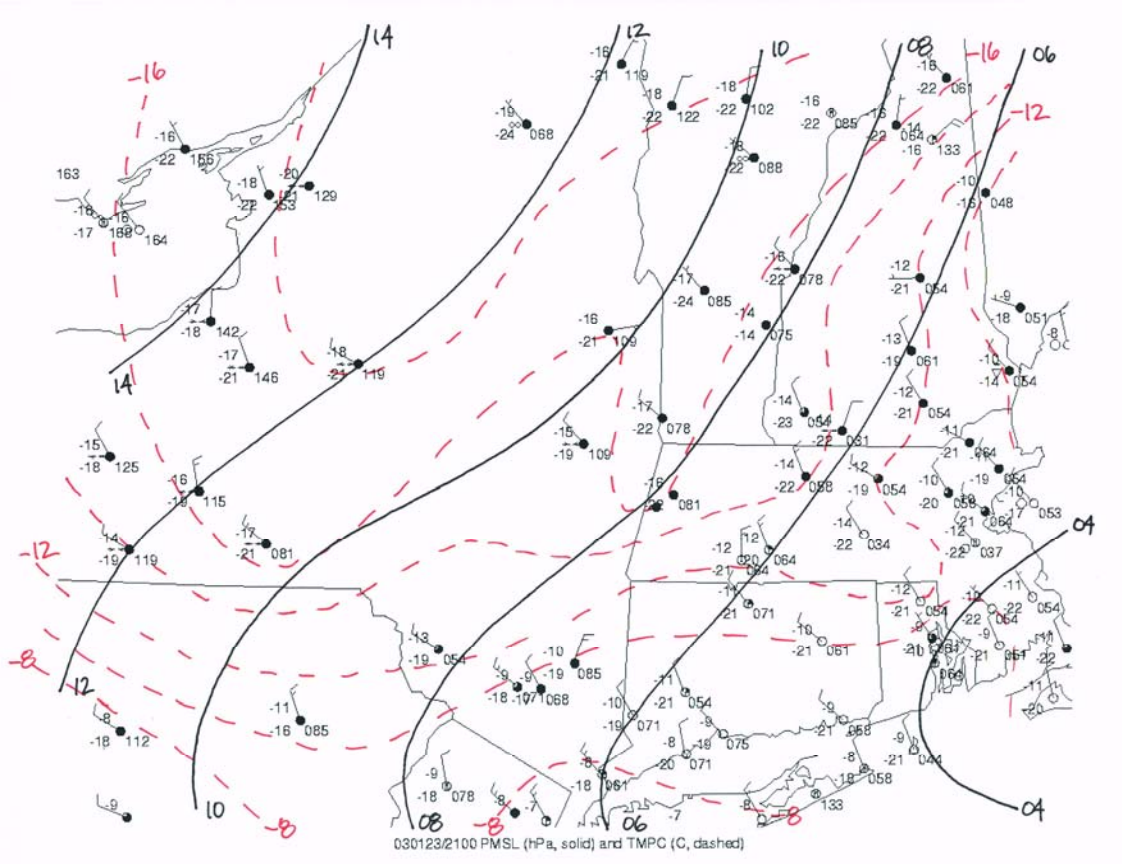

Figure 3.53: As in Fig. 3.16, except for 2100 UTC 23 January 2003.

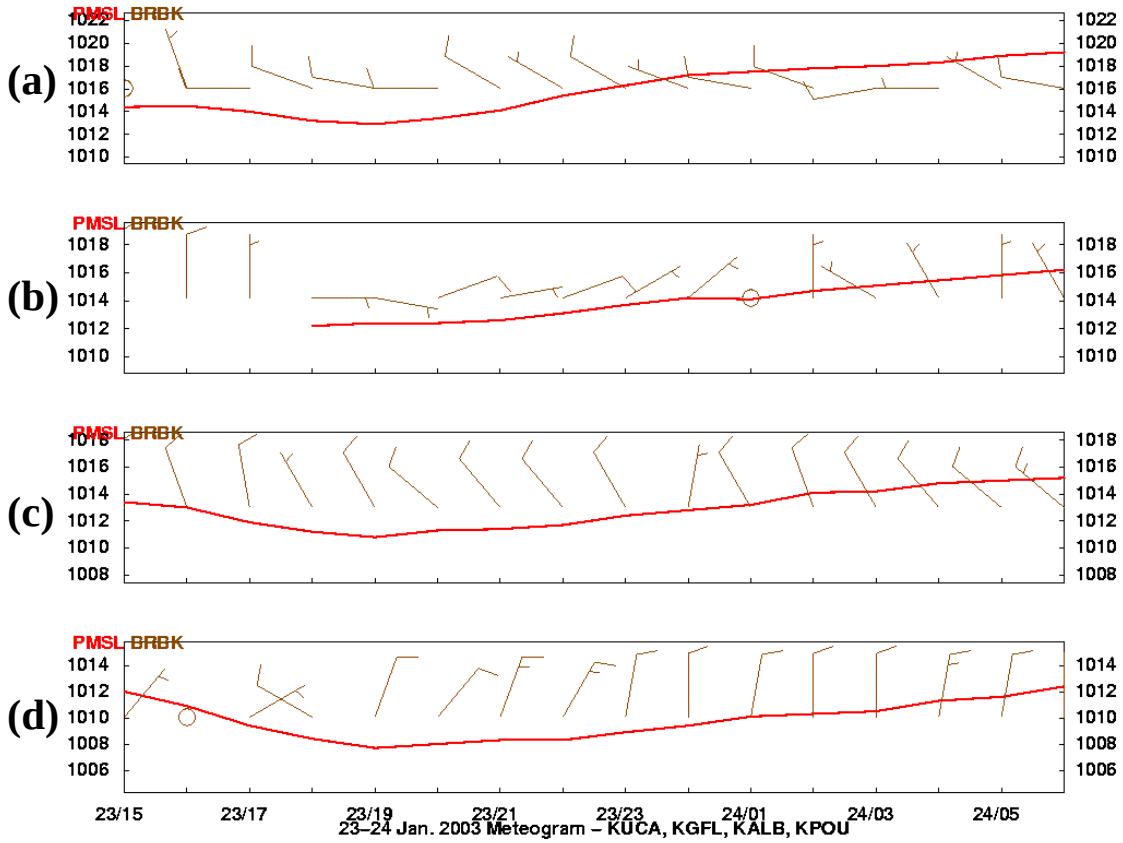

Figure 3.54: As in Fig. 3.17, except from 1500 UTC 23 January to 0600 UTC 24 January 2003. (Data source: the University at Albany DEAS archives, with supplemental data provided by the Historical Weather Data Archives of NSSL).

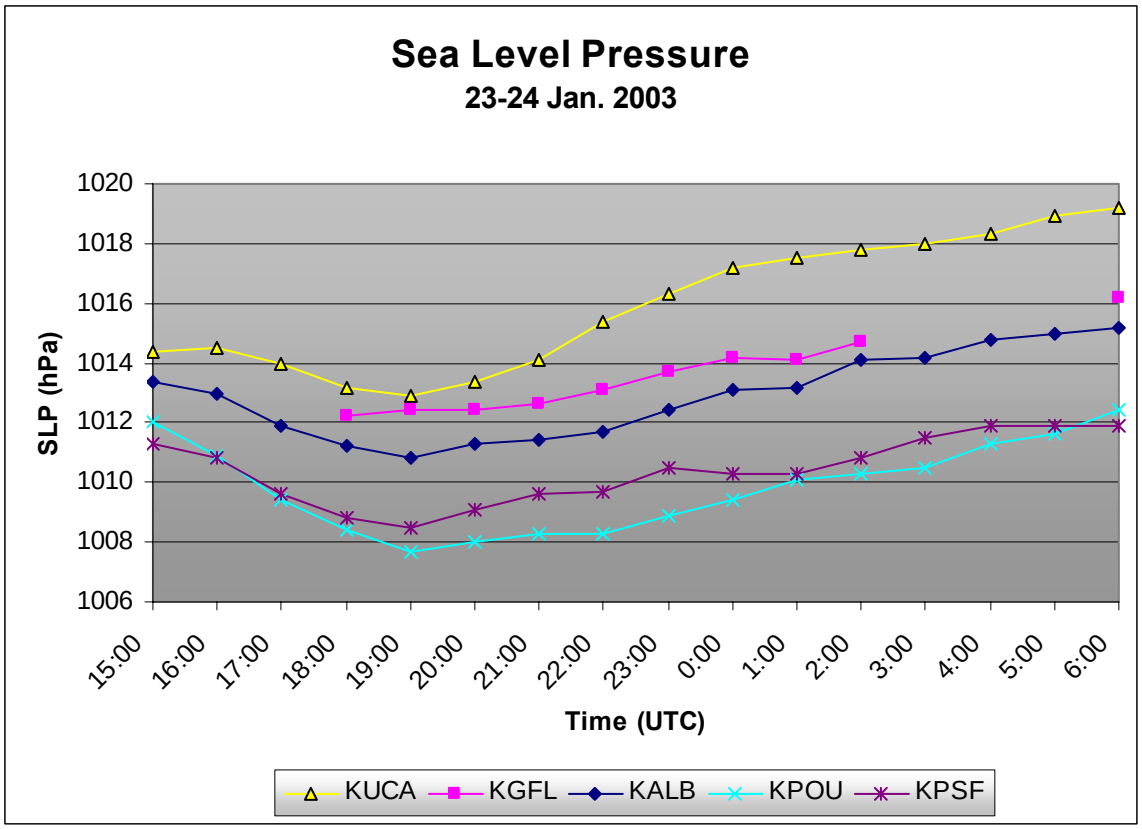

Figure 3.55: As in Fig. 3.18, except from 1500 UTC 23 January to 0600 UTC 24 January 2002. (Data source: the University at Albany DEAS archives, with supplemental data provided by the Historical Weather Data Archives of NSSL).

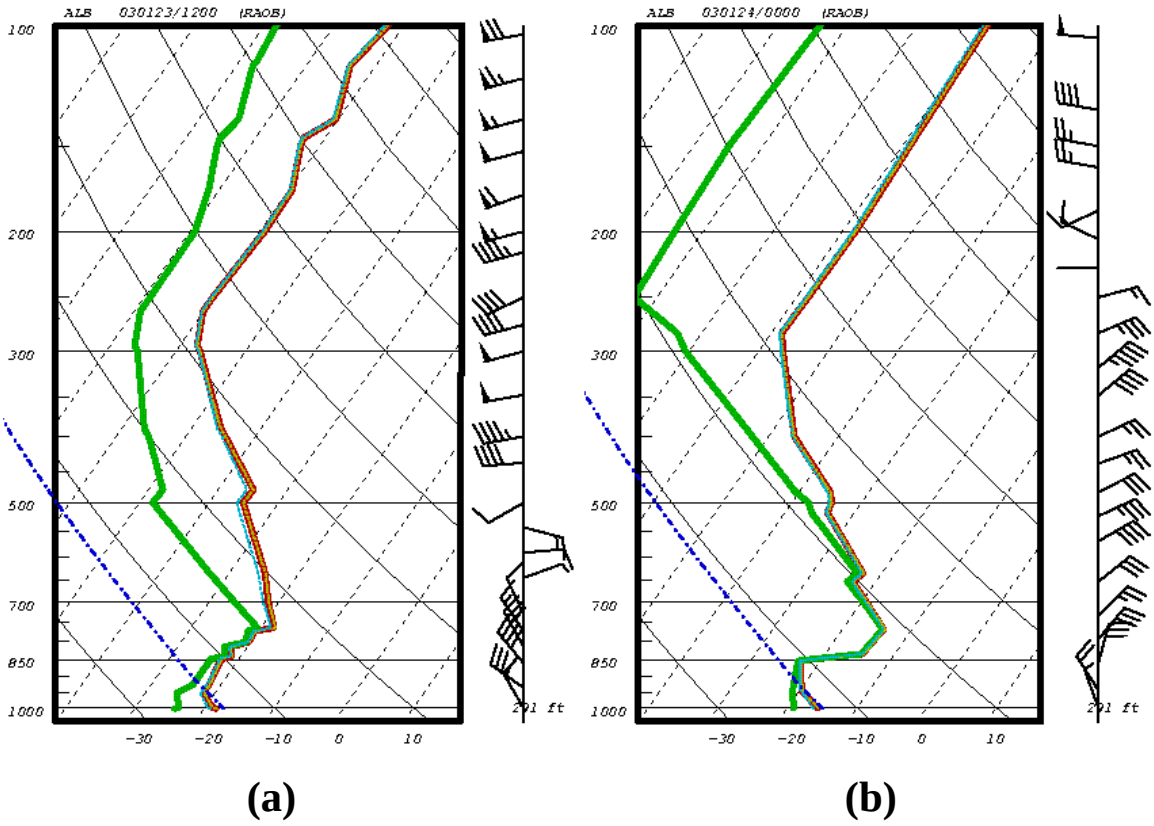

(a) **(b)**

Figure 3.56: As in Fig. 3.19, except for (a) 1200 UTC 23 January 2003 and (b) 0000 UTC 24 January 2003.

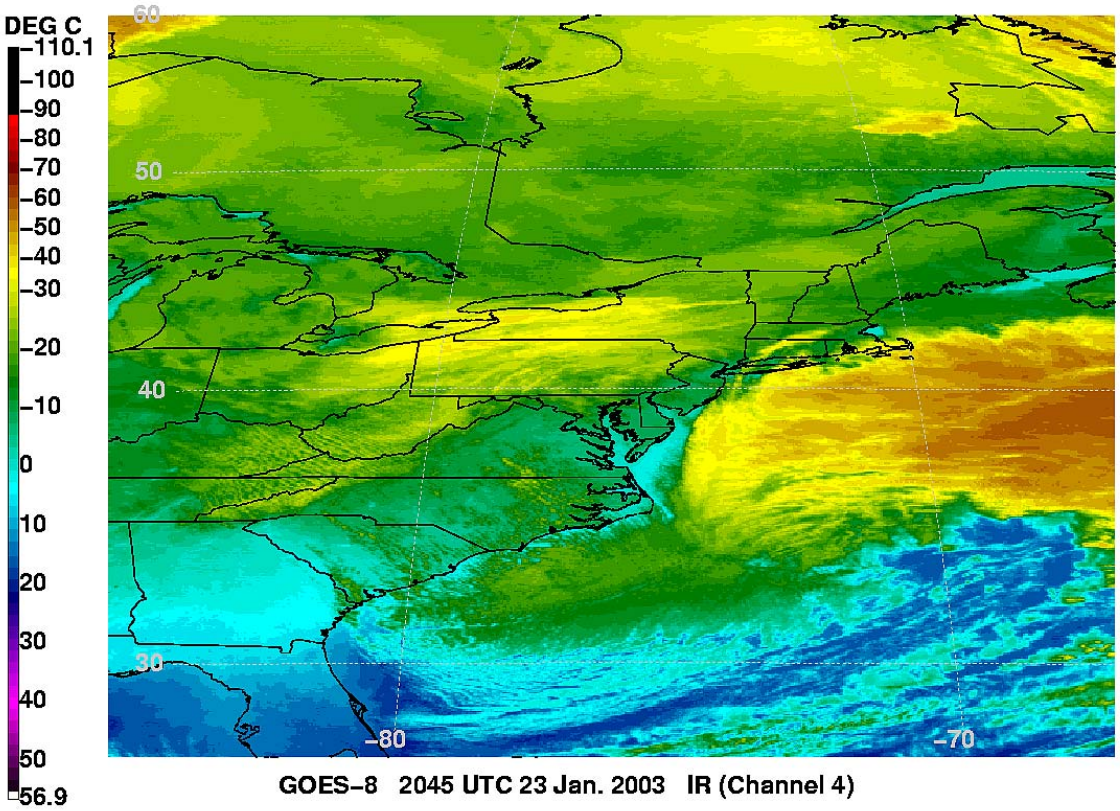

Figure 3.57: As in Fig. 3.23, except for 2045 UTC 23 January 2003.

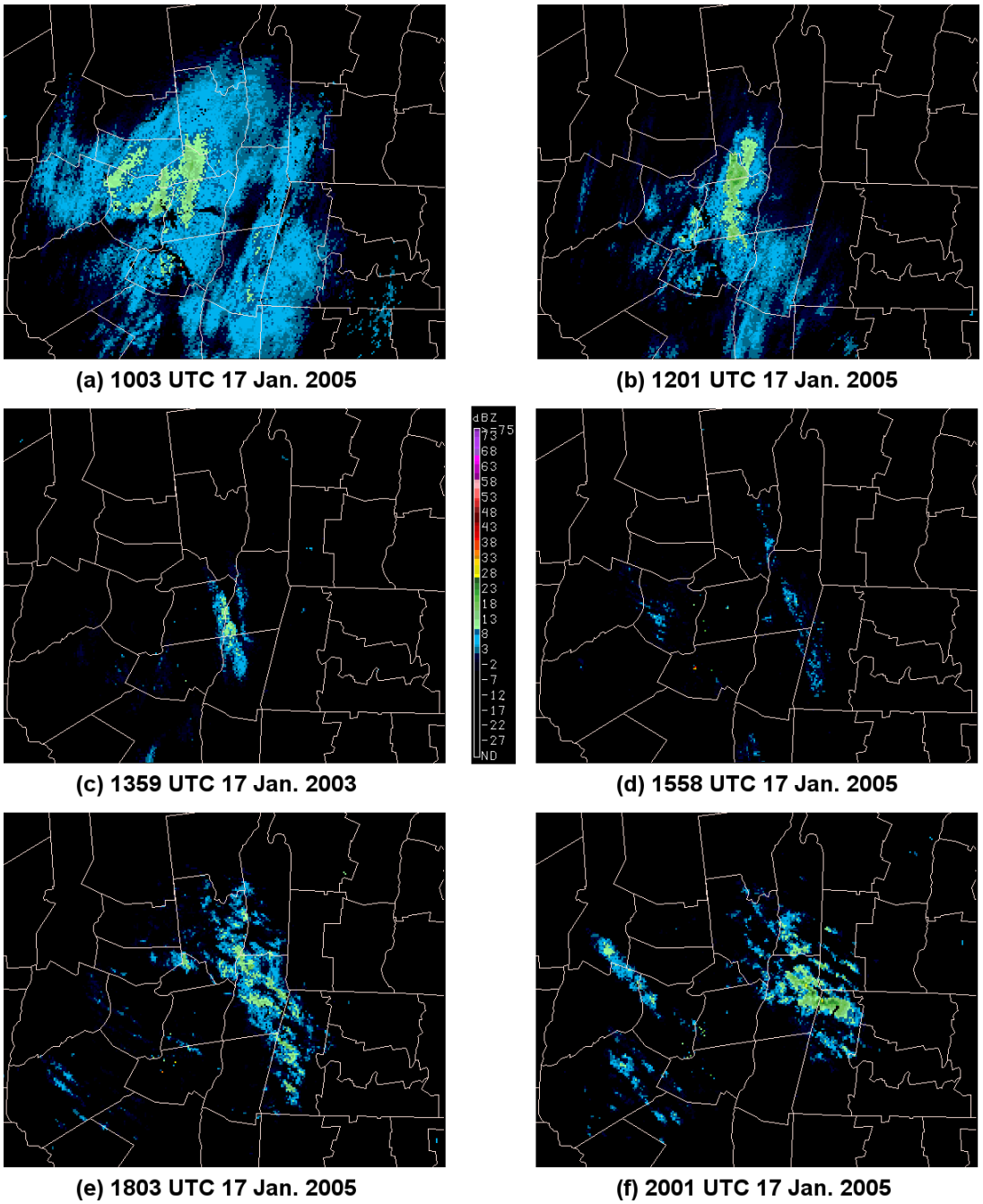

Figure 3.58: As in Fig. 3.15, except for (a) 1003, (b) 1201, (c) 1359, (d) 1558, (e) 1803, and (f) 2001 17 January 2005.

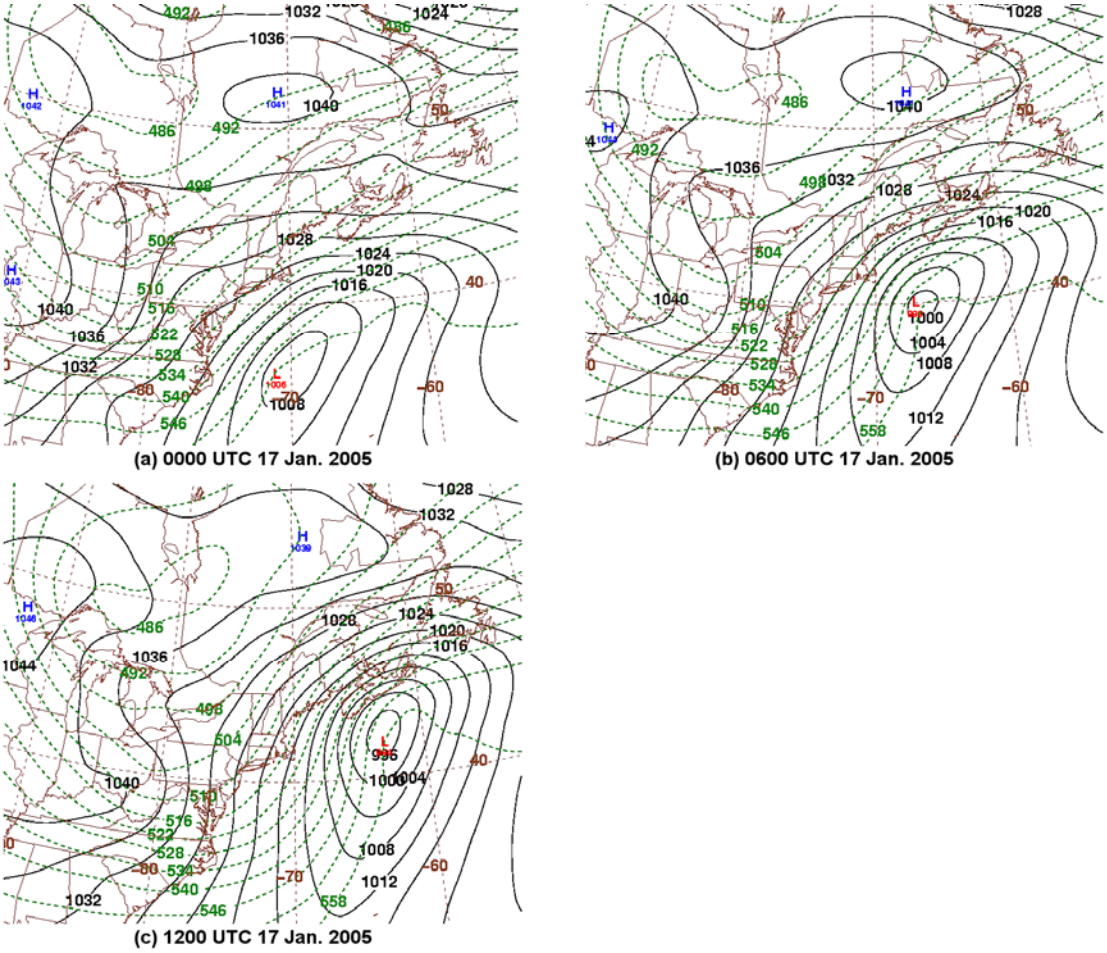

Figure 3.59: As in Fig. 3.7, except for (a) 0000, (b) 0600, and (c) 1200 UTC 17 January 2005.

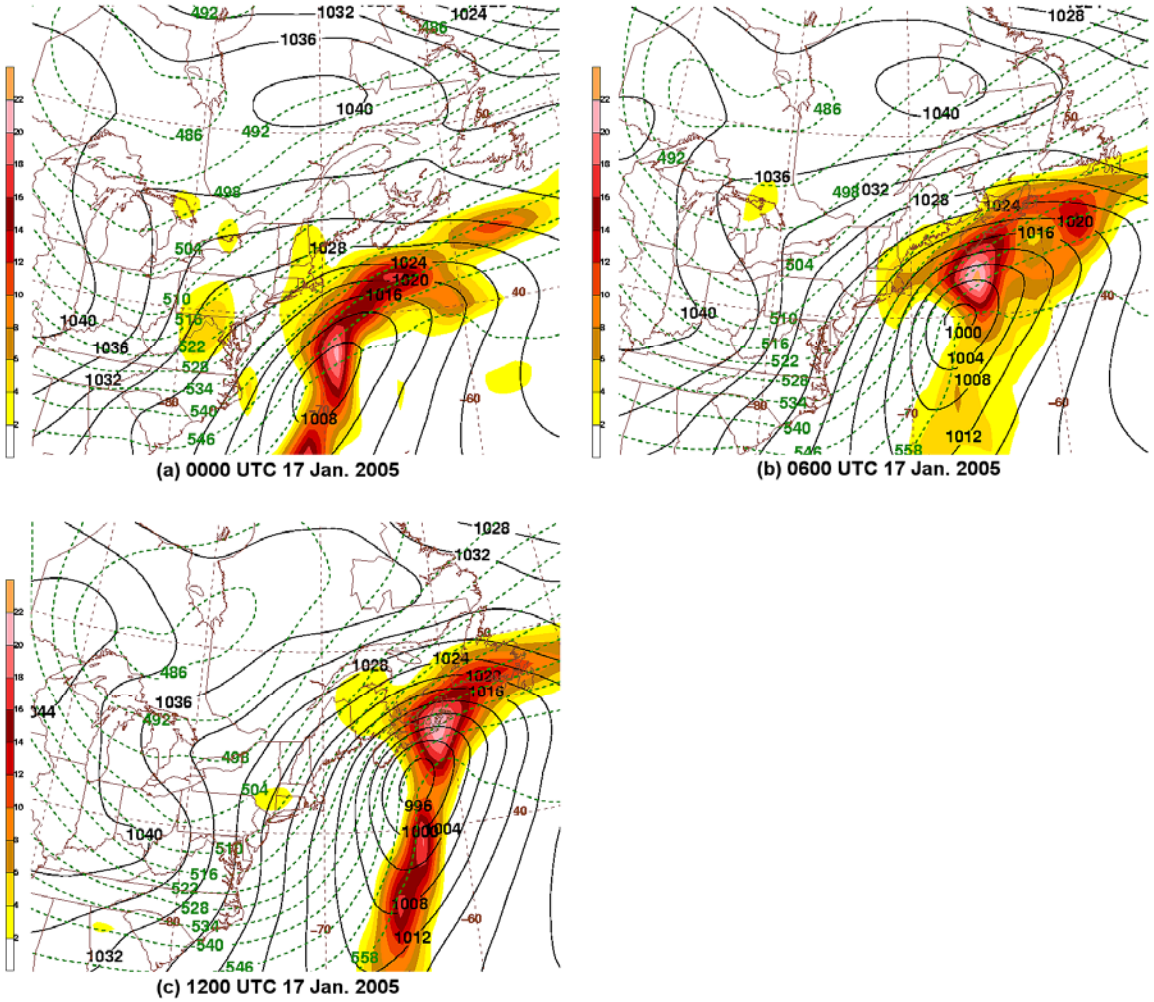

Figure 3.60: As in Fig. 3.10, except for (a) 0000, (b) 0600, and (c) 1200 UTC 17 January 2005.

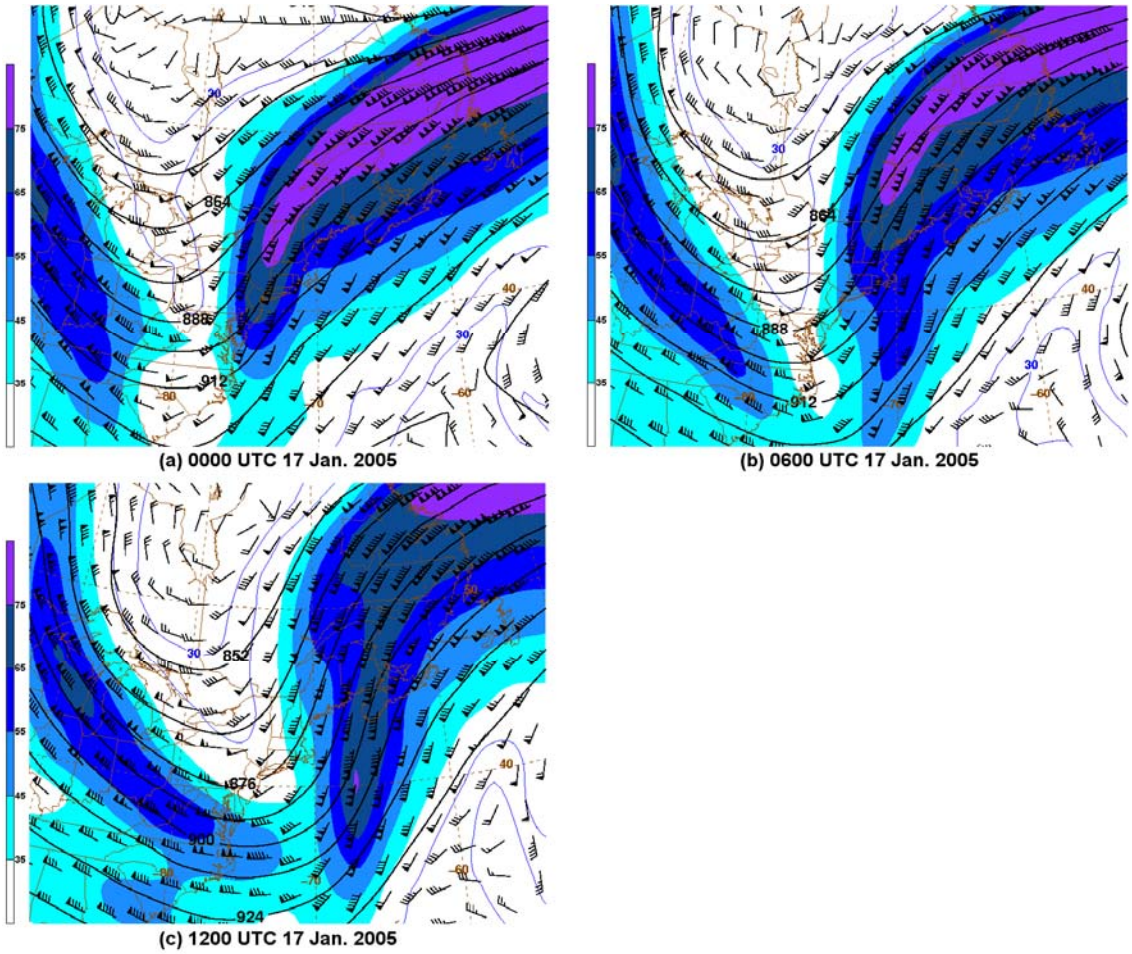

Figure 3.61: As in Fig. 3.13, except for (a) 0000, (b) 0600, and (c) 1200 UTC 17 January 2005.

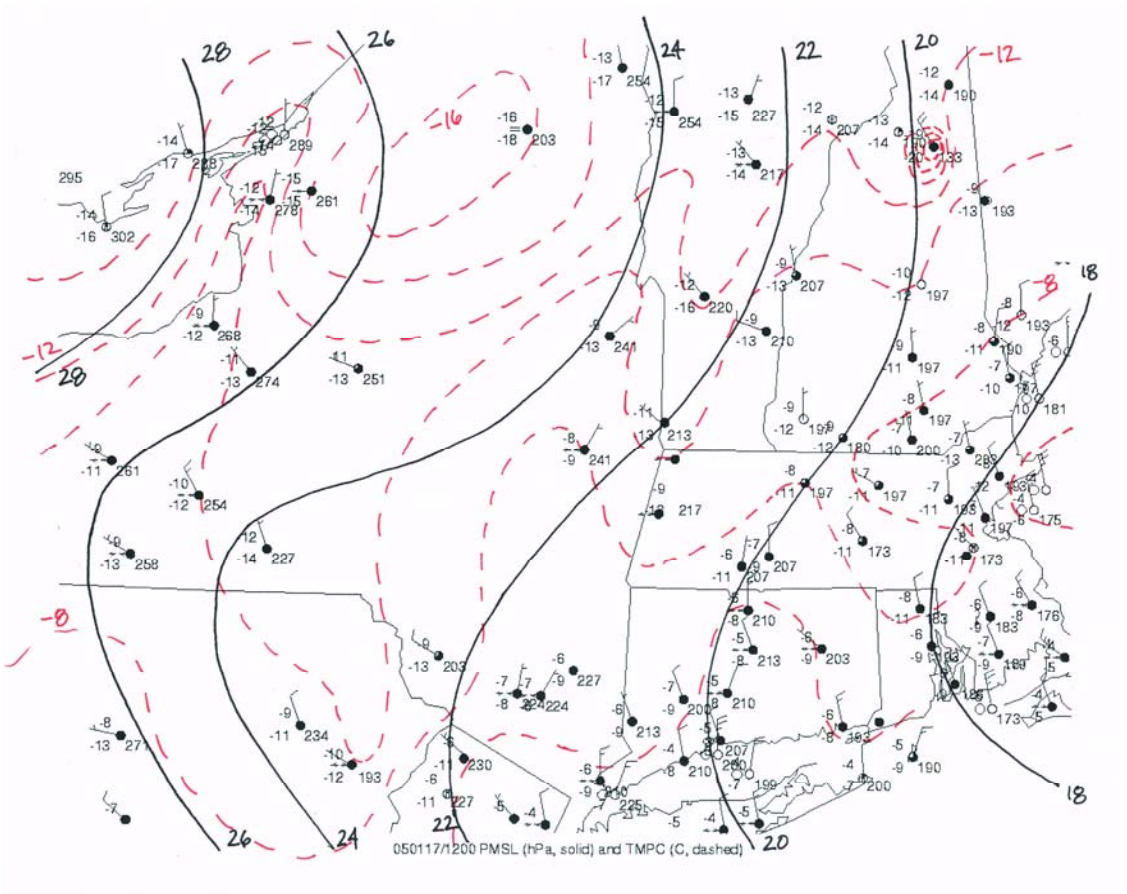

Figure 3.62: As in Fig. 3.16, except for 1200 UTC 17 January 2005.

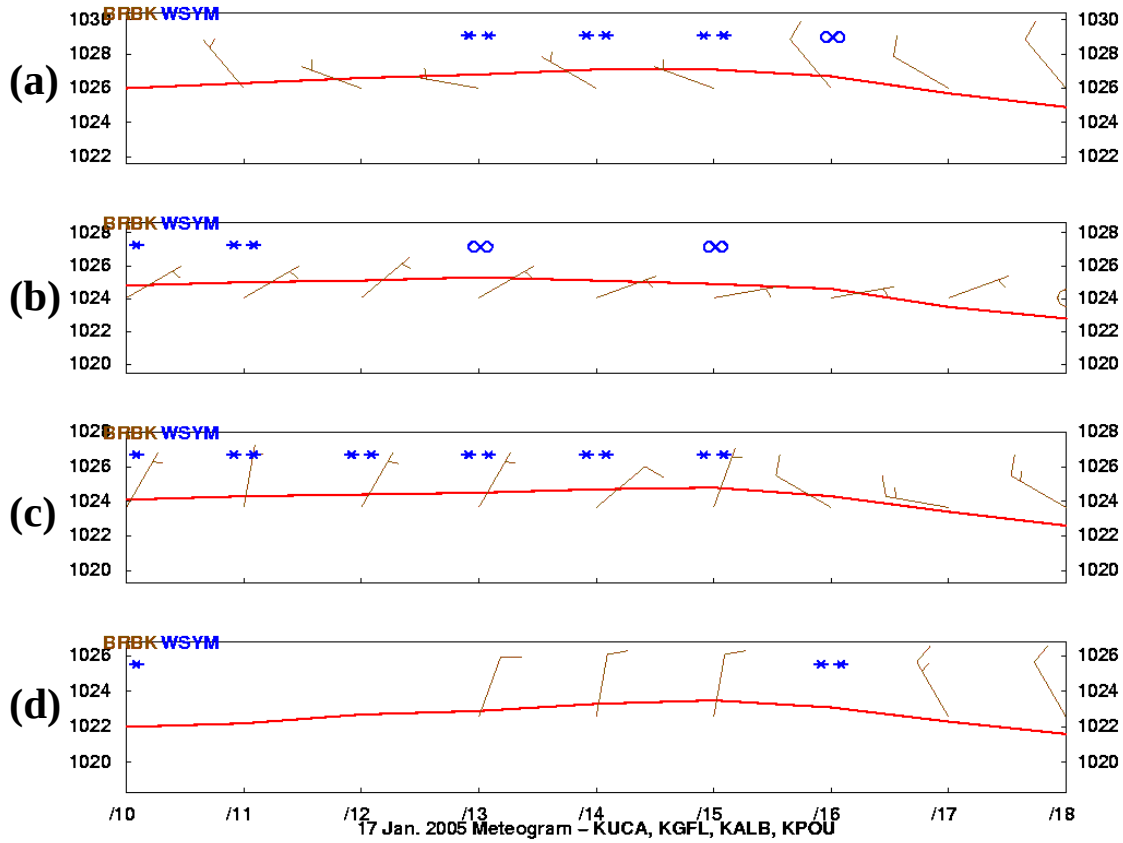

Figure 3.63: As in Fig. 3.17, except from 1000 to 1800 UTC 17 January 2005.

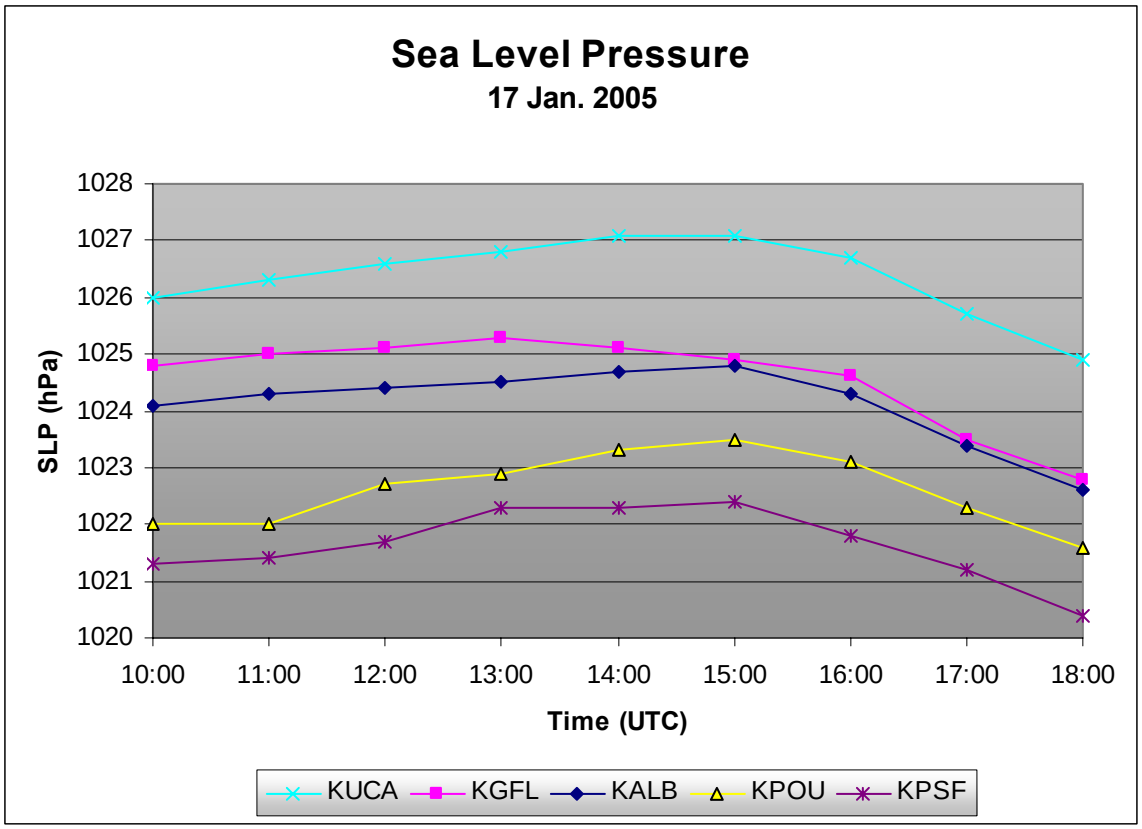

Figure 3.64: As in Fig. 3.18, except from 1000 to 1800 UTC 17 January 2005. (Data source: University at Albany DEAS archives).

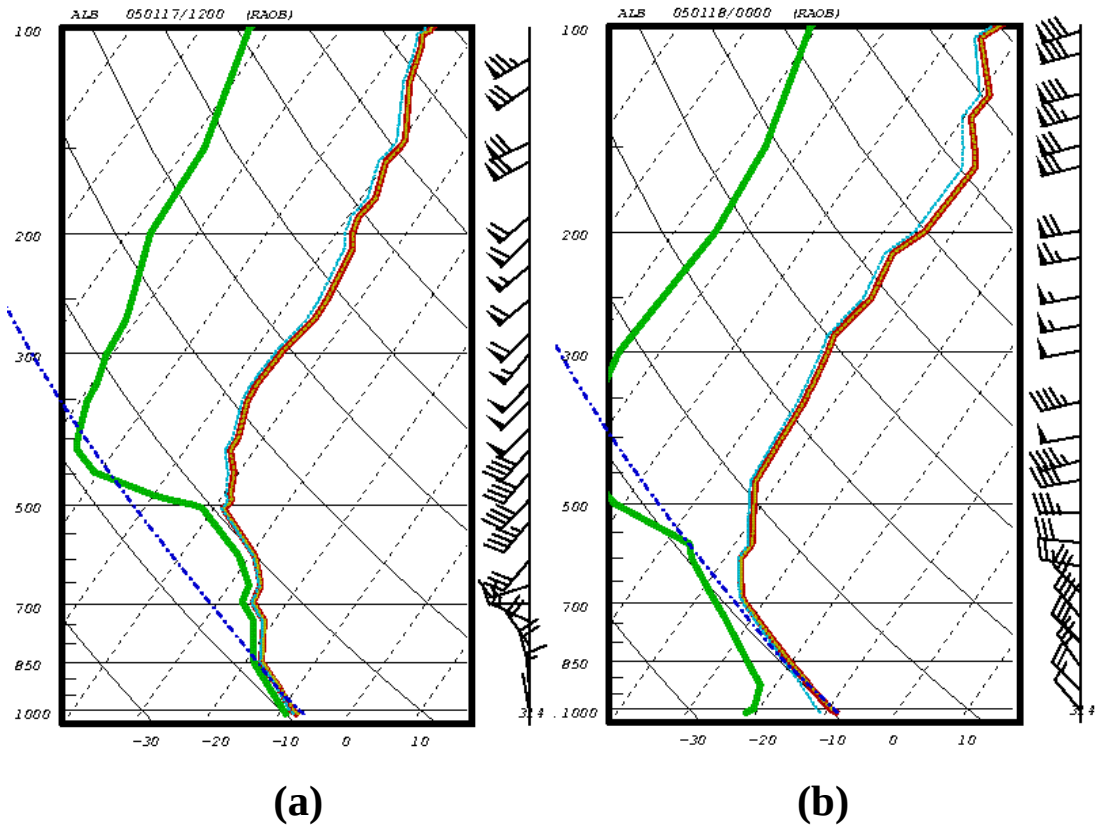

Figure 3.65: As in Fig. 3.19, except for (a) 1200 UTC 17 January 2005 and (b) 0000 UTC 18 January 2005.

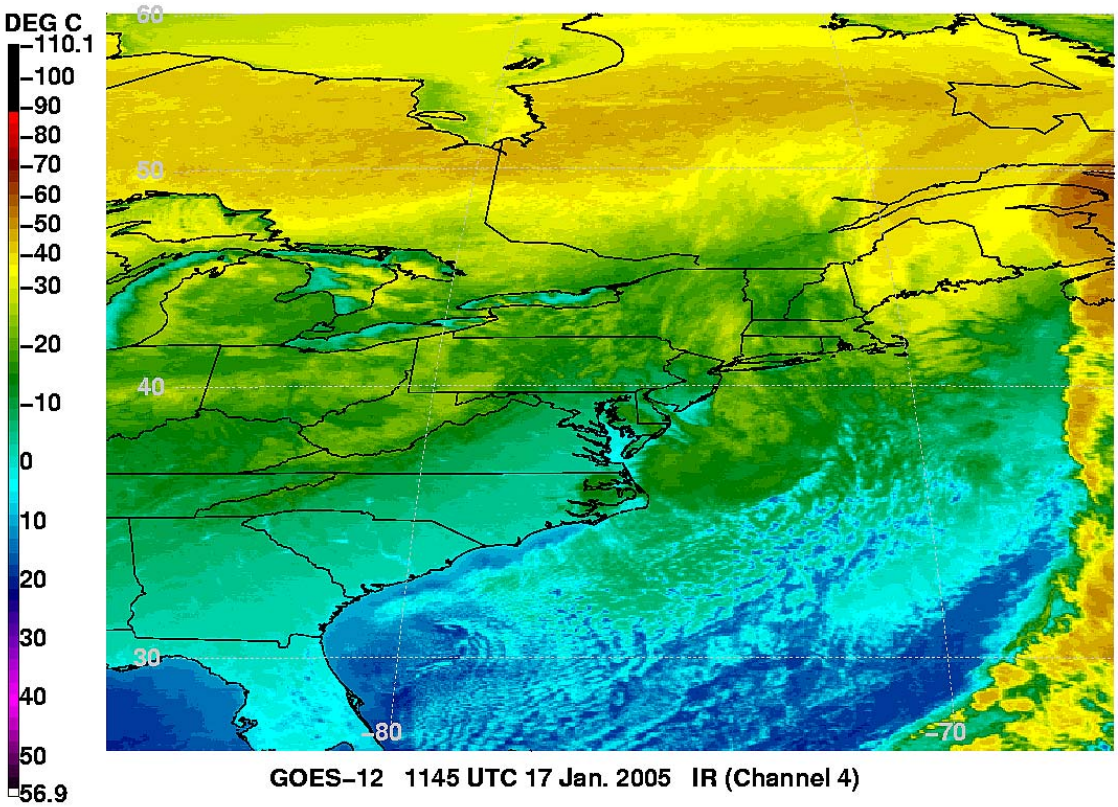

Figure 3.66: As in Fig. 3.23, except from GOES-12 at 1145 UTC 17 January 2005.

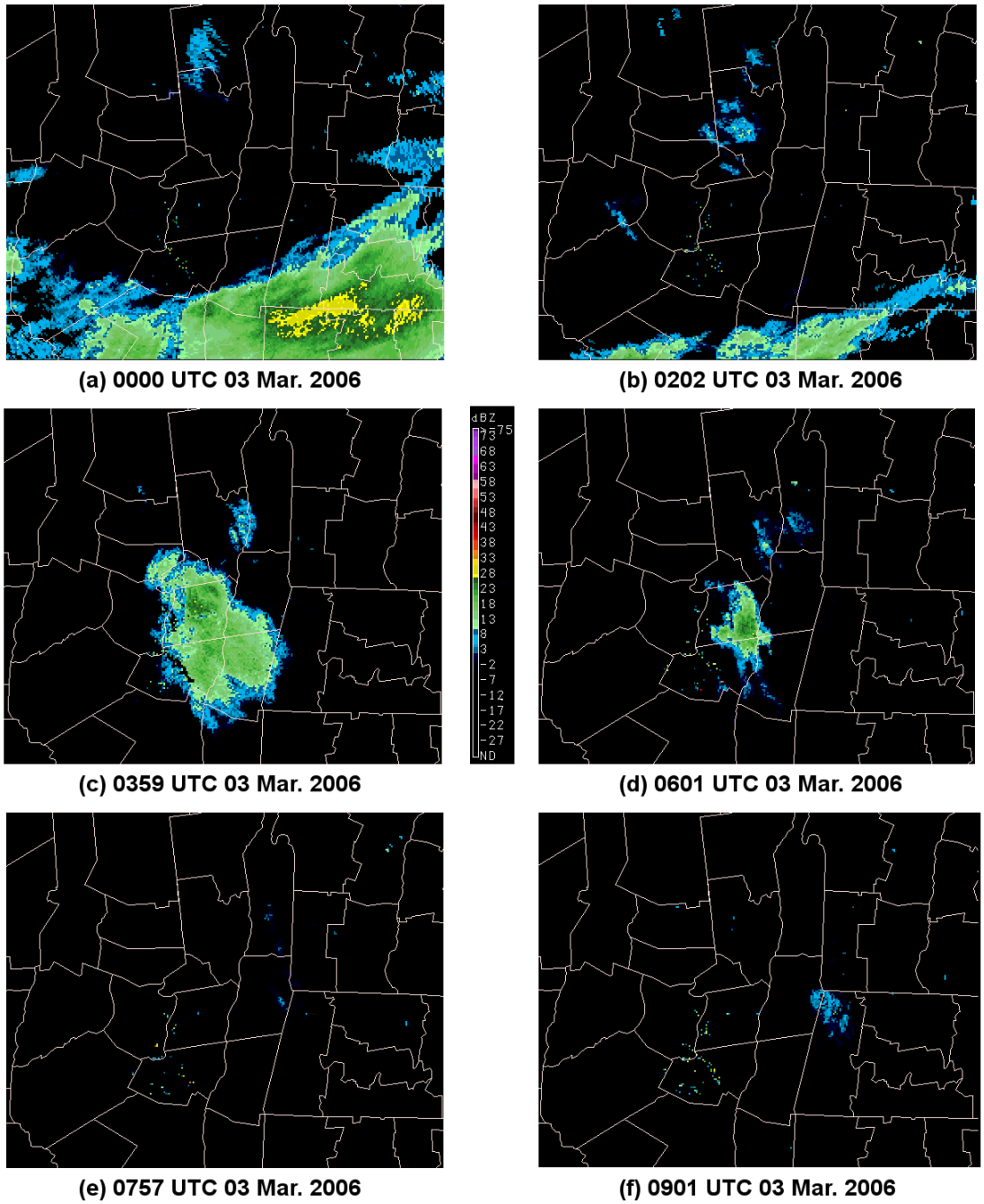

Figure 3.67: As in Fig. 3.15, except for (a) 0000, (b) 0202, (c) 0359, (d) 0601, (e) 0757, and (f) 0901 UTC 3 March 2006.

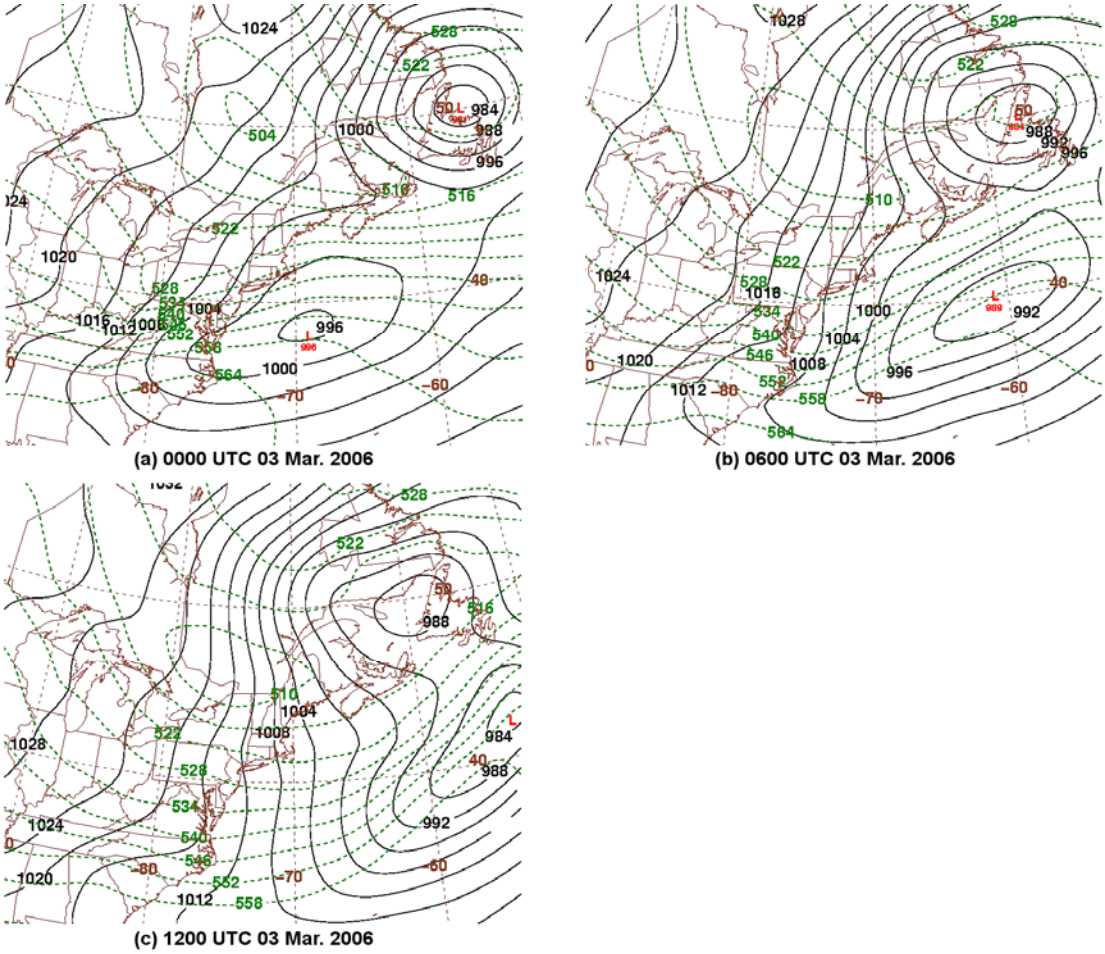

Figure 3.68: As in Fig. 3.7, except for (a) 0000, (b) 0600, and (c) 1200 UTC 3 March 2006.

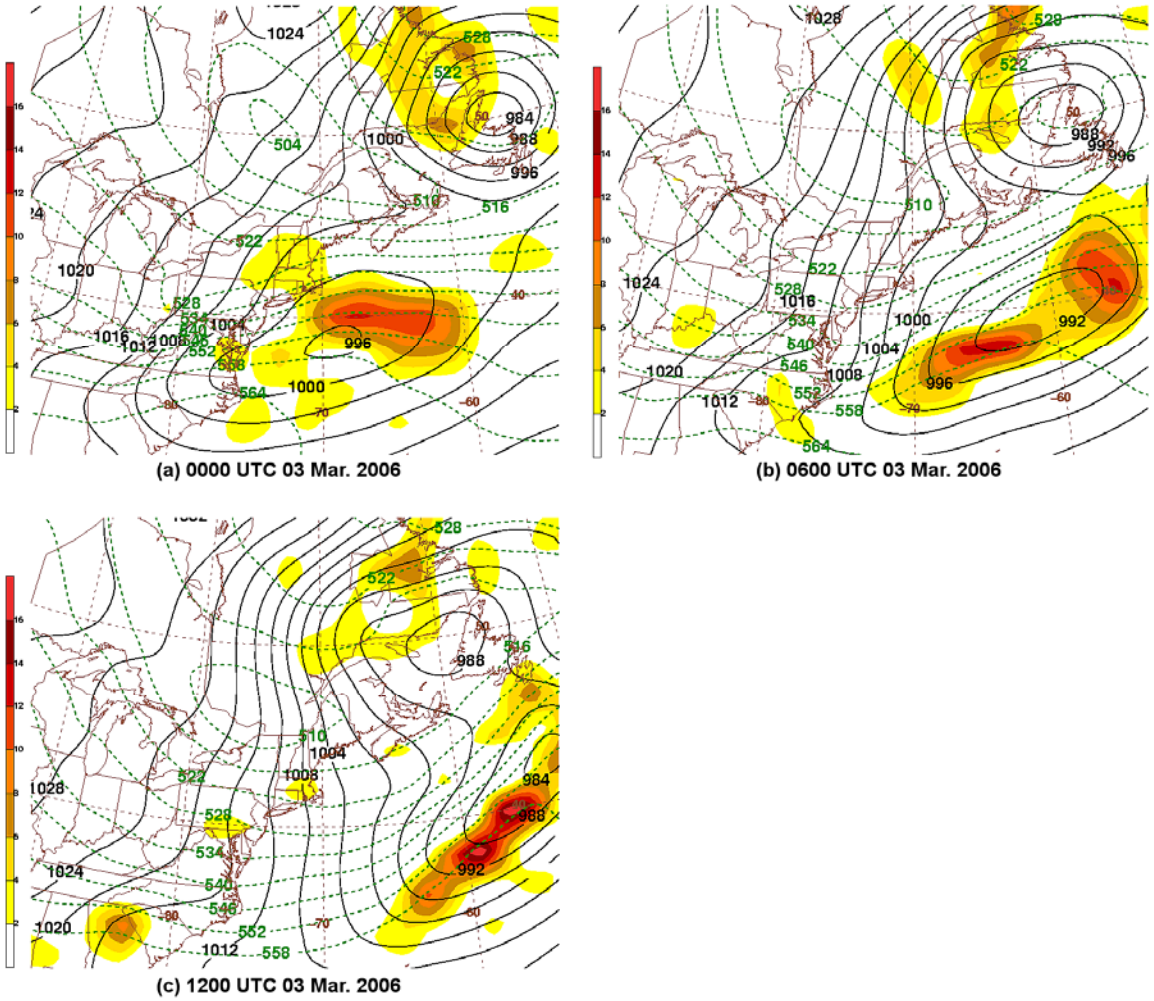

Figure 3.69: As in Fig. 3.10, except for (a) 0000, (b) 0600, and (c) 1200 UTC 3 March 2006.

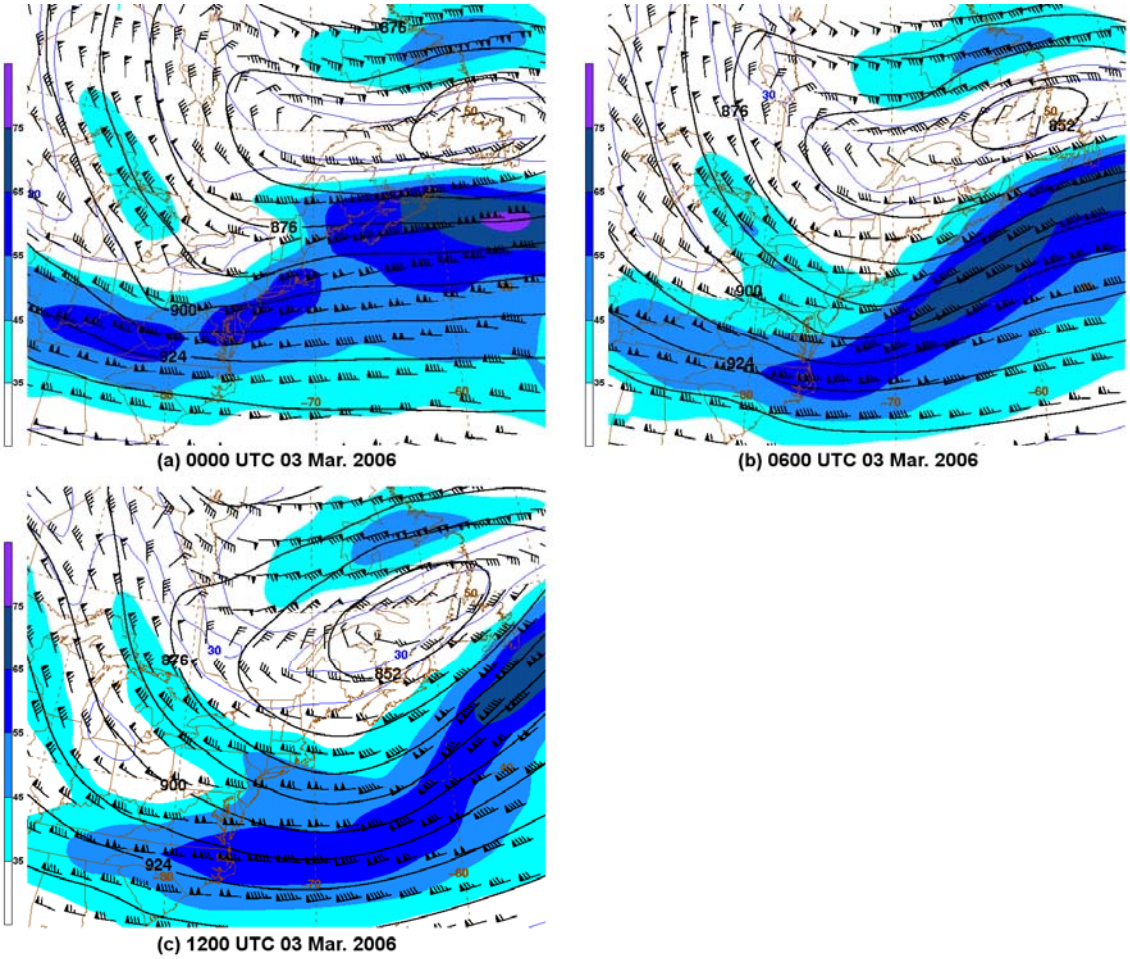

Figure 3.70: As in Fig. 3.13, except for (a) 0000, (b) 0600, and (c) 1200 UTC 3 March 2006.

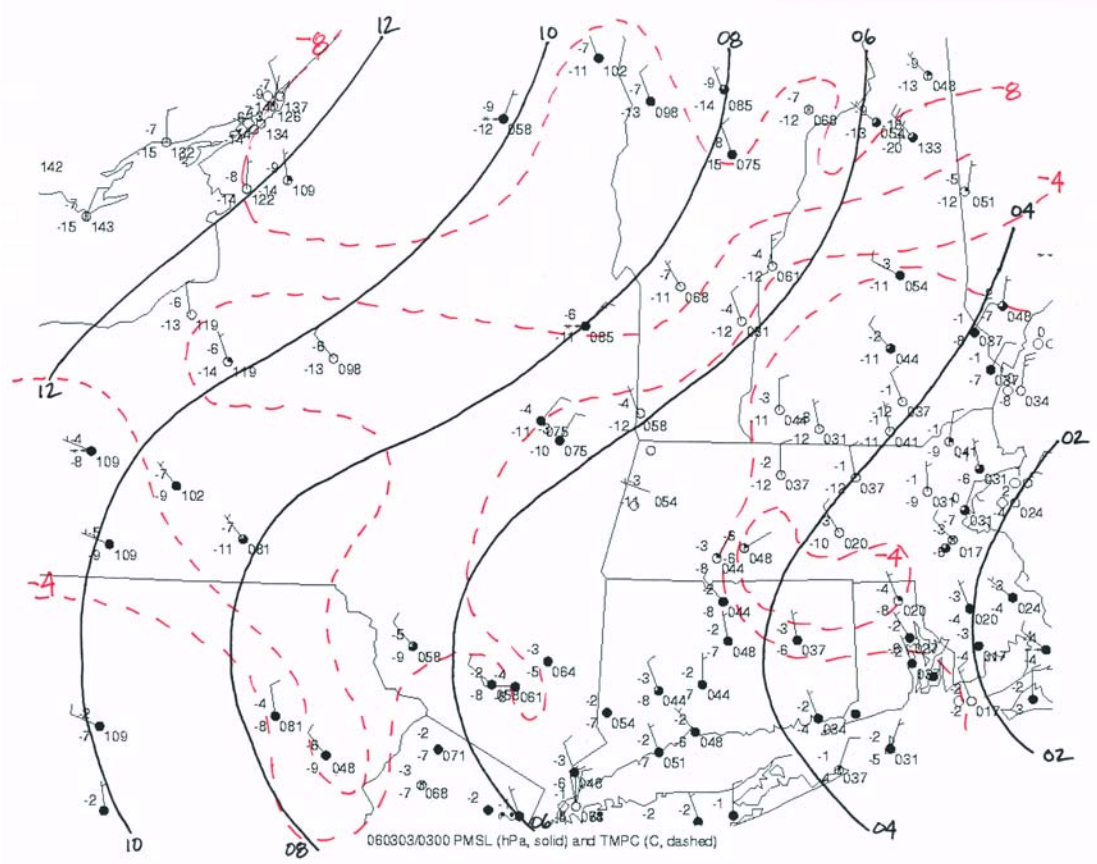

Figure 3.71: As in Fig. 3.16, except for 0300 UTC 3 March 2006.

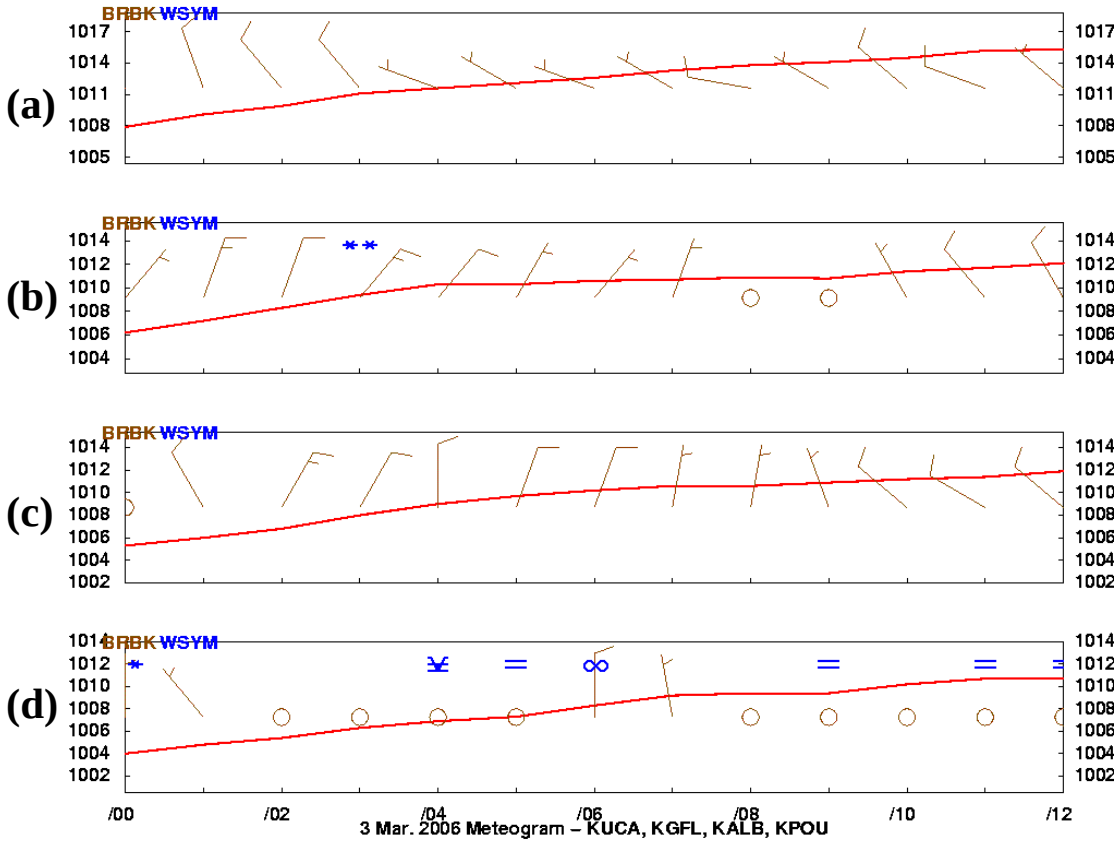

Figure 3.72: As in Fig. 3.17, except from 0000 to 1200 UTC 3 March 2006.

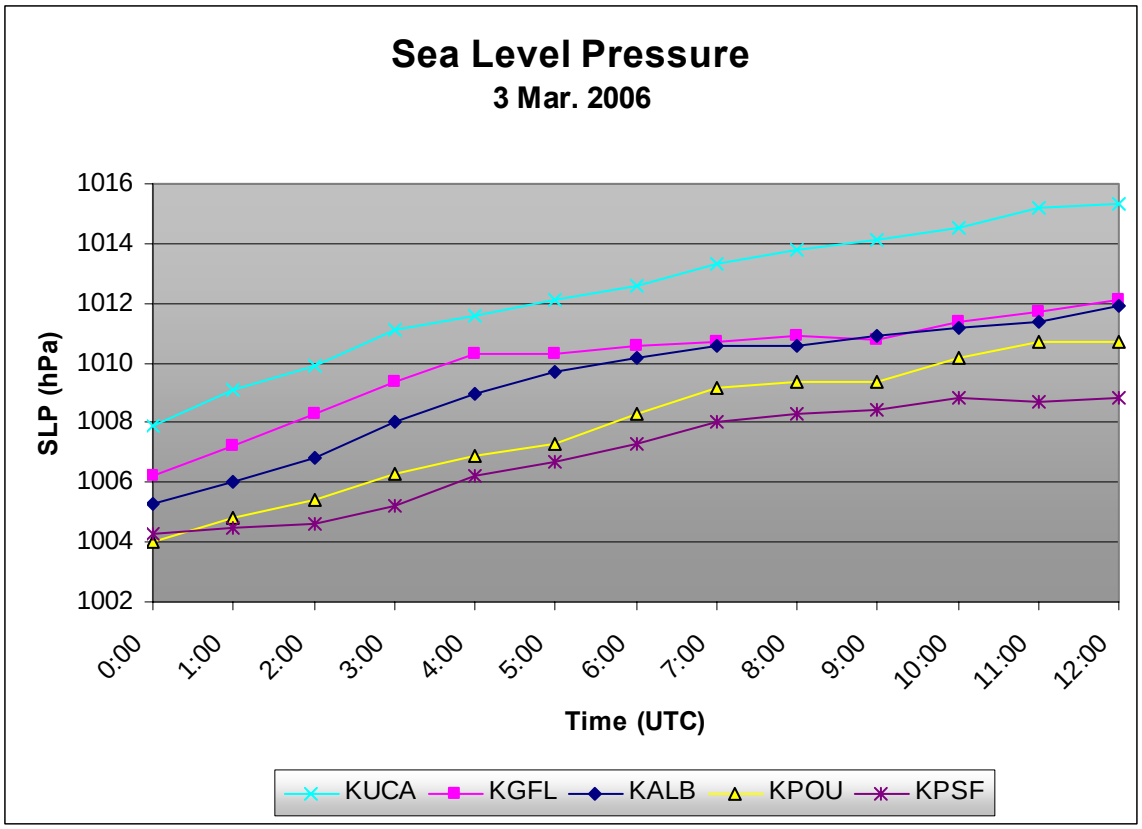

Figure 3.73: As in Fig. 3.18, except from 0000 to 1200 UTC 3 March 2006. (Data source: University at Albany DEAS archives).

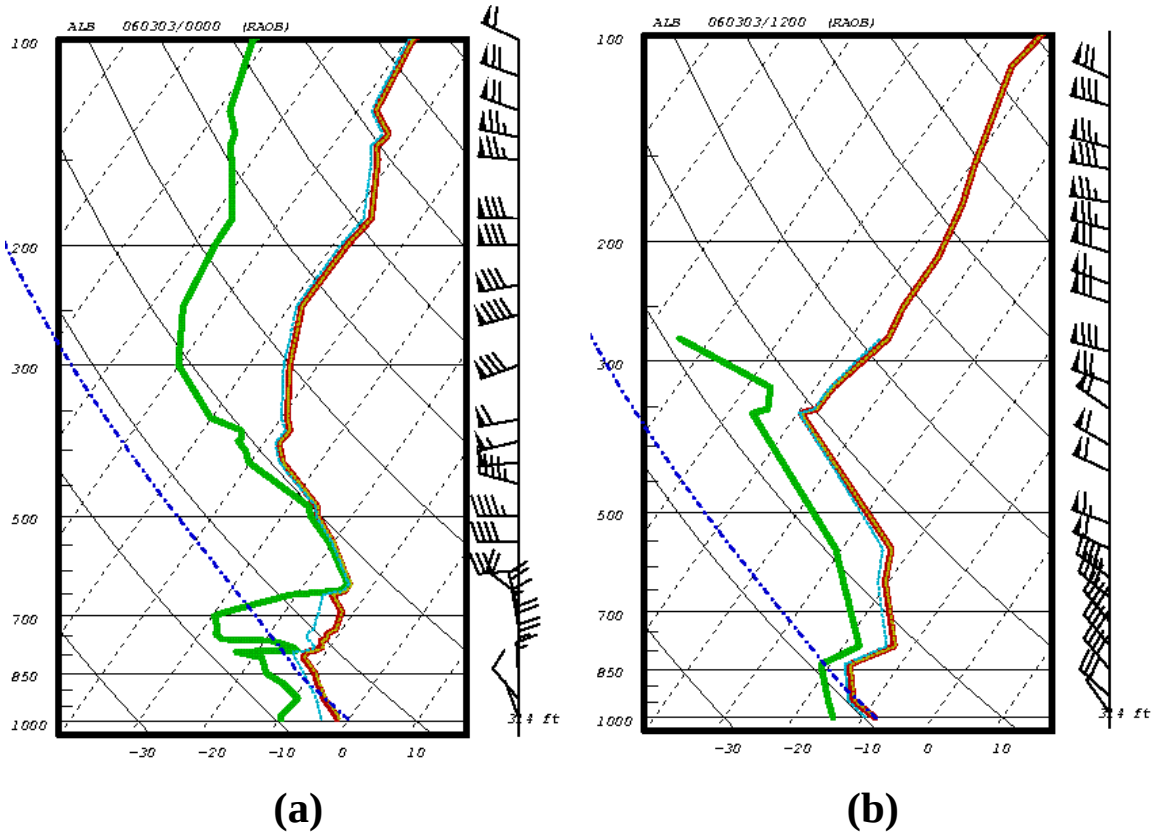

(a) **(b)**

Figure 3.74: As in Fig. 3.19, except for (a) 0000 UTC 3 March 2006 and (b) 1200 UTC 3 March 2006.

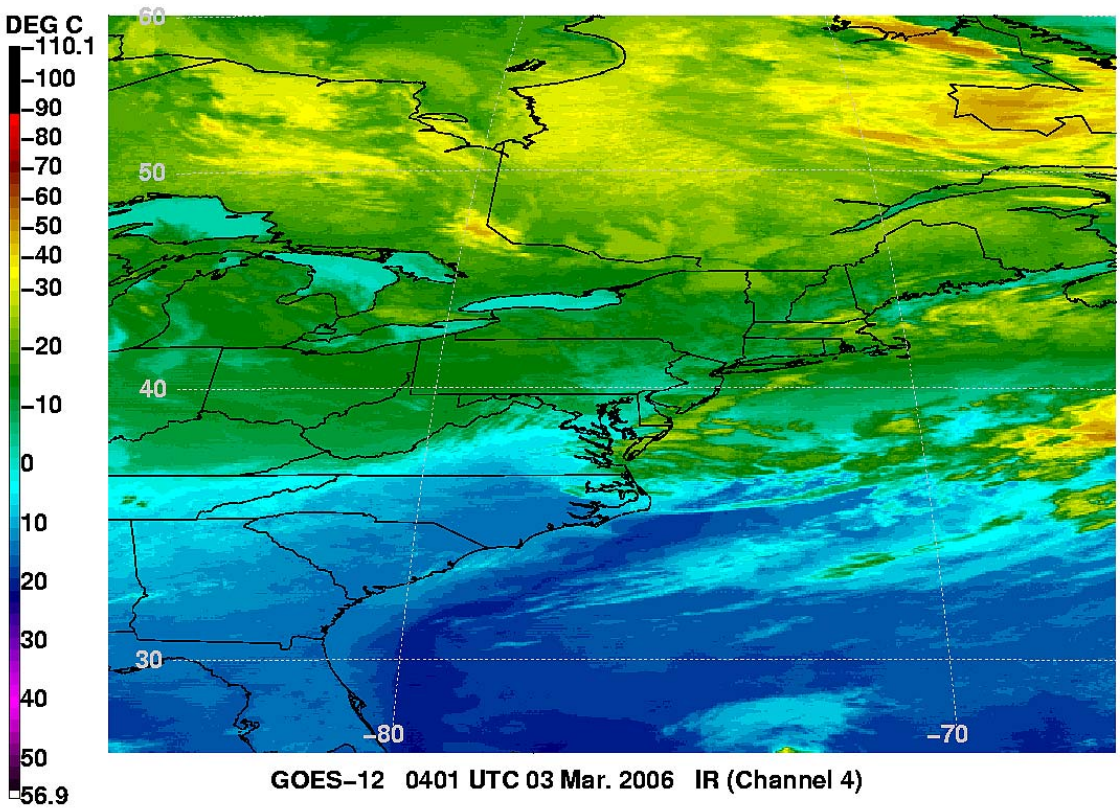

Figure 3.75: As in Fig. 3.23, except from GOES-12 at 0401 UTC 3 March 2006.

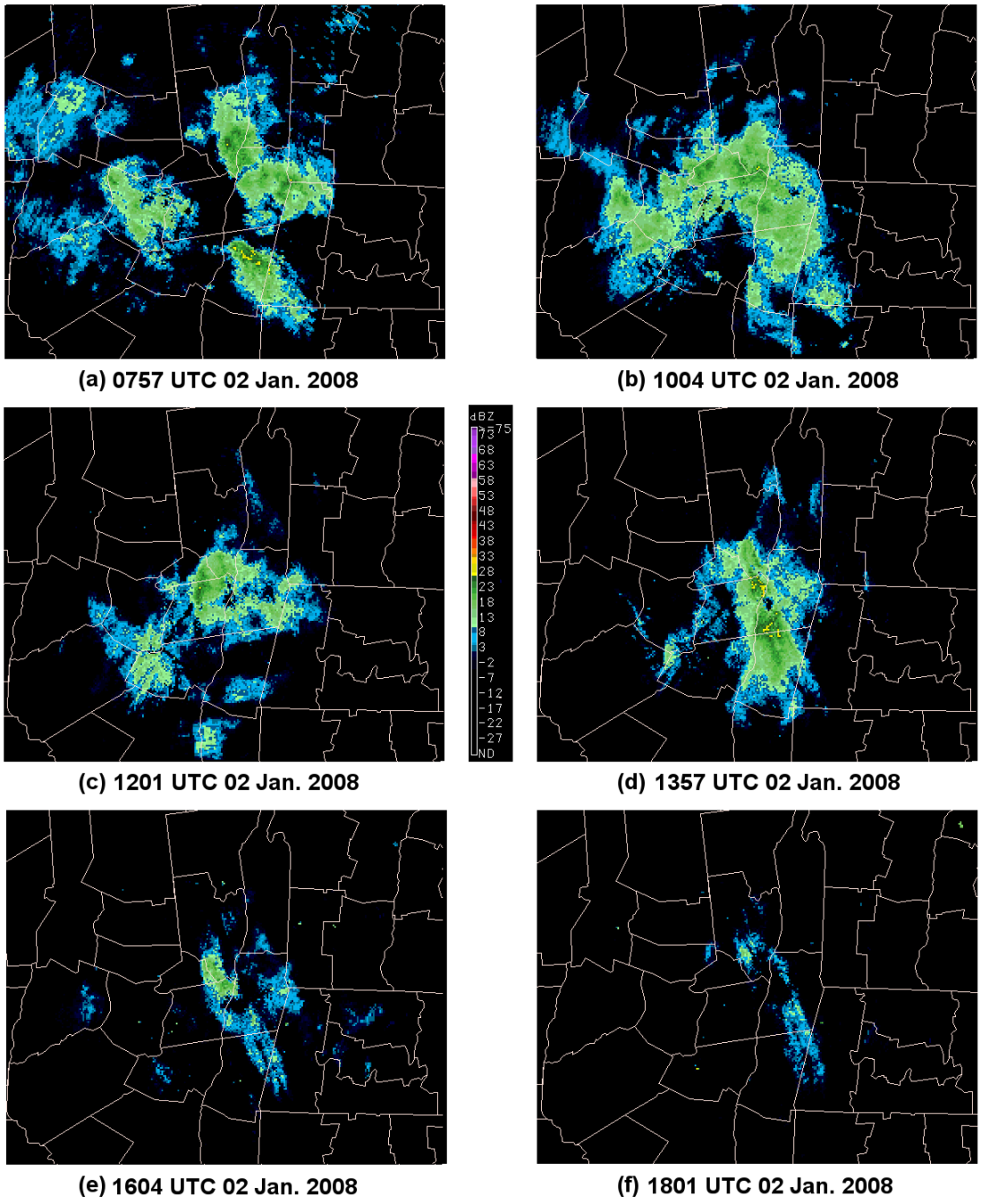

Figure 3.76: As in Fig. 3.15, except for (a) 0757, (b) 1004, (c) 1201, (d) 1357, (e) 1604, and (f) 1801 UTC 2 January 2008.

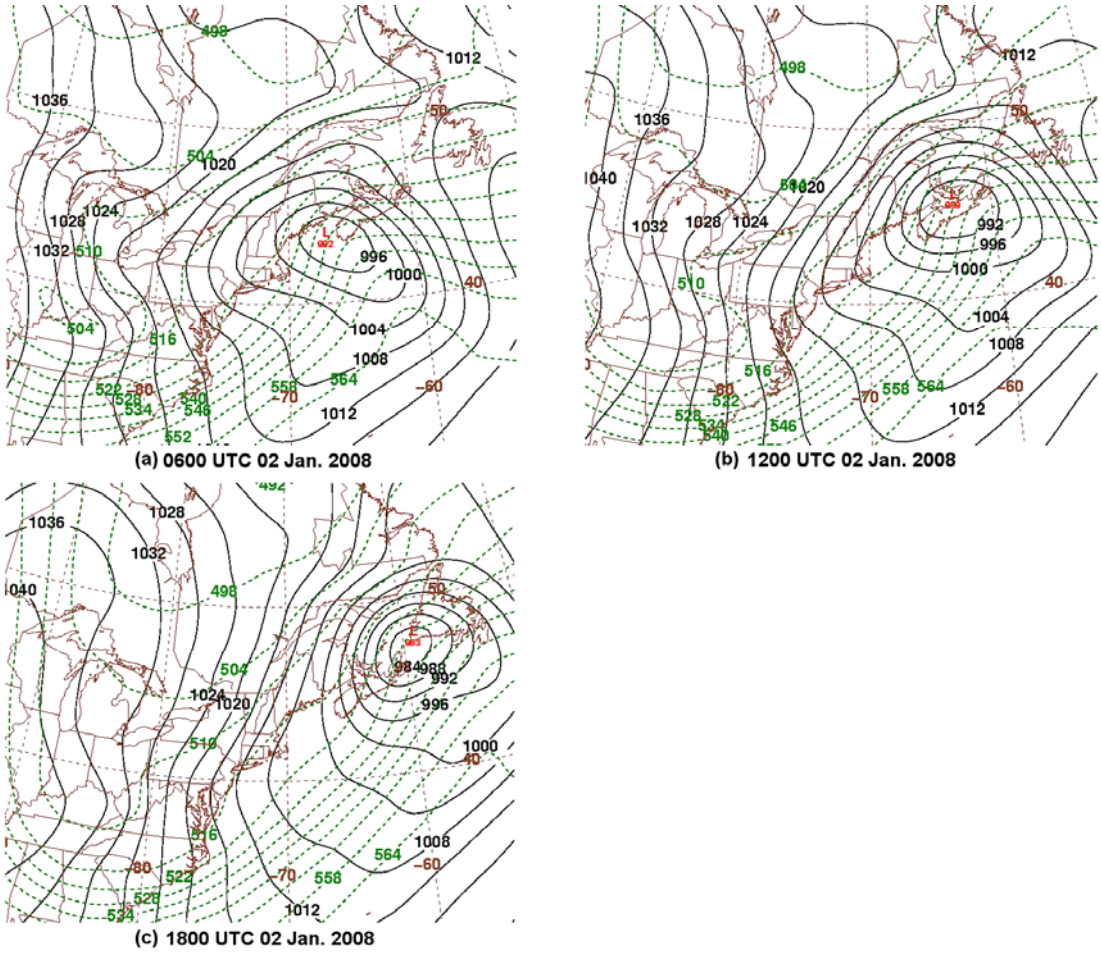

Figure 3.77: As in Fig. 3.7, except for (a) 0600, (b) 1200, and (c) 1800 UTC 2 January 2008.

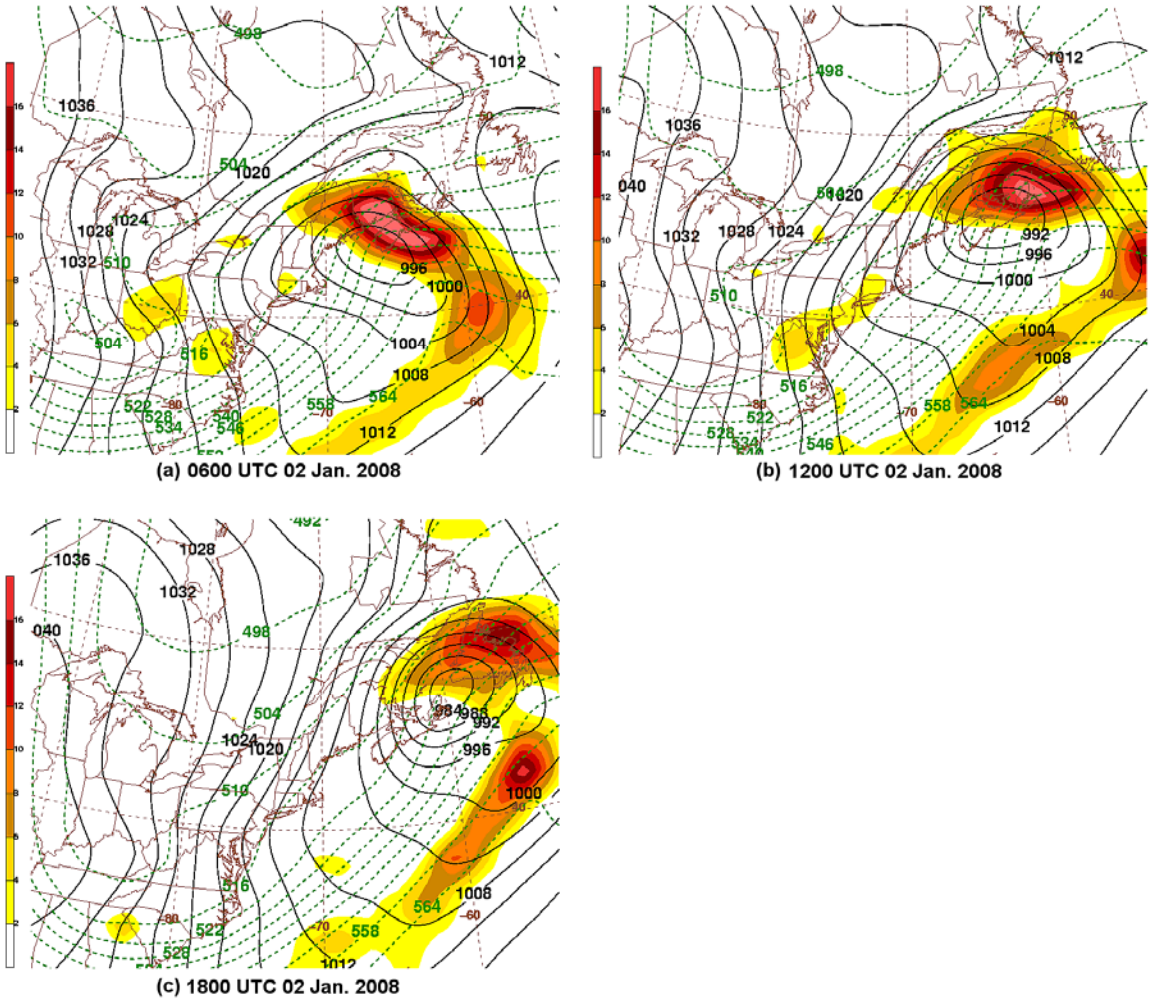

Figure 3.78: As in Fig. 3.10, except for (a) 0600, (b) 1200, and (c) 1800 UTC 2 January 2008.

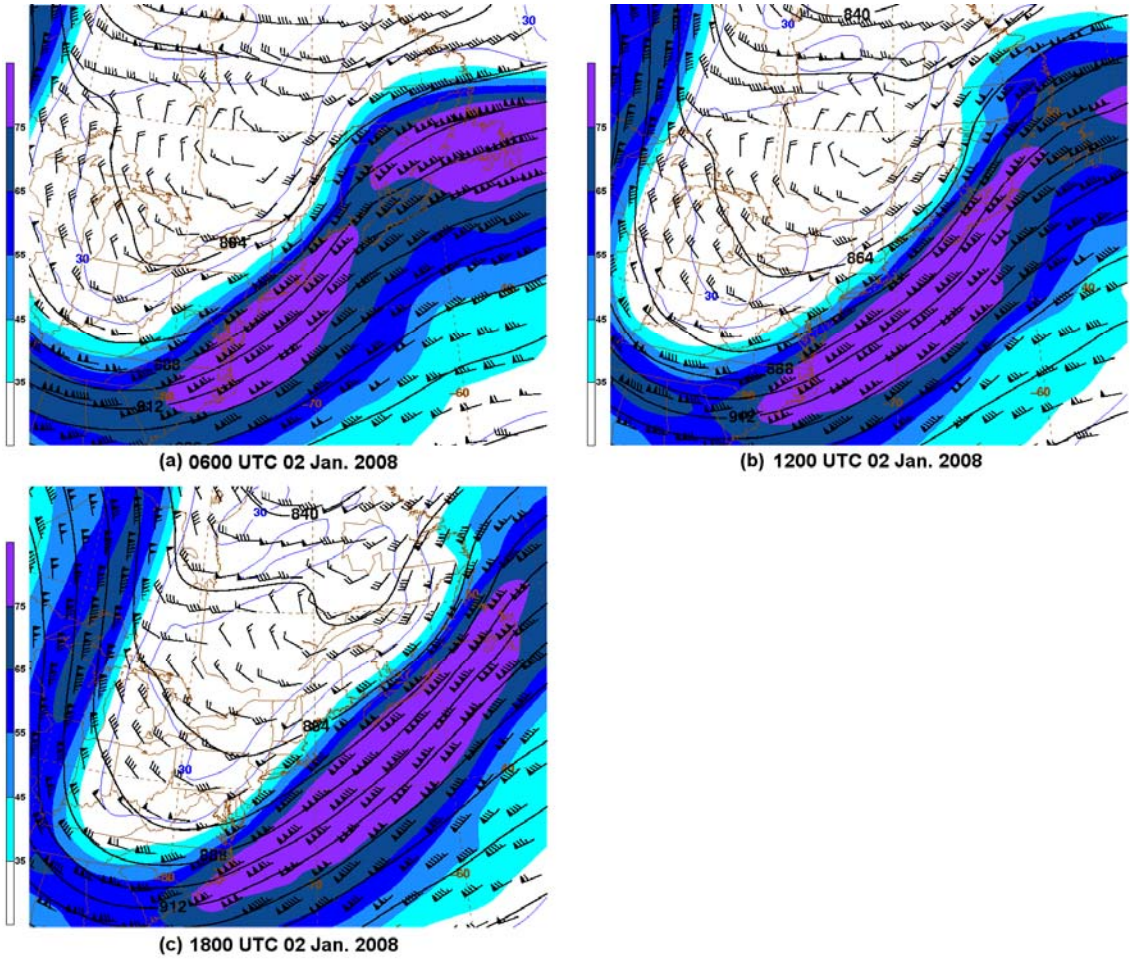

Figure 3.79: As in Fig. 3.13, except for (a) 0600, (b) 1200, and (c) 1800 UTC 2 January 2008.

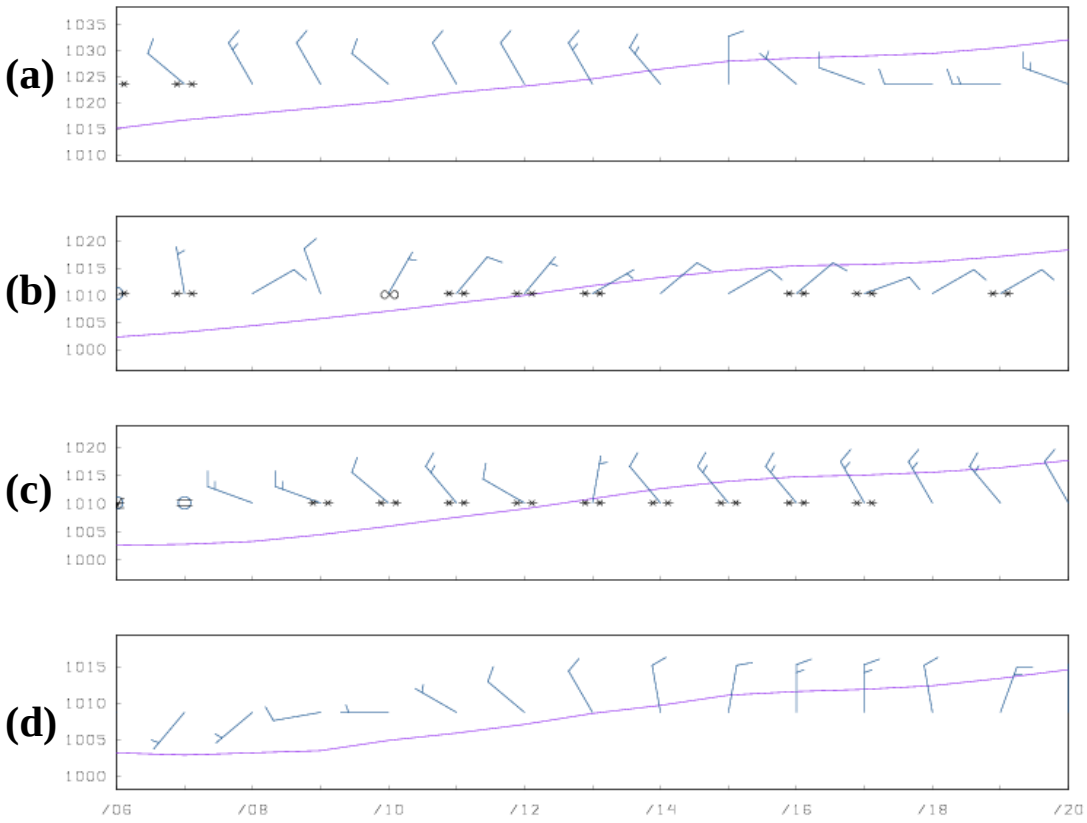

Figure 3.80: As in Fig. 3.17, except from 0600 to 2000 UTC 2 January 2008. (Data source: the Historical Weather Data Archives of NSSL).

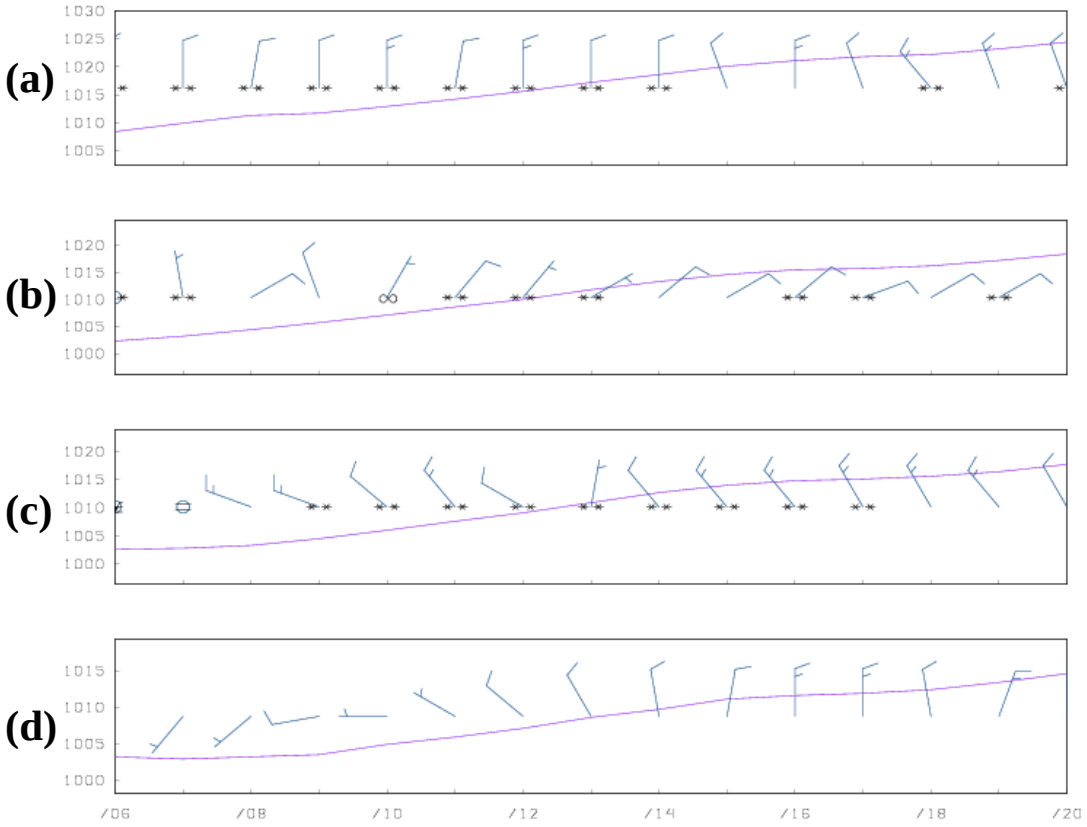

Figure 3.81: As in Fig. 3.80, except for (a) KSYR, (b) KGFL, (c) KALB, and (d) KPOU.

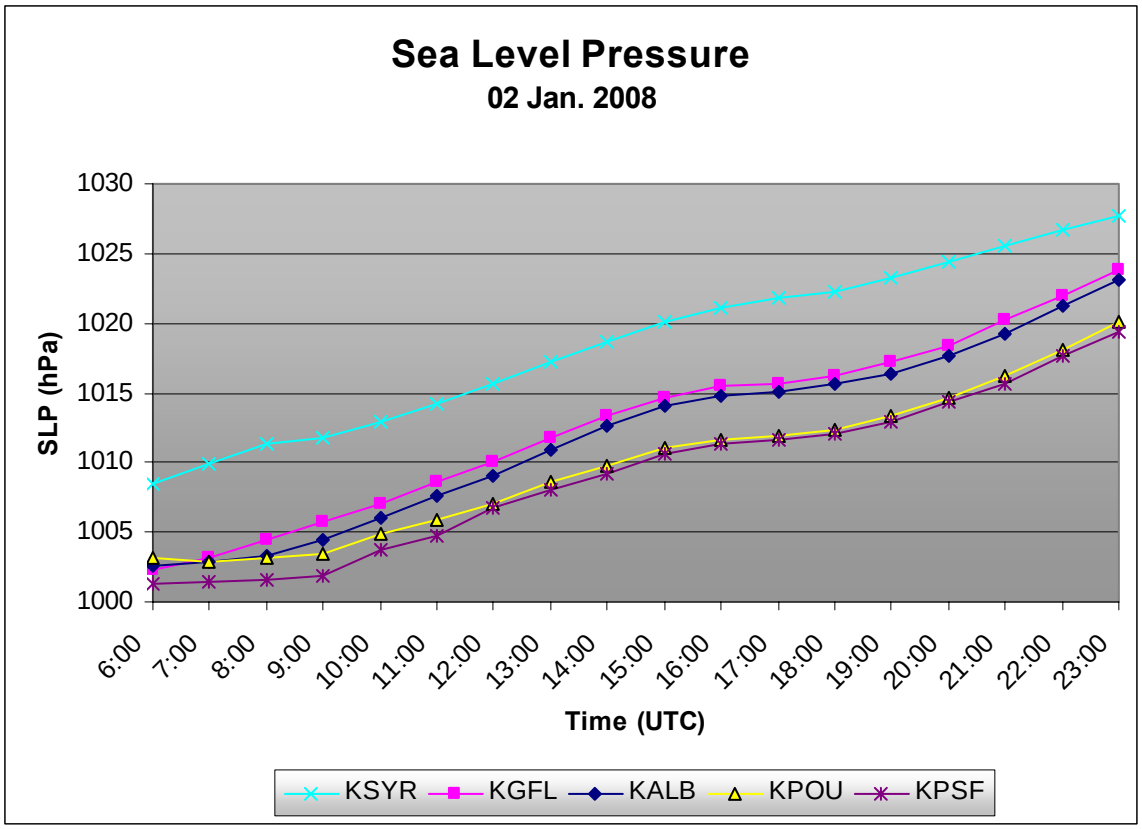

Figure 3.82: Sea level pressure time series (hPa) from 0600 to 2300 UTC 2 January 2008 for KSYR, KGFL, KALB, KPOU, and KPSF (trace and data point markers according to the legend). (Data source: the University at Albany DEAS archives).

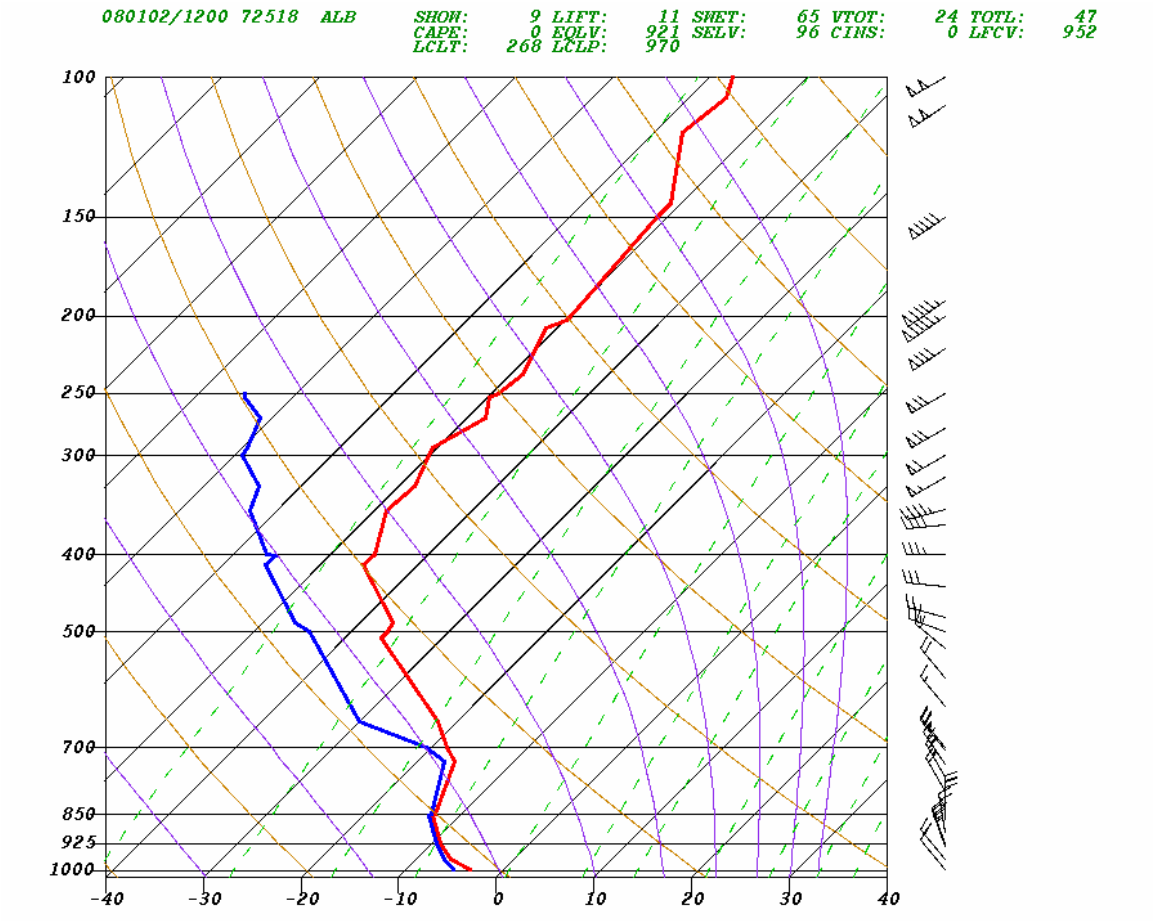

Figure 3.83: Skew *T*–log *p* radiosonde observations at KALY (72518) of air temperature (red line, in °C), dewpoint (blue line, in °C), and wind (to the right of the sounding; m s^{-1}, with pennant, full barb, and half barb denoting 25, 5, and 2.5 m s^{-1}, respectively) for 1200 UTC 2 January 2008. Various thermodynamic parameters are reported in green text at the top of the sounding. (Data source: Ohio State University weather archives).